

# CARMENES input catalogue of M dwarfs

## IV. New rotation periods from photometric time series

E. Díez Alonso<sup>1,2,3</sup>, J. A. Caballero<sup>4</sup>, D. Montes<sup>1</sup>, F. J. de Cos Juez<sup>2</sup>, S. Dreizler<sup>5</sup>, F. Dubois<sup>6</sup>, S. V. Jeffers<sup>5</sup>, S. Lalitha<sup>5</sup>, R. Naves<sup>7</sup>, A. Reiners<sup>5</sup>, I. Ribas<sup>8,9</sup>, S. Vanaverbeke<sup>10,6</sup>, P. J. Amado<sup>11</sup>, V. J. S. Béjar<sup>12,13</sup>, M. Cortés-Contreras<sup>4</sup>, E. Herrero<sup>8,9</sup>, D. Hidalgo<sup>12,13,1</sup>, M. Kürster<sup>14</sup>, L. Logie<sup>6</sup>, A. Quirrenbach<sup>15</sup>, S. Rau<sup>6</sup>, W. Seifert<sup>15</sup>, P. Schöfer<sup>5</sup>, and L. Tal-Or<sup>5,16</sup>

<sup>1</sup> Departamento de Astrofísica y Ciencias de la Atmósfera, Facultad de Ciencias Físicas, Universidad Complutense de Madrid, E-280140 Madrid, Spain; e-mail: [enridiez@ucm.es](mailto:enridiez@ucm.es)

<sup>2</sup> Departamento de Explotación y Prospección de Minas, Escuela de Minas, Energía y Materiales, Universidad de Oviedo, E-33003 Oviedo, Asturias, Spain

<sup>3</sup> Observatorio Astronómico Carda, Villaviciosa, Asturias, Spain (MPC Z76)

<sup>4</sup> Centro de Astrobiología (CSIC-INTA), Campus ESAC, Camino Bajo del Castillo s/n, E-28692 Villanueva de la Cañada, Madrid, Spain

<sup>5</sup> Institut für Astrophysik, Georg-August-Universität Göttingen, Friedrich-Hund-Platz 1, D-37077 Göttingen, Germany

<sup>6</sup> AstroLAB IRIS, Provinciaal Domein “De Palingbeek”, Verbrandemolenstraat 5, B-8902 Zillebeke, Ieper, Belgium

<sup>7</sup> Observatorio Astronómico Naves, Cabrils, Barcelona, Spain (MPC 213)

<sup>8</sup> Institut de Ciències de l’Espai (CSIC-IEEC), Campus UAB, c/ de Can Magrans s/n, E-08193 Bellaterra, Barcelona, Spain

<sup>9</sup> Institut d’Estudis Espacials de Catalunya (IEEC), E-08034 Barcelona, Spain

<sup>10</sup> Vereniging Voor Sterrenkunde, Brugge, Belgium & Centre for mathematical Plasma Astrophysics, Katholieke Universiteit Leuven, Celestijnenlaan 200B, bus 2400, B-3001 Leuven, Belgium

<sup>11</sup> Instituto de Astrofísica de Andalucía (CSIC), Glorieta de la Astronomía s/n, E-18008 Granada, Spain

<sup>12</sup> Instituto de Astrofísica de Canarias, c/ Vía Láctea s/n, E-38205 La Laguna, Tenerife, Spain

<sup>13</sup> Departamento de Astrofísica, Universidad de La Laguna, E-38206 La Laguna, Tenerife, Spain

<sup>14</sup> Max-Planck-Institut für Astronomie, Königstuhl 17, E-69117 Heidelberg, Germany

<sup>15</sup> Landessternwarte, Zentrum für Astronomie der Universität Heidelberg, Königstuhl 12, D-69117 Heidelberg, Germany

<sup>16</sup> School of Geosciences, Raymond and Beverly Sackler Faculty of Exact Sciences, Tel Aviv University, Tel Aviv, 6997801, Israel

Received 27 April 2018; accepted dd Mmm 2018

## ABSTRACT

**Aims.** The main goal of this work is to measure rotation periods of the M-type dwarf stars being observed by the CARMENES exoplanet survey to help distinguish radial-velocity signals produced by magnetic activity from those produced by exoplanets. Rotation periods are also fundamental for a detailed study of the relation between activity and rotation in late-type stars.

**Methods.** We look for significant periodic signals in 622 photometric time series of 337 bright, nearby M dwarfs obtained by long-time baseline, automated surveys (MEarth, ASAS, SuperWASP, NSVS, Catalina, ASAS-SN, K2, and HATNet) and for 20 stars which we obtained with four 0.2–0.8 m telescopes at high geographical latitudes.

**Results.** We present 142 rotation periods (73 new) from 0.12 d to 133 d and ten long-term activity cycles (six new) from 3.0 a to 11.5 a. We compare our determinations with those in the existing literature; we investigate the distribution of  $P_{\text{rot}}$  in the CARMENES input catalogue, the amplitude of photometric variability, and their relation to  $v \sin i$  and pEW(H $\alpha$ ); and we identify three very active stars with new rotation periods between 0.34 d and 23.6 d.

**Key words.** stars: activity – stars: late type – stars: rotation – techniques: photometry

## 1. Introduction

In current exoplanet search programmes, knowledge of the stellar rotation periods is essential in order to distinguish radial-velocity signals induced by real planets or by the rotation of the star itself (Saar & Donahue, 1997; Queloz et al., 2001; Boisse et al., 2011). This is even more important when the goal is to detect weak signals induced by Earth-like exoplanets around low-mass stars (Scalo et al., 2007; Léger et al., 2009; Dumusque et al., 2012; Anglada-Escudé

et al., 2016). For this purpose, star spots on the photosphere of stars can help us because they induce a photometric modulation from which we can infer not only the rotation period of the stars (Kron, 1947; Bouvier et al., 1993; Messina & Guinan, 2002; Strassmeier, 2009), but also long-term activity cycles (Baliunas & Vaughan, 1985; Berdyugina & Järvinen, 2005).

M dwarfs are strongly affected by star spots because of the presence of large active regions on their surfaces,

which are due to the depth of the convective layers (Delfosse et al., 1998; Mullan & MacDonald, 2001; Browning, 2008; Reiners & Basri, 2008; Barnes et al., 2011). As a result, these late-type stars are the most likely to present this kind of modulation in photometric series (Irwin et al., 2011; Kiraga, 2012; West et al., 2015; Suárez Mascareño et al., 2016). The low masses and small radii of M dwarfs also make them ideal targets for surveys aimed at detecting small, low-mass, potentially habitable Earth-like planets (Joshi et al., 1997; Segura et al., 2005; Tarter et al., 2007; Reiners et al., 2010; France et al., 2013). Therefore, the inclusion of M-dwarf targets in exoplanet surveys has increased steadily from the first dedicated radial-velocity searches (Butler et al., 2004; Bonfils et al., 2005; Johnson et al., 2007), through transit searches from the ground and space (Berta et al., 2013; Kopparapu et al., 2013; Crossfield et al., 2015; Dressing & Charbonneau, 2015; Gillon et al., 2016, 2017; Dittmann et al., 2017), to up-to-date searches with specially designed instruments and space missions such as CARMENES (Quirrenbach et al., 2014), HPF (Mahadevan et al., 2014), IRD (Tamura et al., 2012), SPIRou (Artigau et al., 2014), *TESS* (Ricker et al., 2015), or GIARPS (Claudi et al., 2016). As a result, there is a growing number of projects aimed at photometrically following up large samples of M dwarfs in the solar neighbourhood with the goals of determining their rotation periods and discriminating between signals induced by rotation from those induced by the presence of planets (Irwin et al., 2011; Suárez Mascareño et al., 2015; Newton et al., 2016). Some of the targeted M dwarfs have known exoplanets, or are suspected to harbour them, while others are just being monitored by radial-velocity surveys with high-resolution spectrographs. Some exoplanets may transit their stars, although transiting exoplanets around bright M dwarfs are rare (Gillon et al., 2007; Charbonneau et al., 2009).

This work is part of the CARMENES project<sup>1</sup>. It is also the fourth item in the series of papers devoted to the scientific preparation of the target sample being monitored during CARMENES guaranteed time observations (see also Alonso-Floriano et al., 2015a; Cortés-Contreras et al., 2017; Jeffers et al., 2018). Here we present the results of analysing long-term, wide-band photometry of 337 M dwarfs currently being monitored by CARMENES (Reiners et al., 2018b). For many of them we had not been able to find rotation periods in the existing literature (see below).

To determine the rotation periods of our M dwarfs, we make extensive use of public time series of wide-area photometric surveys and databases such as the All-Sky Automated Survey (ASAS; Pojmański, 1997), Northern Sky Variability Survey (NSVS; Woźniak et al., 2004), Wide Angle Search for Planets (SuperWASP; Pollacco et al., 2006), Catalina Real-Time Transient Survey (Catalina; Drake et al., 2009), and The MEarth Project (MEarth; Charbonneau et al., 2009; Irwin et al., 2011). Since the amplitude of the modulations induced by star spots, in the range of millimagnitudes, is also within reach of current amateur facilities (Herrero et al., 2011; Baluev et al., 2015), we also collaborate with amateur astronomers to obtain data for stars that have never been studied by systematic surveys or that need a greater number of observations.

After collecting and cleaning the time series, we look for significant peaks in power spectra, determine probable ro-

tation periods and long activity cycles, compare them with previous determinations and activity indicators when available, and make all our results available to the whole community in order to facilitate the disentanglement of planetary and activity signals in current and forthcoming radial-velocity surveys of M dwarfs.

## 2. Data

### 2.1. Sample of observed M dwarfs

During guaranteed time observations (GTOs), the double-channel CARMENES spectrograph has so far observed a sample of 336 bright, nearby M dwarfs with the goal of detecting low-mass planets in their habitable zone with the radial-velocity method (Quirrenbach et al., 2015; Reiners et al., 2018b); 324 have been presented by Reiners et al. (2018b), 3 did not have enough CARMENES observations at the time the spectral templates were being prepared for the study, and 9 are new spectroscopic binaries (Baroch et al., 2018). Here we investigate the photometric variability of these 336 M dwarfs and of G 34–23 AB (J01221+221AB), which Cortés-Contreras et al. (2017) found to be a close physical binary just before the GTOs started. This results in a final sample size of 337 stars.

As part of the full characterisation of the GTO sample, for each target we have collected all relevant information: astrometry, photometry, spectroscopy, multiplicity, stellar parameters, and activity, including X-ray count rates, fluxes, and hardness ratios, H $\alpha$  pseudo-equivalent widths, reported flaring activity, rotational velocities  $v \sin i$ , and rotational periods  $P_{\text{rot}}$  (Caballero et al., 2016). In particular, for 69 stars of the CARMENES GTO sample we had already collected rotation periods from the existing literature (e.g. Kiraga & Stepień, 2007; Norton et al., 2007; Hartman et al., 2011; Irwin et al., 2011; Kiraga, 2012; Suárez Mascareño et al., 2015; West et al., 2015; Newton et al., 2016, see below).

Of the 337 investigated stars, we were unable to collect or measure any photometric data useful for variability studies for only 3. In these three cases, the M dwarfs are physical companions at relatively small angular separations of bright primaries (J09144+526 = HD 79211, J11110+304 = HD 97101 B, and J14251+518 = θ Boo B). For the other 334 M dwarfs, we looked for peaks in the periodograms of two large families of light curves that we obtained (*i*) from wide-area photometric surveys and public databases, and (*ii*) with 20–80 cm telescopes at amateur and semi-professional observatories. A more detailed photometric survey of particular GTO targets is being carried out within the CARMENES consortium with more powerful telescopes, such as the Las Cumbres Observatory Global Telescope Network (Brown et al., 2013) and the Instituto de Astrofísica de Andalucía 1.5 m and 0.9 m telescopes at the Observatorio de Sierra Nevada. Results of this photometric monitoring extension will be published elsewhere.

In the first four columns of Table A.1 we give the Carmencita identifier (Caballero et al., 2016), discovery name, and 2MASS (Skrutskie et al., 2006) equatorial coordinates of the 337 M dwarfs investigated in this work.

<sup>1</sup> <http://carmenes.caha.es>

**Table 1.** Number of investigated light curves and basic parameters of used public surveys and observatories.

Survey	Location	Instrument configuration	Band	No. of light curves
MEarth	Mount Hopkins, USA	8 × Apogee U42	RG715, $I^a$	184
ASAS	Las Cumbres, Chile	Apogee AP10	$V$	174
SuperWASP	Roque de los Muchachos, Spain	8 × Andor DW436	clear, broad <sup>b</sup>	89
	Sutherland, South Africa		broad <sup>b</sup>	
NSVS	Los Álamos, USA	4 × Apogee AP10	clear <sup>c</sup>	86
Catalina	Mt. Lemmon/Mt. Bigelow, USA	variable <sup>d</sup>	$V_{\text{CSS}}$	37
ASAS-SN	worldwide <sup>e</sup>	FLI ProLine PL230	$V$	14
K2	(Earth-trailing heliocentric orbit)	0.95 m <i>Kepler</i> + 42 × CCD	clear	13
AstroLAB IRIS	Zillebeke, Belgium	0.68 m Keller + SBIG STL-6303E	$B, V$	7
Montcabrer	Cabril, Spain	0.30 m Meade LX200 + SBIG ST-8XME	$R, I$	6
HATNet	Mt. Hopkins, USA Mauna Kea, USA	5+2 × Apogee AP10 <sup>f</sup>	$R_C, I_C$	5
Montsec	San Esteban de la Sarga, Spain	0.80 m Joan Oró + MEIA2 <sup>g</sup>	$R_C$	4
Carda	Villaviciosa, Spain	0.20 m Celestron SC 8" + SBIG ST-7E	clear	3
Total				622

<sup>a</sup> MEarth: broad 715 nm long-pass filter in first (2008–2010) and third seasons (2011+), custom-made  $I_{715-895}$  interference filter in second season (2010–2011).

<sup>b</sup> SuperWASP: from 2006 onwards a broad-band filter was installed with a passband from 400 to 700 nm.

<sup>c</sup> NSVS: unfiltered optical response 450–1000 nm, effective wavelength of  $R$  band.

<sup>d</sup> Catalina: see Christensen et al. (2015) for the latest camera configurations.

<sup>e</sup> ASAS-SN: the network consists of 20 telescopes, distributed among five units in Hawai'i and Texas in the USA, two sites in Chile, and South Africa.

<sup>f</sup> HATNet: see Bakos (2018) for the latest camera configurations.

<sup>g</sup> Montsec: the MEIA2 instrument at the Telescopi Joan Oró on the Observatori Astronomic del Montsec consists of a camera iKon-L with an Andor CCD42-40 chip and a Custom Scientific filter wheel.

## 2.2. Photometric monitoring surveys

We searched for photometric data of our target stars, available through either VizieR (Ochsenbein et al., 2000) or, more often, the respective public web pages of the four main wide-area surveys listed below and summarised in the top part of Table 1.

– MEarth: The MEarth Project<sup>2</sup> (Nutzman & Charbonneau, 2008; Irwin et al., 2011). This consists of two robotically-controlled 0.4 m telescope arrays, MEarth-North at the Fred Lawrence Whipple Observatory on Mount Hopkins, Arizona, and MEarth-South telescope at the Cerro Tololo Inter-American Observatory, Coquimbo. The project monitors the brightness of about 2000 nearby M dwarfs with the goal of finding transiting planets (Berta et al., 2013; Dittmann et al., 2017), but it has also successfully measured rotation periods of M dwarfs (Irwin et al., 2009; Irwin et al., 2011; Newton et al., 2016). On every clear night and for about six months, each star is observed with a cadence of 20 min. In general we used data from three observing batches (2008–2010, 2010–2011, and 2011–2015) from the MEarth-North array ( $\delta = +20$  to  $+60$ ) provided by the fifth MEarth data release DR5, but we also used a few DR6 light curves (2011–2016).

– ASAS: All-Sky Automated Survey<sup>3</sup> (Pojmański, 2002). This is a Polish project devoted to constant photometric monitoring of the whole available sky (approximately 20 million stars brighter than  $V \sim 14$  mag). It consists of two observing stations in Las Cumbres Observatory, Chile (ASAS-3 from 1997 to 2010, ASAS-4 since 2010), and Haleakala Observatory, Hawai'i (ASAS-3N since 2006). Both are equipped with two wide-field instruments observing simultaneously in the  $V$  and  $I$  bands, and a set of smaller narrow-field telescopes and wide-field cameras. We used only the  $V$ -band ASAS-3 data for stars with  $\delta < +28$  deg observed between 1997 and 2006, which are available through the ASAS All Star Catalogue. In particular, we retrieved all light curves within a search radius of 15 arcsec, discarded all data points with C or D quality flags, and computed an average magnitude per epoch of the five ASAS-3 apertures weighted by each aperture magnitude error.

– SuperWASP: Super-Wide Angle Search for Planets<sup>4</sup> (Pollacco et al., 2006). The UK-Spanish WASP consortium runs two identical robotic telescopes of eight lenses each, SuperWASP-North at the Observatorio del Roque de los Muchachos, La Palma, and SuperWASP-South at the South African Astronomical Observatory, Sutherland. WASP has discovered over a hundred exoplanets through transit photometry (Collier Cameron et al., 2007; Barros et al., 2011). For our work, we down-

<sup>2</sup> <http://www.cfa.harvard.edu/MEarth>

<sup>3</sup> <http://www.astroww.edu.pl/asas>

<sup>4</sup> <http://www.superwasp.org>

loaded light curves of the first SuperWASP public data release (DR1 – Butters et al., 2010) from the Czech site<sup>5</sup>. The SuperWASP DR1 contains light curves for about 18 million sources in both hemispheres. Although the two robotic telescopes are still operational, DR1 only provided data collected from 2004 to 2008. The average number of data points per light curve is approximately 6700.

- NSVS: Northern Sky Variability Survey<sup>6</sup> (Woźniak et al., 2004). This was located at Los Álamos National Laboratory, New Mexico. The NSVS catalogue contains data from approximately 14 million objects in the range  $V = 8\text{--}15.5$  mag with a typical baseline of one year from April 1999 to March 2000, and 100–500 measurements for each source. In a median field, bright unsaturated stars have photometric scatter of about 20 mmag. It covered the entire northern hemisphere, and part of the southern hemisphere down to  $\delta = -28$  deg.

In addition to these four main catalogues, which accounted for a total of 533 light curves (86 %), we complemented our dataset with light curves compiled from the Catalina Surveys CSDR2<sup>7</sup> (Catalina; Drake et al., 2009; Drake et al., 2014), K2 (Howell et al., 2014), the All-Sky Automated Survey for Supernovae<sup>8</sup> (ASASSN; Kochanek et al., 2017), and the Hungarian-made Automated Telescope Network<sup>9</sup> (HATNet; Bakos et al., 2004; Bakos, 2018). None of our targets was in the catalogues of the *CoRoT* (Auvergne et al., 2009), *Kepler* (Borucki et al., 2010), or the Transatlantic Exoplanet Survey (TrES; Alonso et al., 2007) surveys. Finally, we did not use other wide surveys, such as Lincoln Near-Earth Asteroid Research (LINEAR; Stokes et al., 2000); XO (McCullough et al., 2005); Kilodegree Extremely Little Telescope (KELT; Pepper et al., 2007), which will soon have an extensive data release (J. Pepper, priv. comm.); HATSouth (Bakos et al., 2013); or the Asteroid Terrestrial-impact Last Alert System (ATLAS; Heinze et al., 2018), with the first data release published after collecting all light curves included in this work. All the public surveys used, amounting 602 light curves, are summarised in Table 1.

### 2.3. Our observations

For 20 GTO M dwarfs without data in public surveys or published periods, or with unreliable or suspect periods in the existing literature (e.g. short  $P_{\text{rot},\text{lit}}$  but low  $v \sin i$  and faint H $\alpha$  emission, or vice versa), we made our own observations in collaboration with amateur and semi-professional astronomical observatories in Spain and Belgium: Carda<sup>10</sup> (MPC Z76) in Asturias, Montcabrer<sup>11</sup> (MPC 213) and Montsec<sup>12</sup> in Barcelona (MPC C65), and AstroLAB IRIS<sup>13</sup> near Ypres. Most of our targets had northern declinations,

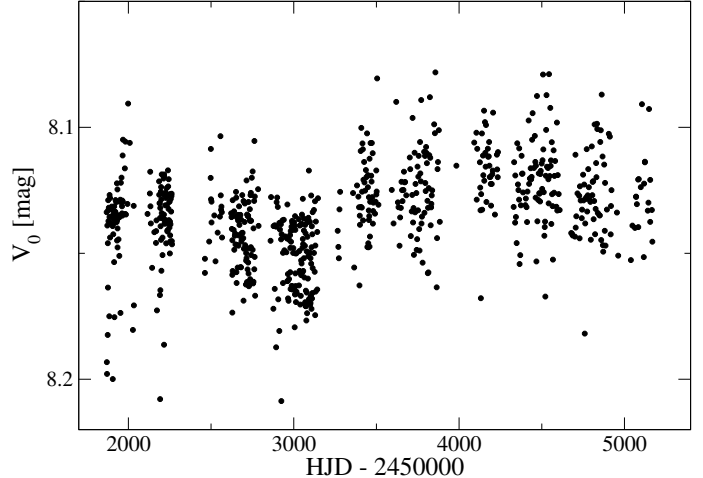


**Fig. 1.** ASAS  $V$ -band photometric data for the M0.5 V star J06105-218 = HD 42581A. It may display an activity cycle modulation with  $P_{\text{cycle}} \sim 8.3$  a superimposed to a rotation period  $P_{\text{rot}} = 27.3$  d (the modulation in the light curve of J15218+209 is similar).

which suitably fit the geographical latitudes of our observatories (between +41.5 deg and +50.8 deg).

The cadence of observations for each target was either continuous every night or just one observation per night during a long run, depending on rule-of-thumb estimations of their rotation periods based on literature values of rotational velocity and H $\alpha$  emission. Exposure times varied widely, from a few seconds to several minutes. We took special care to select enough reference stars with stable light curves and relatively red  $J - K_s$  colours within the respective fields of view (f.o.v.; variable from  $12.3 \times 12.3$  arcmin $^2$  to  $43 \times 43$  arcmin $^2$ ).

For the image reduction and light-curve generation, we used standard calibration procedures (bias and flat-field correction) and widely distributed software such as MaxIm<sup>14</sup>, AstroImageJ<sup>15</sup> (Collins et al., 2017), FotoDif<sup>16</sup>, and LesvePhotometry<sup>17</sup> with parameters appropriate for each observatory, atmospheric condition, and star brightness (see again Table 1).

### 3. Analysis

We searched for significant signals in the periodograms of the 622 light curves compiled or obtained by us as described in Section 2. Prior to this, we cleaned our light curves by discarding outlying data points caused by the combination of target faintness and sub-optimal weather. Some of our M dwarfs could also undergo flaring activity (most flares in our light curves are difficult to identify because of the typical low cadence). We used the same cleaning procedure as Suárez Mascareño et al. (2015, 2016), rejecting iteratively all data points that deviated more than  $2.5\sigma$  from the mean magnitude (which might eventually bias the amplitude of the variations).

<sup>5</sup> <http://wasp.cerit-sc.cz>

<sup>6</sup> <https://skydot.lanl.gov/nsvs/>

<sup>7</sup> <https://catalina.lpl.arizona.edu>

<sup>8</sup> <http://www.astronomy.ohio-state.edu/asassn/>

<sup>9</sup> <https://hatnet.org/>

<sup>10</sup> <http://www.auladeastronomia.es/>

<sup>11</sup> <http://cometas.sytes.net>

<sup>12</sup> <http://www.oadm.cat>

<sup>13</sup> <http://astrolab.be>

<sup>14</sup> <http://diffractionlimited.com/product/maxim-dl/>

<sup>15</sup> <http://www.astro.louisville.edu/software/astroimagej/>

<sup>16</sup> <http://www.astrosurf.com/orodeno/fotodif/>

<sup>17</sup> <http://www.dpobservatory.net/AstroPrograms/Software4VSObservers.php>

**Table 2.** Cycle periods obtained for stars in our sample.

Karmn	Name	$P_{\text{cycle}}$ [a]	FAP [%]	$A_{\lambda}$ [mag]	Survey	$P_{\text{cycle,lit}}$ [a]	FAP <sub>lit</sub> [%]	$A_{\lambda,\text{lit}}$ [mag]	Ref. <sup>a</sup>
J06105-218	HD 42581 A	$8.3 \pm 3.1$	$< 10^{-4}$	0.026	ASAS	$8.4 \pm 0.3$	$< 0.1$	0.0128	SM16
J07361-031	BD-02 2198	$11.5 \pm 1.9$	$< 10^{-4}$	0.035	ASAS	...	...	...	...
J08161+013	GJ 2066	$4.1 \pm 0.7$	$< 10^{-4}$	0.012	ASAS	...	...	...	...
J10122-037	AN Sex	$3.2 \pm 0.4$	$< 10^{-4}$	0.020	ASAS	...	...	...	...
J11477+008	FI Vir	$4.5 \pm 2.0$	0.15	0.012	ASAS	$4.1 \pm 0.3$	1.7	0.0071	SM16
J15218+209	OT Ser	$6.5 \pm 0.8$	$< 10^{-4}$	0.055	ASAS	...	...	...	...
J16303-126	V2306 Oph	$3.9 \pm 1.0$	$< 10^{-4}$	0.014	ASAS	$4.4 \pm 0.2$	$< 0.1$	0.0083	SM16
J19169+051N	V1428 Aql	$3.3 \pm 0.4$	$< 10^{-4}$	0.013	ASAS	$9.3 \pm 1.9$	$< 0.1$	0.0077	SM16
J19346+045	BD+04 4157	$3.0 \pm 0.8$	$< 10^{-4}$	0.013	ASAS	...	...	...	...
J22532-142	IL Aqr	$4.5 \pm 0.7$	$< 10^{-4}$	0.013	ASAS	...	...	...	...

<sup>a</sup> Reference – SM16: Suárez Mascareño et al. (2016).

The last six columns of Table A.1 show the corresponding survey, number of data points  $N_{\text{obs}}$  before and after the cleaning, time interval length  $\Delta t$  between first and last visit, mean  $\bar{m}$  and standard deviation  $\sigma_m$  of the individual magnitudes, and mean error  $\delta m$ . See Section 4.4 for a discussion on the variation of  $\sigma_m$  as a function of  $\bar{m}$ , and the possibility of finding aperiodic or irregular variable stars in our data.

Next, we used the Lomb–Scargle (LS) periodogram (Scargle, 1982) with the `peranso` analysis software (Paunzen & Vanmunster, 2016), which implements multiple light-curve and period analysis functions. We evaluated the significance of the signals found in the periodograms with the Cumming (2004) modification of the Horne & Baliunas (1986) formula. In this way, the false alarm probability (FAP) becomes

$$FAP = 1 - [1 - p(z > z_0)]^M, \quad (1)$$

with  $p(z > z_0)$  being the probability that  $z$ , the target spectral density, is greater than  $z_0$ , the measured spectral density; and  $M$  the number of independent frequencies. In our case,  $p(z > z_0) = e^{-z_0}$ , where  $z_0$  is the peak of the hypothetical signal;  $M = \Delta t \Delta f$ , where  $\Delta t$  is the time baseline,  $\Delta f = f_2 - f_1$ ; and  $f_2$  and  $f_1$  are the maximum and minimum search frequencies, respectively. The `peranso` software also measures amplitudes of light curves.

We searched for significant frequencies with FAP  $< 2\%$  and within the standard frequency interval. On the one hand, we set the highest frequency at the Nyquist frequency to about half of the minimum time interval between consecutive visits (from  $f \sim 100 \text{ d}^{-1}$  for some of our intensive campaigns to  $f \sim 1 \text{ d}^{-1}$  for most of the public-survey light curves). On the other hand, we set the lowest frequency at half the length of the monitoring (typically  $f \sim 0.005 \text{ d}^{-1}$ ). Only in the case of ASAS, the public survey with the longest time baseline (up to ten years), did we search for low frequencies down to  $0.0005 \text{ d}^{-1}$ . For stars with significant signals shorter than 2 d we used a significant frequency oversampling ( $\sim 10\times$ ). When a periodogram displayed several significant peaks, we paid special attention to identifying aliases and picked up the strongest signal with astrophysical meaning (e.g. with  $P_{\text{rot}}$  consistent with existing additional information on the star, especially its rotational velocity,  $v \sin i$ ; see Section 4.3). Figures B.1 to B.9 illustrate our analysis with one representative example of a raw stellar

light curve and corresponding LS periodogram and phase-folded light curve for each dataset with identified period.

There is a justified concern in the literature about the use of the LS periodogram for period determination (e.g. McQuillan et al., 2013). As a result, for the light curves of stars classified as new spectroscopic binaries by Baroch et al. (2018), with K2 data, or with periods shorter than 1 d, or different by more than 10 % from those in the literature (see Section 4.1) we also applied the generalised LS periodogram method (GLS; Zechmeister & Kürster, 2009).

For the spectroscopic binaries and K2 stars, we additionally applied the Gaussian process regression (GP; Rasmussen & Williams, 2005) with the `celerite` package (Foreman-Mackey et al., 2017). To build a celerity model for our case, we defined a covariance/kernel for the GP model, which consisted of a stochastically-driven damped oscillator and a jitter term (Angus et al., 2018). We then wrapped the kernel defined in this way in the GP and computed the likelihood. In all investigated cases except two, the GLS and GP periods were identical within their uncertainties to the LS periods computed with `peranso`. The only two significant differences were J18356+329, for which GLS did not recover  $P_{\text{rot}} = 0.118 \text{ d}$ , the shortest period in our sample and identical to that reported by Hallinan et al. (2008), and J16254+543, for which GLS found  $P_{\text{rot}} = 76.8 \text{ d}$ , a value similar to that in the literature (Suárez Mascareño et al., 2015), but for which the LS algorithm found  $100 \pm 5 \text{ d}$ .

In Table A.2 we show the periods, amplitudes, FAPs, and corresponding surveys of 142 M dwarfs. When available, we show the GLS periods. We tabulate the uncertainty in  $P_{\text{rot}}$  from the full width at half maximum of the corresponding peak in the periodogram (Schwarzenberg-Czerny, 1991). For GLS periods, we tabulate formal uncertainties, which are significantly smaller than the real ones.

When several datasets are available, and even though the periodogram peaks are detected in both, we list the  $P_{\text{rot}}$  of the dataset with the lowest FAP. For the sake of completeness, Table A.2 includes five stars with FAP = 2–10 % for which we recover periods similar to those previously published (Testa et al., 2004; Suárez Mascareño et al., 2015, 2016), but which did not pass our initial FAP criterion. One such period is for J11477+008 = FI Vir, for which Suárez Mascareño et al. (2016) reported a rotation period of 165 d consistent with ours. Its K2 light curve, which spans

**Table 3.** Stars with published rotation periods not recovered in this work.

Karmn	Name	$P_{\text{rot,lit}}$ [d]	Ref. <sup>a</sup>
J03133+047	CD Cet	126.2	New16
J05019-069	LP 656-038	88.5	Kir12
J07274+052	Luyten's star	115.6±19.4	SM15
J09003+218	LP 368-128	0.439	New16
J09360-216	GJ 357	74.3±1.7	SM15
J11033+359	Lalande 21185	48.0	KS07
J13299+102	BD+11 2576	28 ± 2.9	SM15
J11421+267	Ross 905	39.9	SM15
J13457+148	HD 119850	52.3±1.7	SM15
J14010-026	HD 122303	43.4	SM16
J15194-077	HO Lib	132±6.3	SM15
J17578+046	Barnard's star	130	KS07
J18051-030	HD 165222	127.8±3.2	SM15
J22096-046	BD-05 5715	39.2±6.3	SM15

<sup>a</sup> References: KS07: Kiraga & Stepień (2007); Har11: Hartman et al. (2011); Kir12: Kiraga (2012); SM15: Suárez Mascareño et al. (2015); New16: Newton et al. (2016); SM16: Suárez Mascareño et al. (2016).

only 80 d, shows a clear modulation that matches such a long period, the longest one reported by us. Something similar occurs with J13458-179 = LP 798-034, whose K2 light curve shows a 20 mmag peak-to-peak modulation of about three months. We did not find any periods in the existing literature or our ASAS data for this star, which is not listed in Table A.2.

We also looked for long-period cycles in ASAS light curves of stars with identified  $P_{\text{rot}}$  and time baseline  $\Delta t \approx 9$  a. Ten stars have significant signals at  $P_{\text{cycle}} \geq 3.0$  a, and are listed in Table 2. Two of these (J06105-218 and J15218+209) have cycle periods longer than half  $\Delta t$ , and one has a cycle period even longer than the full  $\Delta t$ , but its modulation is very clear (see Fig. 1). Curiously, the star with the longest rotation period and highest FAP, J11477+008, also displays a long-term activity cycle. This flaring M4 dwarf is also the star with the smallest ratio  $P_{\text{cycle}}/P_{\text{rot}} \sim 10$ .

Of the ten values of  $P_{\text{cycle}}$  shown in Table 2, six are new, three are identical within their uncertainties to previous determinations by Suárez Mascareño et al. (2016), and one is revised from 9.3 a to about 3.3 a. There are two additional stars, not listed in Table 2, with significant signals ( $\text{FAP} < 2\%$ ) at 2–3 a, but without identified or reported rotation periods (J06371+175 and J22559+178). It may be that they truly display a long-term modulation overlaid on a low-amplitude rotation period not detected yet, as they could be pole-on.

## 4. Results and discussion

### 4.1. Rotation periods

Of the 142 stars with periods in Table A.2, 69 (49 %) had rotation periods previously reported in the existing literature and tabulated in Carmencita (Caballero et al., 2016); see Table A.2 for full references. Therefore, we present 73 new photometric periods of M dwarfs in this study. This

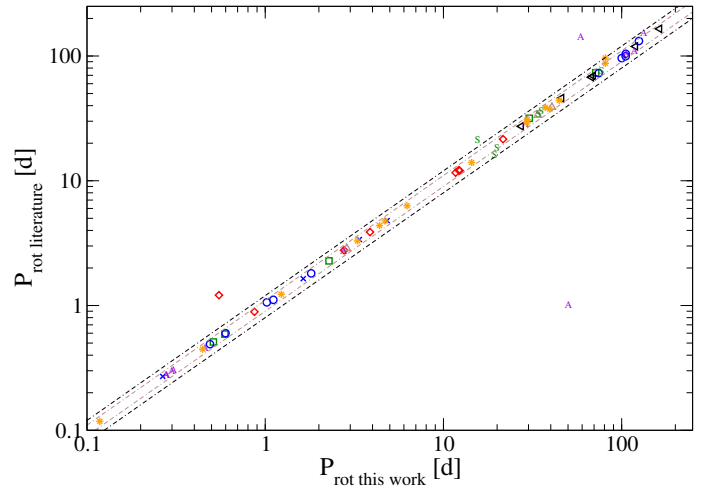


**Fig. 2.** Periods from the literature  $P_{\text{rot,lit}}$  as a function of our period,  $P_{\text{rot},\text{thiswork}}$ , for stars with previously published rotation periods. Dashed lines show 10 % and 20 % deviations from the 1:1 relation. Different symbols and colours stand for the literature source: blue crosses: Norton et al. (2007); green squares: Hartman et al. (2011); blue circles: Irwin et al. (2011); red diamonds: Kiraga (2012); brown up-triangles: Kiraga & Stepień (2007); black left-triangles: Suárez Mascareño et al. (2016); violet A's: Newton et al. (2016); green S's: Mascareño et al. (2018); orange asterisks: Greimel & Robb (1998), Fekel & Henry (2000), Testa et al. (2004), Rivera et al. (2005), Hallinan et al. (2008), Kiraga & Stepień (2013), Suárez Mascareño et al. (2015), West et al. (2015), David et al. (2016), Cloutier et al. (2017), Vida et al. (2017), Lothringer et al. (2018).

number is comparable to the number of new rotation periods of M dwarfs reported by Norton et al. (2007), Irwin et al. (2011), and Suárez Mascareño et al. (2016), but is far lower than other more comprehensive searches by Hartman et al. (2011), Kiraga (2012), and Newton et al. (2017). However, there is a fundamental difference in the samples; ours exclusively contains bright, nearby M dwarfs that are targets of dedicated exoplanet surveys. In particular, the mean  $J$ -band magnitude and heliocentric distance of our CARMENES GTO sample are only 7.7 mag and 11.6 pc (cf. Caballero et al., 2016), much brighter and closer than any M dwarf sample photometrically investigated previously.

We were not able to recover the rotation periods of 14 stars reported by Kiraga & Stepień (2007), Kiraga (2012), Suárez Mascareño et al. (2015), and Newton et al. (2016), and listed in Table 3. In most of these cases, unrecovered published  $P_{\text{rot,lit}}$  values were long, of low significance, and came from low-cadence, relatively noisy, ASAS data.

In Fig. 2 we compare the rotation periods that we found and those reported in the existing literature for the 69 stars in common. Except for four discordant stars, the agreement is excellent, with maximum deviations rarely exceeding 10 %, and with virtually all values identical within their uncertainties. There are four outliers with deviations between  $P_{\text{rot,lit}}$  and  $P_{\text{rot},\text{thiswork}}$  larger than 20 %:

- J00051+457 = GJ 2. A rotation period of 21.2 d was previously measured by Suárez Mascareño et al. (2015) from a series of high-resolution spectroscopy of activity

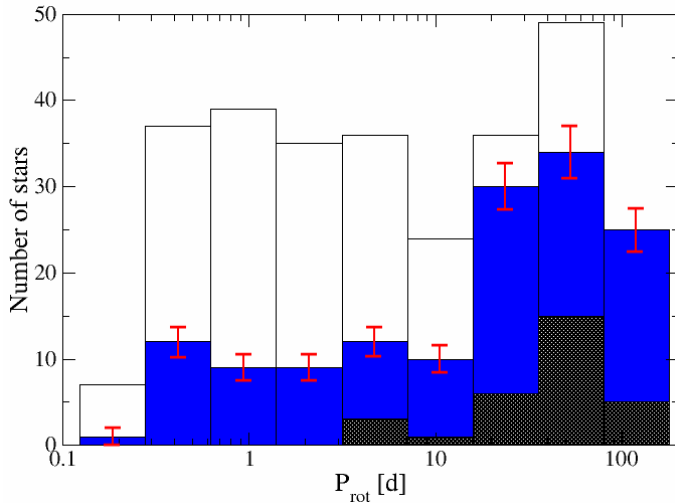


**Fig. 3.** Distribution of rotation periods in our work (shaded, with Poissonian uncertainties) and in Carmencita (white). Rotation periods found with ASAS are shaded darker. The size of the bins follows the definitions given by Freedman & Diaconis (1981). Compare with Fig. 3 in Newton et al. (2016).

indicators, while we measure 15.37 d on an ASAS light curve;

- J16570–043 = LP 686–027. This is an active, ‘RV-loud star’ ( $\text{pEW}(\text{H}\alpha) = -4.2 \pm 0.1 \text{ \AA}$  and  $v \sin i \approx 10.1 \text{ km s}^{-1}$  (Jeffers et al., 2018; Reiners et al., 2018b; Tal-Or et al., 2018). Our analysis of the ASAS data reproduced the 1.21 d period of Kiraga (2012), but with an FAP  $\gg 5\%$ . However, our analysis of NSVS data, with  $\sim 4$  more epochs and a baseline  $\sim 9$  times longer than ASAS, resulted in a shorter  $P_{\text{rot}} \sim 0.55$  d with a lower FAP = 1.4%;
- J18363+136 = Ross 149. We found two significant signals in our ASAS data of roughly the same power at 1.02 d and 50.2 d, which are aliases of one another. The first period is identical to  $P_{\text{rot,lit}} = 1.017$  d discovered by Newton et al. (2016) in MEarth data. However, we tabulate the 50.2 d period based on the very slow rotation velocity of the star ( $v \sin i < 2 \text{ km s}^{-1}$ ; Reiners et al. 2018b);
- J20260+585 = Wolf 1069. Newton et al. (2016) reported a possible or uncertain period of 142.09 d. With MEarth data, we found instead a signal at 59.0 d. However, neither of the two signals is visible in the SuperWASP dataset.

#### 4.2. Period distribution

Using MEarth data, Newton et al. (2016) reported that the distribution of M-dwarf rotation periods displays a lack of stars with intermediate rotation periods around 30 d. This lack at intermediate periods could be understood as a bimodal  $P_{\text{rot}}$  distribution, with peaks at 0.5–2 d and 50–100 d, and a valley in between. While there is a significant overabundance of periods larger than 30 d in our sample, as illustrated in Fig. 3, the distribution of periods shorter than 30 d (and longer than 0.5 d) is flat within Poissonian statistics. Therefore, we see only one wide peak in the period distribution at  $P_{\text{rot}} = 20$ –120 d or, conversely, a lack

of stars with intermediate and short rotation periods  $P_{\text{rot}} = 0.6$ –20 d. However, rather than contradicting the results presented by Newton et al. (2016), we attribute the lack of short periods to the different temporal sampling of the surveys used (see below). The authors also stated that the rotators with the highest quality grade were biased towards such short periods, while the sparse temporal sampling of most surveys used here (excluding SuperWASP and MEarth) prevented us from detecting periods of a few days. If the available periods for the  $\sim 2200$  Carmencita stars are taken into account (cf. Fig. 3), the peak at  $P_{\text{rot}} = 20$ –120 d becomes much less apparent, and the period distribution is rather flat from 0.6 d to 8 d, approximately. There might be a dip at  $P_{\text{rot}} = 8$ –20 d.

Regarding survey sampling, we analysed the distribution of time elapsed between consecutive exposures of our light curves. The SuperWASP distribution has two peaks, one very narrow at slightly less than one minute (the CCD read-out time) and another wider peak, centred at 10–20 min, a bit more optimistic than the 40 min stated by Pollacco et al. (2006). The NSVS distribution also has two peaks, one at around 1 min and the other at 1 d, much wider and sparser than SuperWASP and with a baseline of only one year (Woźniak et al., 2004). Together with SuperWASP, the MEarth dataset is, with a field cadence of between 15 and 40 min ( $\sim 20$  min according to Irwin et al. 2011) and ‘sequentially for the entire time [that] they are above airmass 2’, the most appropriate one for sampling the  $P_{\text{rot}} = 0.6$ –20 d interval. The ASAS sampling is much poorer than the other three main surveys, with a peak of the distribution centred at around one week. The nominal sampling value of 2 d (Pojmański, 2002) is attained only for some bright stars and during a fraction of the observing time. However, the sampling strategy and the very long duration of the ASAS survey, of several years, makes it excellent for searching for periods longer than 20 d.

This partly explains the apparent lack of rotation periods in the range between 0.6 and 20 d of GTO stars with respect to Carmencita stars in Fig. 3. Our GTO stars are brighter than the rest of the Carmencita stars (Alonso-Floriano et al., 2015a) so the observed lack of shorter periods in our sample is probably caused by the inclusion of bright ASAS targets, combined with the observational cadence of ASAS, which is optimised towards detecting long periods. We thus have a combination of a Malmquist bias and a sampling effect.

A larger (volume- or magnitude-limited) sample of M dwarfs with a homogeneous, denser, longer monitoring could be needed to settle the question if there is a real lack of rotation periods between 0.6 d or 8 d and 20 d at low stellar masses. We may have to wait for the 8.4 m Large Synoptic Survey Telescope, which will monitor the entire available sky every three nights on average.

#### 4.3. Activity

##### 4.3.1. RV-loud stars

A comprehensive study linking rotational velocity, H $\alpha$  emission, and rotation periods of M dwarfs was already presented by Jeffers et al. (2018) in a previous publication of this series. Using different tracers of magnetic activity, it can be seen that the rotational velocity increases with M-dwarf activity until saturation in rapid rotators (Stauffer et

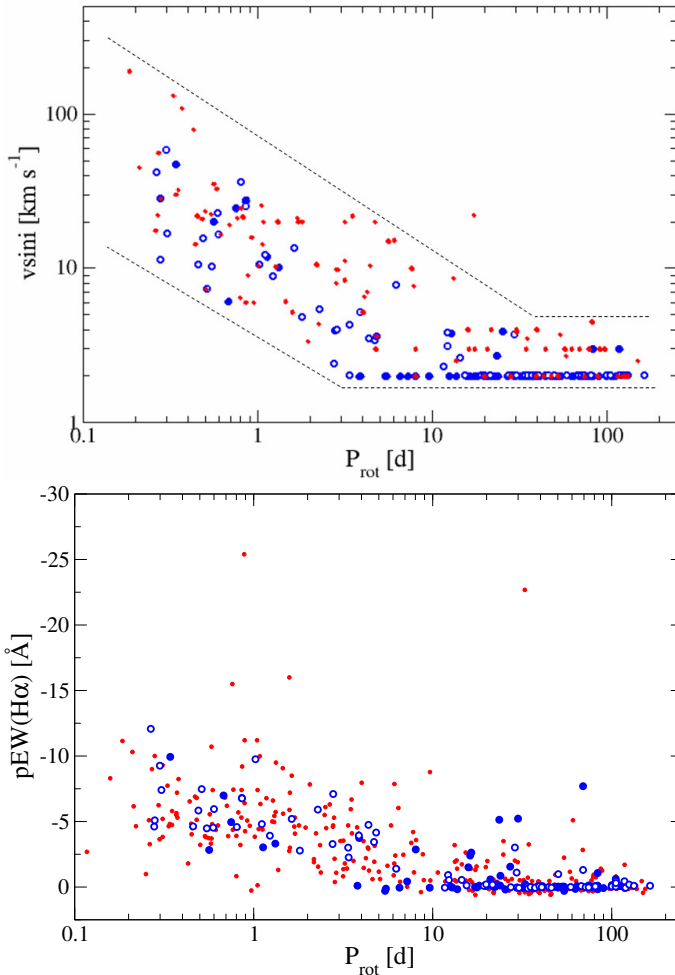


**Fig. 4.**  $v \sin i$  vs.  $P_{\text{rot}}$  (top panel) and pEW(H $\alpha$ ) vs.  $P_{\text{rot}}$  (bottom panel) for stars with new (blue filled circles) and re-computed rotation periods in this study (blue open circles) and stars in Carmencita with previously published rotation periods (red dots). In the top panel, the dotted lines indicate the lower and upper envelopes of the  $v \sin i$ - $P_{\text{rot}}$  relation, and most of the values at  $v \sin i = 2$  or  $3 \text{ km s}^{-1}$  are upper limits. Compare with Figs. 6 and 8 in Jeffers et al. (2018). Here we present 154 new or improved  $v \sin i$ - $P_{\text{rot}}$  and pEW(H $\alpha$ )- $P_{\text{rot}}$  pairs, with periods from this work and velocities and H $\alpha$  equivalent widths from Reiners et al. (2018b). Outlier stars in both panels are discussed in the text.

al., 1984; Hawley et al., 1996; Delfosse et al., 1998; Kiraga & Stepień, 2007; Mohanty & Basri, 2003; Reiners et al., 2009; Browning et al., 2010; Newton et al., 2017, and references therein).

As a complement to these studies, we present the following brief discussion on the rotation periods of the most active stars in our sample, most of which were tabulated by Tal-Or et al. (2018). They presented a list of 31 RV-loud stars: CARMENES GTO M-dwarf targets that displayed large-amplitude radial-velocity variations due to activity. Most of these stars, close to activity saturation, were also part of the investigation on wing asymmetries of H $\alpha$ , Na I D, and He I lines in CARMENES spectra by Fuhrmeister et al. (2018). We found rotation periods from photometric time series for all of them except

for nine stars<sup>18</sup>, which are either extremely active (e.g. Barta 161 12, LP 022–420), too faint and late for the surveys used (e.g. vB 8, 2MASS J20091824–0113377), or both (e.g. LSPM J1925+0938). The most active of these nine stars without an identified period could actually be variable, but irregular (see below).

As expected from their typically large  $v \sin i$  values, most of the other 22 RV-loud stars have short or very short rotation periods: 20 stars have  $P_{\text{rot}} < 10 \text{ d}$ , and 11 have  $P_{\text{rot}} < 1 \text{ d}$ . The list of RV-loud stars with identified periods contains some very well-known variable stars, such as V388 Cas, V2689 Ori, YZ CMi, DX Cnc, GL Vir, OT Ser, V1216 Sgr, V374 Peg, EV Lac, and GT Peg. However, there are three such RV-loud stars for which there was no published value of rotation period. Of these, two have identified periods shorter than one day: J02088+494 = G 173–039 ( $P_{\text{rot}} = 0.748 \text{ d}$ ) and J04472+206 = RX J0447.2+2038 ( $P_{\text{rot}} = 0.342 \text{ d}$ ). They both have high rotational velocities of  $v \sin i \approx 24$ – $48 \text{ km s}^{-1}$  (Reiners et al., 2018a; Tal-Or et al., 2018). The third star without a previously reported rotation period is J19169+051S = V1298 Aql (vB 10,  $P_{\text{rot}} = 23.6 \text{ d}$ ), which has a slow rotational velocity of only  $2.7 \text{ km s}^{-1}$ , but it does have an M8.0 V spectral type (Alonso-Floriano et al., 2015a; Kaminski et al., 2018) and has long been known to display variability of up to 0.2 mag peak-to-peak in  $V$  band (Herbig, 1956; Liebert et al., 1978).

The 31 RV-loud stars in Tal-Or et al. (2018) are not the only CARMENES GTO M-dwarf targets that display large-amplitude radial-velocity variations due to activity, as all stars with ten or fewer observations during the first 20 months of operation were discarded from the study. In total, 46 stars in our sample have rotation periods shorter than  $10 \text{ d}$ , and 19 shorter than  $1 \text{ d}$ . Of the latter, only seven were not tabulated as RV-loud stars by Tal-Or et al. (2018): four M4.0–5.5 dwarfs with previously reported rotation period and  $v \sin i > 16 \text{ km s}^{-1}$ , the strong X-ray emitter RBS 365 (J02519+224, M4.0 V,  $v \sin i = 27.4 \pm 0.6 \text{ km s}^{-1}$ ), the  $\beta$  Pictoris moving group candidate 1RXS J050156.7+010845 (J05019+011, M4.0 V,  $v \sin i = 6.1 \pm 0.9 \text{ km s}^{-1}$ ; see Alonso-Floriano et al. 2015b and references therein), and the unconfirmed close astrometric binary G 34–23 AB (J01221+221 AB; not in the GTO sample, see Section 2). Because of the magnitude difference between the two components in the pair ( $\Delta I = 0.86 \pm 0.12 \text{ mag}$  according to Cortés-Contreras et al. 2017) the most likely variable is the primary, G 34–23 A. New analyses of RV scatter and activity of CARMENES GTO stars, including the other six single stars just described and the three RV-loud stars with new periods described above, most of them with  $P_{\text{rot}} < 1 \text{ d}$ , are ongoing and will be presented elsewhere.

#### 4.3.2. Linking $P_{\text{rot}}$ , $v \sin i$ , H $\alpha$ , and $A$

We go deeper into the  $P_{\text{rot}}$ - $v \sin i$  discussion with the top panel in Fig. 4. To build this plot we took 305 rotation periods and rotation velocities from the existing literature and compiled in the Carmencita catalogue (see references

<sup>18</sup> J01352–072 = Barta 161 12, J09449–123 = G 161–071, J12156+526 = StKM 2–809, J14173+454 = RX J1417.3+4525, J15499+796 = LP 022–420, J16555–083 = vB 8, J18189+661 = LP 071–165, J19255+096 = LSPM J1925+0938, and J20093–012 = 2MASS J20091824–0113377.

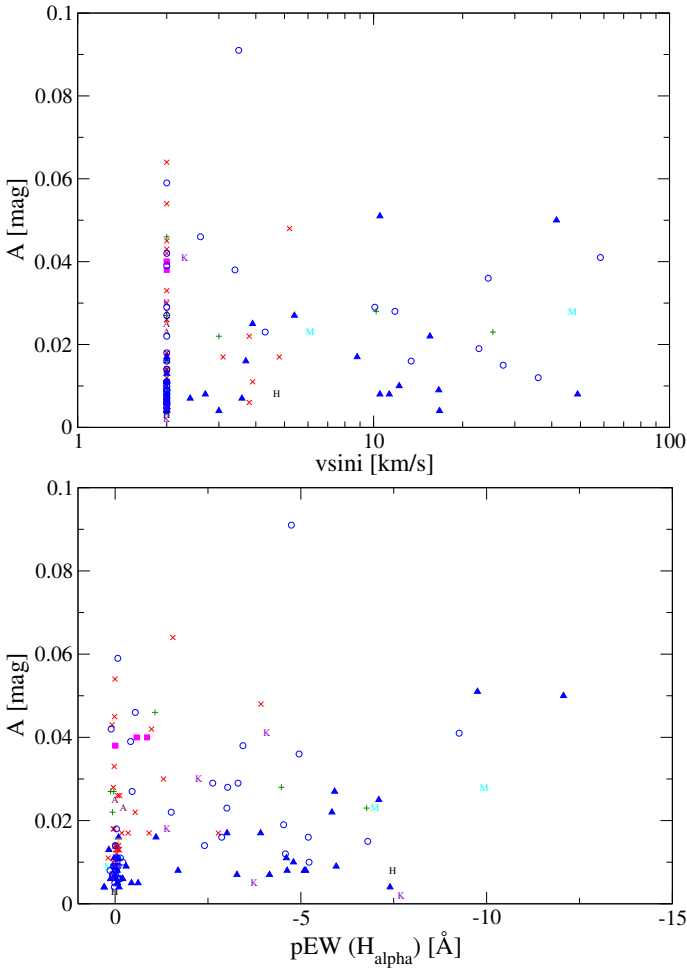


**Fig. 5.** Our amplitude of photometric variability as a function of  $v \sin i$  (top panel) and pEW(H $\alpha$ ) (bottom panel). Red crosses: ASAS data, blue triangles: MEarth, blue open circles: SuperWASP, green pluses: NSVS, magenta squares: AstroLAB IRIS, maroon C's: ASAS-SN, black H's: HATNet, violet K's: K2, cyan M's: Montcabrer, orange T's: Montsec.

in Section 2.1). As expected and widely discussed by West et al. (2015) and Jeffers et al. (2018), among others, the shorter the rotation period  $P_{\text{rot}}$  of an M dwarf, the higher the rotation velocity  $v \sin i$ . The vertical width is due to the indetermination in inclination angle  $i$  and the spread in spectral types, and thus stellar radii  $R$  according to the formula

$$v \sin i = \frac{2\pi R \sin i}{P_{\text{rot}}} \quad (2)$$

We can outline conservative lower and upper envelopes of the  $P_{\text{rot}}-v \sin i$  relation. The horizontal regime at long periods and low rotational velocities is due to the instrumental limit in determining  $v \sin i$  from high-resolution spectra, not to any real astrophysical effect on the stars.

<sup>19</sup>

<sup>19</sup> An ultra-high-resolution spectrograph of  $\mathcal{R} \gtrsim 200,000$  at an 8 m-class telescope would be needed to measure rotational velocities of a large sample of M dwarfs with an accuracy of  $1 \text{ km s}^{-1}$  (Reiners et al., 2018b).

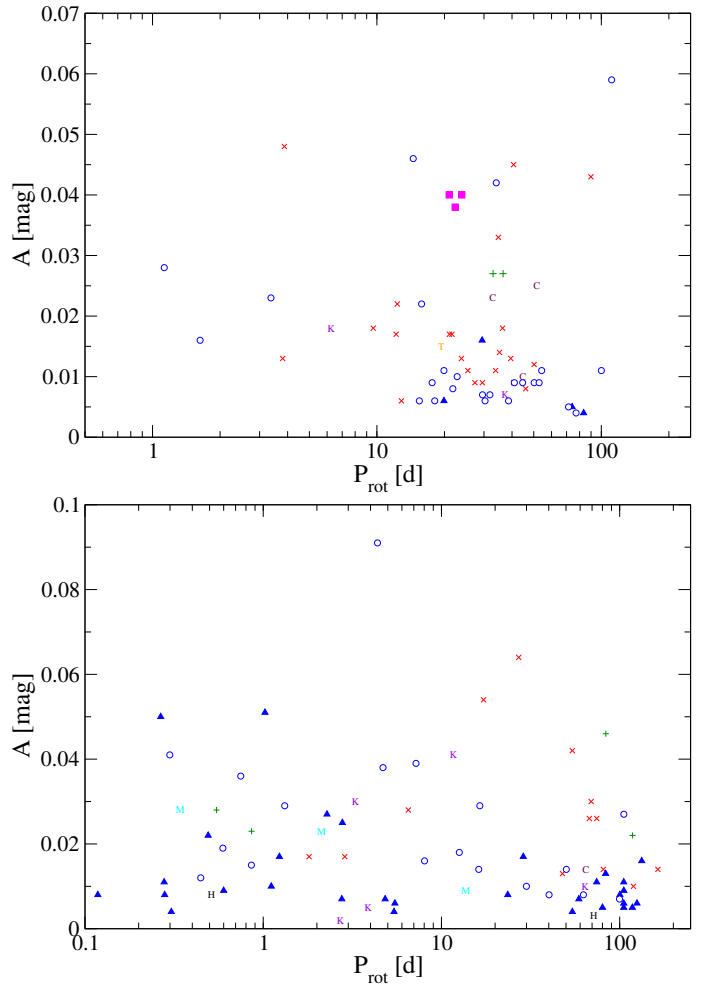


**Fig. 6.** Our amplitude of photometric variability as a function of rotation period for M0.0 – M3.0 V stars (top panel) and M3.5 – M8.5 V stars (bottom panel). Same symbol legend as in Fig. 5.

In our plot there is only one outlier, G 131–047 AB (J00169+200 AB), which has  $P_{\text{rot}} = 17.3$  d from West et al. (2015) and  $v \sin i = 22 \text{ km s}^{-1}$  from Mochnacki et al. (2002). The star, a non-GTO star from Carmencita, is another unconfirmed close astrometric binary with components separated by only 1.08 arcsec (Cortés-Contreras et al., 2017), so it might also be a double-line spectroscopic binary. A double narrow cross-correlation function could appear to Mochnacki et al. (2002) as a single wide function, which would explain the high rotational velocity for its rotation period. In any case, our plot will be a reference for future studies of the  $P_{\text{rot}}-v \sin i$  relation, as we used the most precise values of rotational velocities (Reiners et al., 2018b) and of rotation periods (this study), together with an exhaustive compilation of data for nearby bright M dwarfs.

In the bottom panel of Fig. 4 we also link our rotation periods and those compiled in Carmencita with the corresponding pseudo-equivalent widths of the H $\alpha$  line, pEW(H $\alpha$ ), possibly the most widely used activity indicator in low-mass stars. From the plot, again, the shorter the rotation period, the stronger the H $\alpha$  emission (cf. Jeffers et al., 2018). And again, there are outliers. The most remarkable ones, with  $\text{pEW(H}\alpha\text{)} < -20 \text{ \AA}$ , are J07523+162 = LP 423-031 and J08404+184 = AZ Cnc. They just dis-

played well-documented flaring activity during their spectroscopic observations (Haro & Chavira, 1966; Jankovics et al., 1978; Dahn et al., 1985; Shkolnik et al., 2009; Reiners & Basri, 2010; Alonso-Floriano et al., 2015a). Other stars at the outer boundary of the general distribution have either moderate flaring activity (slightly larger  $|p\text{EW}(\text{H}\alpha)|$  for their  $P_{\text{rot}}$ ) or early M spectral types (slightly smaller  $|p\text{EW}(\text{H}\alpha)|$  for their  $P_{\text{rot}}$ ).

We searched for correlations between amplitude  $A$  and  $P_{\text{rot}}$ ,  $v \sin i$ , and  $p\text{EW}(\text{H}\alpha)$ , as illustrated in Figs. 5 and 6. However, contrary to our expectations, we did not find that the most active stars (fastest rotators, strongest  $\text{H}\alpha$  emitters) always have the largest photometric amplitudes. For example, the star with the largest amplitude measured in our sample,  $A_{\text{SuperWASP}} = 0.091$  mag, is the most strongly active star J22468+443 = EV Lac (Pettersen et al., 1984; Favata et al., 2000; Zhilyaev et al., 2000; Osten et al., 2005, 2010), while the star with the third largest amplitude,  $A_{\text{SuperWASP}} = 0.059$  mag, is J14257+236W = BD+24 2733A, a relatively inactive M0.0 V star with  $P_{\text{rot}} \approx 111$  d,  $v \sin i < 2 \text{ km s}^{-1}$ , and absent  $\text{H}\alpha$  emission (Maldonado et al., 2017; Reiners et al., 2018b; Jeffers et al., 2018).

Previous works have investigated the relation between  $A$  and  $P_{\text{rot}}$ . Hartman et al. (2011) found no correlation for K and early to mid M dwarf stars if  $P_{\text{rot}} < 30$  d, and an anti-correlation if  $P_{\text{rot}} > 30$  d. They found no correlation for mid to late M dwarfs. Newton et al. (2016) analysed the MEarth sample in two groups,  $0.25M_{\odot} < M < 0.5M_{\odot}$  and  $0.08M_{\odot} < M < 0.25M_{\odot}$ , and found an anti-correlation  $A - P_{\text{rot}}$  in the first group and no correlation in the second group. We repeated the same exercise separating our sample in early to mid (M0.0 – 3.0 V;  $N=63$ ) and mid to late (M3.5 – 8.5 V;  $N=78$ ) stars (Fig. 6). We performed a Spearman rank correlation analysis and obtained a relation coefficient of  $-0.24$  with  $p$ -value 0.06 for early to mid stars, and a coefficient of  $-0.21$  with  $p$ -value 0.06 for mid to late stars. Therefore, in both cases we found a suggestive (but non-significant) anti-correlation between  $A$  and  $P_{\text{rot}}$ . We note the overabundance of M0.0 – 3.0 V stars with periods  $P_{\text{rot}} = 10 - 100$  d with respect to M3.5 – 8.5 V stars).

#### 4.4. Aperiodic variables

We also looked for aperiodic or irregular variable stars that display a large scatter in their light curves, but for which we failed to find any significant periodicity. For this reason, we used the common approach of plotting the standard deviation  $\sigma(m)$  of each individual light curve as a function of the mean magnitude  $\bar{m}$  (see e.g. Caballero et al. 2010 for a practical application). We performed this exercise for only three of the main surveys because average magnitudes of MEarth light curves were set to zero, different pass bands and instrumental set-ups must not be mixed up, and the complementary surveys and our own observations do not have enough data points for a robust analysis.

The  $\sigma(m)$  versus  $\bar{m}$  plots for ASAS, SuperWASP, and NSVS are shown in Fig. 7. All NSVS stars follow the expected trend for their mean magnitude (see Irwin et al. 2007 for a detailed description of virtually all parameters affecting  $\sigma(m)$  in a photometric survey). Of the SuperWASP stars, only J09003+218 = LP 368-128, a faint M6.5 V (Dupuy & Liu, 2012; Alonso-Floriano et al., 2015a), has a much larger scatter than its peers. Newton et al. (2016)

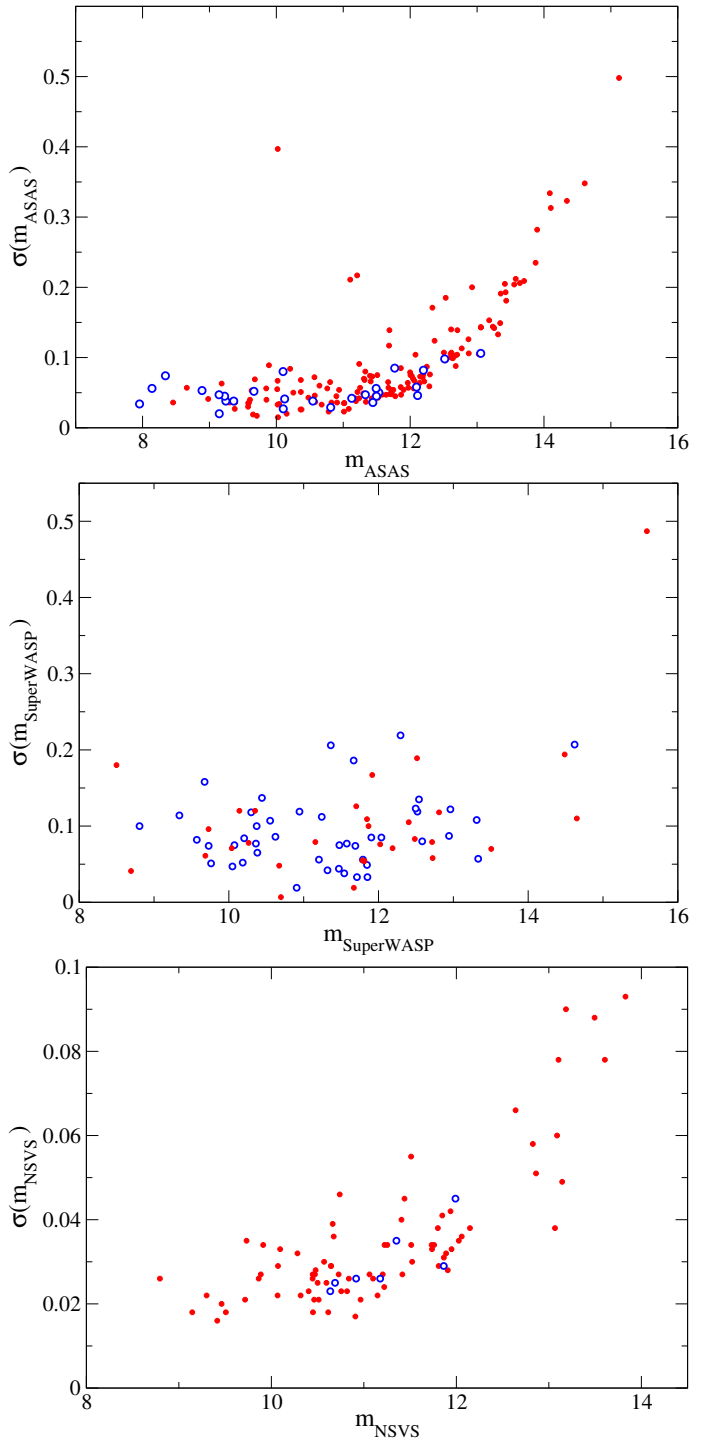


**Fig. 7.** Standard deviation  $\sigma(m)$  vs. mean  $\bar{m}$  for ASAS, SuperWASP, and NSVS magnitudes. Blue open circles and red filled circles represent stars with and without  $P_{\text{rot}}$  computed in this work, respectively. Most of the structure, specifically in the top and bottom panels, is not of astrophysical origin but related to the different sources of noise.

found a period of 0.439 d that we did not reproduce in our datasets (Table 3). However, we attribute its large  $\sigma(m)$ , of about 0.5 mag, to its magnitude, which is over 1 mag fainter than the second-faintest star in the SuperWASP sample. Finally, there are three outliers among the ASAS stars: J12248-182 = Ross 695, J04520+064 = Wolf 1539,

J09307+003 = GJ 1125. We ascribe the origin of their large  $\sigma(m)$  to their short angular separation to bright background stars that contaminate the ASAS light curves. In the three cases, they are located at variable angular separations  $\rho \approx 25\text{--}50$  arcsec to stars 1.2–2.5 mag brighter in the  $V$  band than our M dwarfs. As a result, the variability observed is not intrinsic to the stars themselves.

A few aperiodic or irregular variable stars also appeared in our monitoring with amateur and semi-professional telescopes. For example, with Carda we measured intra-night trends of over 0.030 mag in the known variable star J05337+019 = V371 Ori, and a 15 min, 0.030 mag-amplitude flare in the poorly investigated, X-ray emitting star J06574+740 = 2MASS J06572616+7405265.

#### 4.5. Long-period cycles

Baliunas et al. (1996) suggested the observable  $P_{\text{cycle}}/P_{\text{rot}}$  to study the relation between cycle and rotation periods. They proposed  $P_{\text{cycle}}/P_{\text{rot}} \sim D^i$ , being  $D$  the dynamo number and  $i$  the slope of the relation. Slopes  $i \sim 1$  would imply no correlation, while values different from unity would imply a correlation between the length of the cycle and rotation period. Previous works have explored this relation (Oláh et al., 2009; Gomes da Silva et al., 2012; Suárez Mascareño et al., 2016) and find a weak correlation for F, G, and K stars. Here we repeated the exercise restricting the analysis to M dwarf stars. For this, we carefully selected 47 single, inactive M dwarfs with previous published  $P_{\text{cycle}}$  and  $P_{\text{rot}}$  (Savanov, 2012; Robertson et al., 2013; Suárez Mascareño et al., 2016; Wargelin et al., 2017; Küker et al., 2018; Mascareño et al., 2018) and the stars of our sample for which we have found  $P_{\text{cycle}}$  and  $P_{\text{rot}}$  (see Table 2). In our sample of field M dwarfs we did not include fast-rotating, probably very young M dwarfs tabulated by Vida et al. (2013, 2014) and Distefano et al. (2016, 2017).

Figure 8 shows the plot  $P_{\text{cycle}}/P_{\text{rot}}$  versus  $1/P_{\text{rot}}$  in log-log scale. We found a slope  $i = 1.01 \pm 0.06$ , in agreement with the results of Savanov (2012) and Suárez Mascareño et al. (2016), who also did not find a correlation between  $P_{\text{cycle}}$  and  $P_{\text{rot}}$  in M dwarfs.

## 5. Conclusions

As a complement to the CARMENES survey for exoplanets, we searched for rotation periods from photometric series of 337 M dwarfs. We collected public data from long-term monitoring surveys (MEarth, ASAS, SuperWASP, NSVS, Catalina, ASAS-SN, K2, and HATNet). For 20 stars without data in these public surveys or for those with poor data, we carried out photometric monitoring in collaboration with amateur observatories. In total, we investigated 622 light curves of 334 M dwarfs. We analysed each light curve by computing LS periodograms and identifying significant signals. In some cases, we also applied GLS and Gaussian processes analyses. We found 142 signals that we interpret as rotation periods. Of these, 73 are new and 69 match or even improve previous determinations found in the existing literature. We also found long activity cycles for ten stars of the sample, six of which we report here for the first time. We explored the relation between  $P_{\text{cycle}}$  and  $P_{\text{rot}}$  for a sample of 47 M dwarfs with previous reported cycle and rotation periods, and the ten M dwarfs with cycle

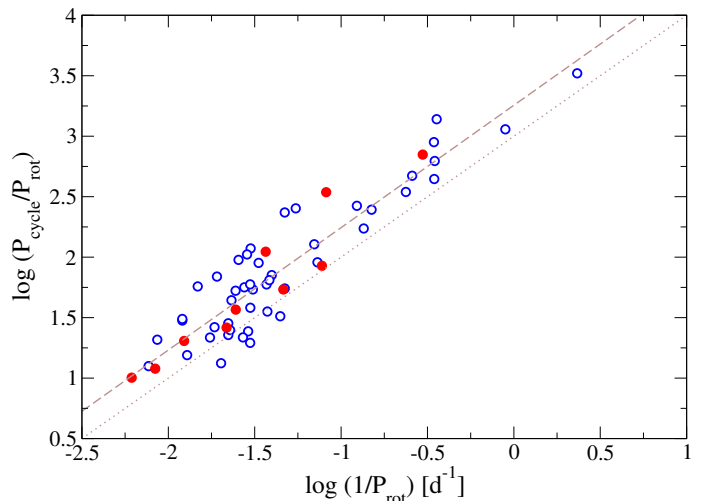


**Fig. 8.**  $P_{\text{cycle}}/P_{\text{rot}}$  vs.  $1/P_{\text{rot}}$  in log-log scale for M dwarf stars with previous published  $P_{\text{cycle}}$  and  $P_{\text{rot}}$  (blue open circles) and stars with new  $P_{\text{cycle}}$  from this work (red filled circles). Dashed ( $i = 1.01$ ) and dotted ( $i = 1.00$ , with arbitrary offset) lines mark our sample fit and non-correlation, respectively.

and rotation periods presented in this work, and did not find any correlation between  $P_{\text{cycle}}$  and  $P_{\text{rot}}$ .

Although the main aim of this work was to catalogue rotation periods of M dwarfs being searched for exoplanets with the radial-velocity method, and therefore to be able to discriminate between stellar activity and true exoplanet signals, we also presented results on (i) the absence of a lack of stars with intermediate periods at about 30 d with respect to stars with shorter periods in the rotation period distribution; (ii) the link between rotation period and activity, especially through rotational velocity and  $H\alpha$  pseudo-equivalent width; (iii) the identification of three very active, possibly young stars with new rotation periods between 0.34 d and 23.6 d; and (iv) the lack of apparent correlation between amplitude of photometric variability and  $P_{\text{rot}}$ ,  $v \sin i$ , and pEW( $H\alpha$ ).

The CARMENES Consortium will continue to improve or find new rotation periods, using them to discard or confirm radial-velocity exoplanets, and will make them public for use by other groups worldwide.

**Acknowledgements.** We thank the anonymous referee for the careful review, F. García de la Cuesta for observing J05019+011 from Observatorio Astronómico La Vara, Luarca, Spain. CARMENES is an instrument for the Centro Astronómico Hispano-Alemán de Calar Alto (CAHA, Almería, Spain). CARMENES is funded by the German Max-Planck-Gesellschaft (MPG), the Spanish Consejo Superior de Investigaciones Científicas (CSIC), the European Union through FEDER/ERF FICTS-2011-02 funds, and the members of the CARMENES Consortium (Max-Planck-Institut für Astronomie, Instituto de Astrofísica de Andalucía, Landessternwarte Königstuhl, Institut de Ciències de l’Espai, Institut für Astrophysik Göttingen, Universidad Complutense de Madrid, Thüringer Landessternwarte Tautenburg, Instituto de Astrofísica de Canarias, Hamburger Sternwarte, Centro de Astrobiología and Centro Astronómico Hispano-Alemán), with additional contributions by the Spanish Ministerio de Ciencia, Innovación y Universidades (under grants AYA2016-79425-C3-1/2/3-P, AYA2017-89121-P, AYA2018-84089), the German Science Foundation (DFG), the Klaus Tschira Stiftung, the states of Baden-Württemberg and Niedersachsen, the Junta de Andalucía, and by the Principado de Asturias (under grant FC-15-GRUPIN14-017). This research made use of the SIMBAD and VizieR,

operated at Centre de Données astronomiques de Strasbourg, France, and NASA's Astrophysics Data System.

## References

- Alonso, R., Brown, T. M., Charbonneau, D., et al. 2007, *Transiting Extrapolar Planets Workshop*, 366, 13
- Alonso-Floriano, F. J., Morales, J. C., Caballero, J. A., et al. 2015a, *A&A*, 577, A128
- Alonso-Floriano, F. J., Caballero, J. A., Cortés-Contreras, M., Solano, E., & Montes, D. 2015b, *A&A*, 583, A85
- Anglada-Escudé, G., Amado, P. J., Barnes, J., et al. 2016, *Nature*, 536, 437
- Angus, R., Morton, T., Aigrain, S., Foreman-Mackey, D., & Rajpaul, V. 2018, *MNRAS*, 474, 2094
- Artigau, É., Kouach, D., Donati, J.-F., et al. 2014, *Proc. SPIE*, 9147, 914715
- Auvergne, M., Bodin, P., Boisnard, L., et al. 2009, *A&A*, 506, 411
- Baliunas, S. L., & Vaughan, A. H. 1985, *ARA&A*, 23, 379
- Baliunas, S. L., Donahue, R. A., Soon, W. H., et al. 1995, *ApJ*, 438, 269
- Baliunas, S. L., Nesme-Ribes, E., Sokoloff, D., & Soon, W. H. 1996, *ApJ*, 460, 848
- Baluev, R. V., Sokov, E. N., Shaidulin, V. S., et al. 2015, *MNRAS*, 450, 3101
- Bakos, G., Noyes, R. W., Kovács, G., et al. 2004, *PASP*, 116, 266
- Bakos, G. Á., Csabry, Z., Penev, K., et al. 2013, *PASP*, 125, 154
- Bakos, G. Á. 2018, *Handbook of Exoplanets*, eds. H. Deeg & J. A. Belmonte, in press (eprint arXiv:1801.00849)
- Barnes, J. R., Jeffers, S. V., & Jones, H. R. A. 2011, *MNRAS*, 412, 1599
- Baroch, D., Morales, J. C., Ribas, I., et al. 2018, arXiv:1808.06895
- Barros, S. C. C., Faedi, F., Collier Cameron, A., et al. 2011, *A&A*, 525, A54
- Berdyugina, S. V., & Järvinen, S. P. 2005, *AN*, 326, 283
- Berta, Z. K., Irwin, J., & Charbonneau, D. 2013, *ApJ*, 775, 91
- Boisse, I., Bouchy, F., Hébrard, G., et al. 2011, *Physics of Sun and Star Spots*, 273, 281
- Bonfils, X., Forveille, T., Delfosse, X., et al. 2005, *A&A*, 443, L15
- Borucki, W. J., Koch, D., Basri, G., et al. 2010, *Science*, 327, 977
- Bouvier, J., Cabrit, S., Fernandez, M., Martin, E. L., & Matthews, J. M. 1993, *A&A*, 272, 176
- Brown, T. M., Baliber, N., Bianco, F. B., et al. 2013, *PASP*, 125, 1031
- Browning, M. K. 2008, *ApJ*, 676, 1262
- Browning, M. K., Basri, G., Marcy, G. W., West, A. A., & Zhang, J. 2010, *AJ*, 139, 504
- Butler, R. P., Vogt, S. S., Marcy, G. W., et al. 2004, *ApJ*, 617, 580
- Butters, O. W., West, R. G., Anderson, D. R., et al. 2010, *A&A*, 520, L10
- Caballero, J. A., Cornide, M., & de Castro, E. 2010, *AN*, 331, 257
- Caballero, J. A., Cortés-Contreras, M., Alonso-Floriano, F. J., et al. 2016, 19th Cambridge Workshop on Cool Stars, Stellar Systems, and the Sun (CS19), 148
- Chabrier, G., Gallardo, J., & Baraffe, I. 2007, *A&A*, 472, L17
- Charbonneau, D., Berta, Z. K., Irwin, J., et al. 2009, *Nature*, 462, 891
- Claudi, R., Benatti, S., Carleo, I., et al. 2016, *Proc. SPIE*, 9908, 99081A
- Cloutier, R., Astudillo-Defru, N., Doyon, R., et al. 2017, *A&A*, 608, A35
- Correia, A. C. M., Couetdic, J., Laskar, J., et al. 2010, *A&A*, 511, A21
- Cortés-Contreras, M., Béjar, V. J. S., Caballero, J. A., et al. 2017, *A&A*, 597, A47
- Collier Cameron, A., Bouchy, F., Hébrard, G., et al. 2007, *MNRAS*, 375, 951
- Collins, K. A., Kielkopf, J. F., Stassun, K. G., & Hessman, F. V. 2017, *AJ*, 153, 77
- Christensen, E. J., Carson Fuls, D., Gibbs, A. R., et al. 2015, *AAS/Division for Planetary Sciences Meeting Abstracts*, 47, 308.19
- Crossfield, I. J. M., Petigura, E., Schlieder, J. E., et al. 2015, *ApJ*, 804, 10
- Cumming, A. 2004, *MNRAS*, 354, 1165
- Dahn, C., Green, R., Keel, W., et al. 1985, *Information Bulletin on Variable Stars*, 2796, 1
- David, T. J., Hillenbrand, L. A., Petigura, E. A., et al. 2016, *Nature*, 534, 658
- Delfosse, X., Forveille, T., Perrier, C., & Mayor, M. 1998, *A&A*, 331, 581
- Distefano, E., Lanza, A. C., Lanza, A. F., Messina, S., & Spada, F. 2016, *A&A*, 591, A43
- Distefano, E., Lanza, A. C., Lanza, A. F., Messina, S., & Spada, F. 2017, *A&A*, 606, A58
- Dittmann, J. A., Irwin, J. M., Charbonneau, D., et al. 2017, *Nature*, 544, 333
- Donati, J.-F., Forveille, T., Collier Cameron, A., et al. 2006, *Science*, 311, 633
- Drake, A. J., Djorgovski, S. G., Mahabal, A., et al. 2009, *ApJ*, 696, 870
- Drake, A. J., Graham, M. J., Djorgovski, S. G., et al. 2014, *ApJS*, 213, 9
- Dressing, C. D., & Charbonneau, D. 2015, *ApJ*, 807, 45
- Dumasque, X., Pepe, F., Lovis, C., et al. 2012, *Nature*, 491, 207
- Dupuy, T. J., & Liu, M. C. 2012, *ApJS*, 201, 19
- Favata, F., Reale, F., Micela, G., et al. 2000, *A&A*, 353, 987
- Fekel, F. C., & Henry, G. W. 2000, *AJ*, 120, 3265
- Foreman-Mackey, D., Agol, E., Ambikasaran, S., & Angus, R. 2017, *AJ*, 154, 220
- France, K., Froning, C. S., Linsky, J. L., et al. 2013, *ApJ*, 763, 149
- Freeman, D. & Diaconis, P. 1981, *Probability Theory and Related Field*, 57, 4, 453
- Fuhrmeister, B., Czesla, S., Schmitt, J. H. M. M., et al. 2018, *A&A*, 615, A14
- Gillon, M., Pont, F., Demory, B.-O., et al. 2007, *A&A*, 472, L13
- Gillon, M., Triaud, A. H. M. J., Fortney, J. J., et al. 2012, *A&A*, 542, A4
- Gillon, M., Jehin, E., Lederer, S. M., et al. 2016, *Nature*, 533, 221
- Gillon, M., Triaud, A. H. M. J., Demory, B.-O., et al. 2017, *Nature*, 542, 456
- Gomes da Silva, J., Santos, N. C., Bonfils, X., et al. 2012, *A&A*, 541, A9
- Greimel, R., & Robb, R. M. 1998, *Information Bulletin on Variable Stars*, 4652, 1
- Hallinan, G., Antonova, A., Doyle, J. G., et al. 2008, *ApJ*, 684, 644
- Haro, G., & Chavira, E. 1966, *Vistas in Astronomy*, 8, 89
- Hartman, J. D., Bakos, G. Á., Noyes, R. W., et al. 2011, *AJ*, 141, 166
- Hawley, S. L., Gizis, J. E., & Reid, I. N. 1996, *AJ*, 112, 2799
- Heinze, A. N., Tonry, J. L., Denneau, L., et al. 2018, *ApJ*, subm., eprint arXiv:1804.02132
- Herbig, G. H. 1956, *PASP*, 68, 531
- Herrero, E., Morales, J. C., Ribas, I., & Naves, R. 2011, *A&A*, 526, L10
- Horne, J. H., & Baliunas, S. L. 1986, *ApJ*, 302, 757
- Howell, S. B., Sobeck, C., Haas, M., et al. 2014, *PASP*, 126, 398
- Irwin, J., Irwin, M., Aigrain, S., et al. 2007, *MNRAS*, 375, 1449
- Irwin, J., Charbonneau, D., Nutzman, P., & Falco, E. 2009, *Transiting Planets*, IAU symposium, 253, 37
- Irwin, J., Berta, Z. K., Burke, C. J., et al. 2011, *ApJ*, 727, 56
- Jankovics, I., Tsvetkova, K. P., & Tsvetkov, M. K. 1978, *Information Bulletin on Variable Stars*, 1454, 1
- Jeffers, S. V., Schöfer, P., Lamert, A., et al. 2018, *A&A*, 614, A76
- Johnson, J. A., Butler, R. P., Marcy, G. W., et al. 2007, *ApJ*, 670, 833
- Joshi, M. M., Haberle, R. M., & Reynolds, R. T. 1997, *Icarus*, 129, 450
- Kaminski, A., Trifonov, T., Caballero, J. A., et al. 2018, *A&A*, in press, eprint arXiv:1808.01183
- Kiraga, M., & Stepien, K. 2007, *Acta Astron.*, 57, 149
- Kiraga, M. 2012, *Acta Astron.*, 62, 67
- Kiraga, M., & Stepien, K. 2013, *Acta Astron.*, 63, 53
- Kochanek, C. S., Shappee, B. J., Stanek, K. Z., et al. 2017, *PASP*, 129, 104502
- Kopparapu, R. K., Ramirez, R., Kasting, J. F., et al. 2013, *ApJ*, 765, 131
- Korhonen, H., Vida, K., Husarik, M., et al. 2010, *AN*, 331, 772
- Kron, G. E. 1947, *PASP*, 59, 261
- Küker, M., Rüdiger, G., Oláh, K., & Strassmeier, K. G. 2018, eprint arXiv:1804.02925
- Léger, A., Rouan, D., Schneider, J., et al. 2009, *A&A*, 506, 287
- Liebert, J., Kron, R. G., & Spinrad, H. 1978, *PASP*, 90, 718
- Lothringer, J. D., Benneke, B., Crossfield, I. J. M., et al. 2018, *ApJ*, subm., eprint arXiv:1801.00412
- Luger, R., Sestovic, M., Kruse, E., et al. 2017, *Nature Astronomy*, 1, 0129

- Mahadevan, S., Ramsey, L. W., Terrien, R., et al. 2014, Proc. SPIE, 9147, 91471G
- Maldonado, J., Scandariato, G., Stelzer, B., et al. 2017, A&A, 598, A27
- McCullough, P. R., Stys, J. E., Valenti, J. A., et al. 2005, PASP, 117, 783
- McQuillan, A., Aigrain, S., & Mazeh, T. 2013, MNRAS, 432, 1203
- Messina, S., & Guinan, E. F. 2002, A&A, 393, 225
- Messina, S., Desidera, S., Turatto, M., Lanzafame, A. C., & Guinan, E. F. 2010, A&A, 520, A15
- Mochnacki, S. W., Gladders, M. D., Thomson, J. R., et al. 2002, AJ, 124, 2868
- Mohanty, S., & Basri, G. 2003, ApJ, 583, 451
- Morin, J., Donati, J.-F., Petit, P., et al. 2008, MNRAS, 390, 567
- Mullan, D. J., & MacDonald, J. 2001, ApJ, 559, 353
- Newton, E. R., Irwin, J., Charbonneau, D., et al. 2016, ApJ, 821, 93
- Newton, E. R., Irwin, J., Charbonneau, D., et al. 2017, ApJ, 834, 85
- Norton, A. J., Wheatley, P. J., West, R. G., et al. 2007, A&A, 467, 785
- Nutzman, P., & Charbonneau, D. 2008, PASP, 120, 317
- Ochsenbein, F., Bauer, P., & Marcout, J. 2000, A&AS, 143, 23
- Oláh, K., Kolláth, Z., Granzer, T., et al. 2009, A&A, 501, 703
- Osten, R. A., Hawley, S. L., Allred, J. C., Johns-Krull, C. M., & Roark, C. 2005, ApJ, 621, 398
- Osten, R. A., Godet, O., Drake, S., et al. 2010, ApJ, 721, 785
- Paunzen, E., & Vannmunder, T. 2016, AN, 337, 239
- Pepper, J., Pogge, R. W., DePoy, D. L., et al. 2007, PASP, 119, 923
- Pettersen, B. R., Coleman, L. A., & Evans, D. S. 1984, ApJ, 282, 214
- Pojmański, G. 1997, Acta Astron., 47, 467
- Pojmański, G. 2002, Acta Astron., 52, 397
- Pollacco, D. L., Skillen, I., Collier Cameron, A., et al. 2006, PASP, 118, 1407
- Queloz, D., Henry, G. W., Sivan, J. P., et al. 2001, A&A, 379, 279
- Quirrenbach, A., Amado, P. J., Seifert, W., et al. 2012, Proc. SPIE, 8446, E0R
- Quirrenbach, A., Amado, P. J., Caballero, J. A., et al. 2014, Proc. SPIE, 9147, E1F
- Quirrenbach, A., Caballero, J. A., Amado, P. J. et al. 2015, 18th Cambridge Workshop on Cool Stars, Stellar Systems, and the Sun, Proceedings of the conference held at Lowell Observatory, 8-14 June 2014. Edited by G. van Belle and H.C. Harris., pp. 897–906
- Quirrenbach, A., Amado, P. J., Caballero, J. A., et al. 2016, Proc. SPIE, 9908, E12
- Rasmussen, C. E. & Williams, C. K. I., Gaussian Processes for Machine Learning, The MIT Press, November 2006. ISBN: 9780262182539
- Reiners, A., & Basri, G. 2007, ApJ, 656, 1121
- Reiners, A., & Basri, G. 2008, ApJ, 684, 1390
- Reiners, A., & Basri, G. 2010, ApJ, 710, 924
- Reiners, A., Basri, G., & Browning, M. 2009, ApJ, 692, 538
- Reiners, A., Bean, J. L., Huber, K. F., et al. 2010, ApJ, 710, 432
- Reiners, A., Ribas, I., Zechmeister, M., et al. 2018a, A&A, 609, L5
- Reiners, A., Zechmeister, M., Caballero, J. A., et al. 2018b, A&A, 612, A49
- Ricker, G. R., Winn, J. N., Vanderspek, R., et al. 2015, JATIS, 1, 014003
- Rivera, E. J., Lissauer, J. J., Butler, R. P., et al. 2005, ApJ, 634, 625
- Robertson, P., Endl, M., Cochran, W. D., & Dodson-Robinson, S. E. 2013, ApJ, 764, 3
- Saar, S. H., & Donahue, R. A. 1997, ApJ, 485, 319
- Savanov, I. S. 2012, Astronomy Reports, 56, 716
- Scalo, J., Kaltenegger, L., Segura, A. G., et al. 2007, Astrobiology, 7, 85
- Segura, A., Kasting, J. F., Meadows, V., et al. 2005, Astrobiology, 5, 706
- Scargle, J. D. 1982, ApJ, 263, 835
- Schwarzenberg-Czerny, A. 1991, MNRAS, 253, 198
- Shkolnik, E., Liu, M. C., & Reid, I. N. 2009, ApJ, 699, 649
- Skrutskie, M. F., Cutri, R. M., Stiening, R., et al. 2006, AJ, 131, 1163
- Stauffer, J. R., Hartmann, L., Soderblom, D. R., & Burnham, N. 1984, ApJ, 280, 202
- Strassmeier, K. G. 2009, A&A Rev., 17, 251
- Stokes, G. H., Evans, J. B., Viggh, H. E. M., Shelly, F. C., & Pearce, E. C. 2000, Icarus, 148, 21
- Suárez Mascareño, A., Rebolo, R., González Hernández, J. I., & Esposito, M. 2015, MNRAS, 452, 2745
- Suárez Mascareño, A., Rebolo, R., & González Hernández, J. I. 2016, A&A, 595, A12
- Suárez Mascareño, A., Rebolo, R., González Hernández, J. I., et al. 2018, A&A, 612, A89
- Tal-Or, L., Zechmeister, M., Reiners, A., et al. 2018, A&A, 614, A122
- Tamura, M., Suto, H., Nishikawa, J., et al. 2012, Proc. SPIE, 8446, 84461T
- Tarter, J. C., Backus, P. R., Mancinelli, R. L., et al. 2007, Astrobiology, 7, 30
- Testa, P., Drake, J. J., & Peres, G. 2004, ApJ, 617, 508
- Vida, K., Kriskovics, L., & Oláh, K. 2013, AN, 334, 972
- Vida, K., Oláh, K., & Szabó, R. 2014, MNRAS, 441, 2744
- Vida, K., Kriskovics, L., Oláh, K., et al. 2016, A&A, 590, A11
- Vida, K., Kővári, Z., Pál, A., Oláh, K., & Kriskovics, L. 2017, ApJ, 841, 124
- Wargelin, B. J., Saar, S. H., Pojmański, G., Drake, J. J., & Kashyap, V. L. 2017, MNRAS, 464, 3281
- West, A. A., Weisenburger, K. L., Irwin, J., et al. 2015, ApJ, 812, 3
- Woźniak, P. R., Vestrand, W. T., Akerlof, C. W., et al. 2004, AJ, 127, 2436
- Zechmeister, M., & Kürster, M. 2009, A&A, 496, 577
- Zhilyaev, B. E., Romanyuk, Y. O., Verlyuk, I. A., et al. 2000, A&A, 364, 641

## Appendix A: Long tables

**Table A.1.** M dwarfs searched for photometric periods.

Karmn	Name	$\alpha$ (J2000.0)	$\delta$ (J2000.0)	Survey	$N_{\text{obs}}/N_{\text{used}}$	$\Delta t$ [a]	$\bar{m}$ [mag]	$\sigma_m$ [mag]	$\overline{\delta m}$ [mag]
J00051+457	GJ 2	00:05:10.78	+45:47:11.6	SuperWASP NSVS ASAS Catalina NSVS	5126/4400 69/69 181/172 160/140 106/105	1.645 0.397 7.863 4.285 0.397	10.185 9.300 13.899 11.897 11.889	0.052 0.022 0.282 0.056 0.032	0.027 0.010 0.122 0.050 0.020
J00067-075	GJ 1002	00:06:43.26	-07:32:14.7	ASAS NSVS	181/172 106/105	4.285 0.397	11.897 11.889	0.096 0.032	0.050 0.020
J00162+198E	LP 404-062	00:16:16.08	+19:51:51.5	ASAS MEarth-2010 MEarth-2010 MEarth-2014	317/282 935/910 935/933 282/278	6.855 2.562 0.720 2.704	11.690 0.000 0.000 0.000	0.139 0.007 0.009 0.015	0.114 0.004 0.003 0.011
J00162+198W	EZ Psc AB	00:16:14.63	+19:51:37.6	ASAS NSVS	316/305 202/193	6.855 0.585	11.684 10.595	0.117 0.025	0.110 0.011
J00183+440	GX And	00:18:22.57	+44:01:22.2	SuperWASP MEarth-2011 MEarth-2014-tel02	1233/1102 622/585 2328/2127	1.047 0.448 2.710	8.498 0.000 0.001	0.180 0.015 0.017	0.125 0.007 0.006
J00184+440	GQ And	00:18:25.50	+44:01:37.6	MEarth-2011 MEarth-2014-tel02	622/578 2326/2161	0.448 2.710	0.000 0.000	0.015 0.011	0.007 0.006
J00286-066	GJ 1012	00:28:39.48	-06:39:48.1	ASAS	389/368	9.030	11.861	0.085	0.040
J00389+306	Wolf 1056	00:38:58.79	+30:36:58.4	SuperWASP	12312/12309	4.112	10.944	0.119	0.018
J00570+450	G 172-030	00:57:02.61	+45:05:09.9	SuperWASP NSVS	3576/3334 52/52	1.645 0.331	9.729 9.415	0.096 0.016	0.016 0.010
J01013+613	GJ 47	01:01:20.06	+61:21:56.0	NSVS	105/103	0.706	10.095	0.033	0.011
J01019+541	G 218-020	01:01:59.53	+54:10:57.8	MEarth-2016-tel01 MEarth-2014-tel06 SuperWASP ASAS-SN	2549/2531 1678/1621 4983/4724 372/361	4.068 0.776 3.962 2.729	0.001 0.000 12.521 15.274	0.010 0.010 0.218 0.079	0.003 0.003 0.016 0.074
J01025+716	BD+70 68	01:02:32.13	+71:40:47.6	ASAS-SN NSVS	474/468 228/215	0.585 0.706	10.066 13.494	0.026 0.088	0.006 0.087
J01026+623	BD+61 195	01:02:38.96	+62:20:42.2	MEarth-2010 MEarth-2011 MEarth-2014	207/190 1268/1227 175/158	1.386 0.593 2.677	0.005 0.000 0.000	0.027 0.014 0.022	0.002 0.003 0.003
J01033+623	V388 Cas	01:03:19.72	+62:21:55.7	MEarth-2011	1268/1254	0.593	0.000	0.021	0.003
J01048-181	GJ 1028	01:04:53.69	-18:07:29.3	ASAS NSVS	136/128 101/89	9.005 0.276	14.610 12.827	0.348 0.058	0.181 0.042
J01056+284	GJ 1029 AB	01:05:37.32	+28:29:34.0	MEarth-2010 SuperWASP	760/738 4695/3975	1.361 4.112	0.000 14.383	0.007 0.171	0.003 0.092
J01125-169	YZ Cet	01:12:30.53	-16:59:57.0	ASAS	461/439	9.006	12.095	0.058	0.028
J01221+221	G 034-023	01:22:10.28	+22:09:03.2	SuperWASP	4643/4199	4.115	12.520	0.119	0.031
J01339-176	LP 768-113	01:33:58.00	-17:38:23.5	ASAS	462/444	9.027	13.055	0.106	0.052
J01352-072	Barta 161 12	01:35:13.93	-07:12:51.8	ASAS	397/380	8.981	13.436	0.181	0.076
J01433+043	GJ 70	01:43:20.15	+04:19:17.2	ASAS NSVS	322/301 121/119	8.899 0.460	10.937 10.072	0.054 0.029	0.020 0.010
J01518+644	G 244-037	01:51:51.08	+64:26:06.1	NSVS	122/115	0.706	10.570	0.030	0.015
J02002+130	TZ Ari	02:00:12.79	+13:03:11.2	ASAS MEarth-2010 MEarth-2011	141/131 1298/1247 1009/957	6.05820 0.362 0.258	12.365 0.001 0.010	0.124 0.047 0.161	0.040 0.006 0.005
J02015+637	G 244-047	02:01:35.33	+63:46:11.9	Carda	1147/1111	0.041	10.41	0.012	0.004
J02070+496	G 173-037	02:07:03.83	+49:38:44.1	SuperWASP	4440/4175	4.038	11.668	0.186	0.021
J02088+494	G 173-039	02:08:53.60	+49:26:56.6	SuperWASP NSVS	6662/6099 221/220	4.041 0.712	12.497 11.407	0.123 0.040	0.029 0.015
J02123+035	BD+02 348	02:12:20.91	+03:34:31.1	ASAS	330/311	8.921	10.042	0.034	0.019
J02222+478	BD+47 612	02:22:14.63	+47:52:48.1	SuperWASP NSVS	3414/3004 53/52	3.443 0.572	9.572 8.795	0.082 0.026	0.028 0.010
J02336+249	GJ 102	02:33:37.17	+24:55:39.2	SuperWASP ASAS MEarth-2010 MEarth-2014 NSVS Catalina	5884/5176 215/196 111/106 166/160 129/121 377/349	4.077 6.976 1.282 2.369 0.698 8.098	12.404 13.057 -0.001 0.001 11.733 11.343	0.105 0.143 0.007 0.008 0.034 0.112	0.033 0.066 0.003 0.004 0.016 0.005
J02358+202	BD+19 381	02:35:53.28	+20:13:11.9	SuperWASP ASAS NSVS	3092/2712 215/196 59/58	3.904 6.976 0.616	10.552 13.057 9.886	0.107 0.143 0.027	0.025 0.066 0.010
J02362+068	BX Cet	02:36:15.36	+06:52:19.1	ASAS	215/196	6.976	13.057	0.143	0.066
J02442+255	VX Ari	02:44:15.38	+25:31:25.0	SuperWASP ASAS	2808/2592 183/174	4.025 6.912	10.443 10.581	0.137 0.037	0.025 0.015
J02519+224	RBS 365	02:51:54.09	+22:27:30.0	SuperWASP ASAS	3359/3047 340/322	4.044 6.976	12.541 13.181	0.135 0.153	0.043 0.130
J02530+168	Teegarden's Star	02:53:00.85	+16:52:53.3	MEarth-2010 MEarth-2011 MEarth-2010-tel01 MEarth-2014-tel08	514/506 528/475 2228/2130 1719/1688	1.392 0.713 2.388 0.381	0.000 0.032 0.000 0.000	0.010 0.275 0.012 0.011	0.006 0.005 0.004 0.004
J02565+554W	Ross 364	02:56:34.35	+55:26:14.5	SuperWASP	4135/3998	4.041	10.264	0.078	0.023

**Table A.1.** M dwarfs searched for photometric periods (cont.).

Karmn	Name	$\alpha$ (J2000.0)	$\delta$ (J2000.0)	Survey	$N_{\text{obs}}/N_{\text{used}}$	$\Delta t$ [a]	$\bar{m}$ [mag]	$\sigma_m$ [mag]	$\overline{\delta m}$ [mag]
J03133+047	CD Cet	03:13:22.99	+04:46:29.4	NSVS	104/103	0.616	9.508	0.018	0.010
				ASAS	200/182	8.792	14.103	0.313	0.182
J03181+382	HD 275122	03:18:07.42	+38:15:08.2	MEarth-2010	1068/1011	1.170	0.001	0.021	0.003
J03213+799	GJ 133	03:21:21.76	+79:58:02.2	SuperWASP	6609/5222	1.449	10.361	0.077	0.023
				AstroLAB IRIS	199/195	1.041	11.089	0.022	0.006
J03217-066	G 077-046	03:21:46.89	-06:40:24.2	ASAS	488/457	9.030	11.331	0.047	0.021
J03463+262	HD 23453	03:46:20.12	+26:12:56.0	SuperWASP	2315/2097	3.635	9.686	0.061	0.028
				ASAS	226/212	6.978	9.580	0.035	0.015
J03473-019	G 080-021	03:47:23.33	-01:58:19.5	ASAS	376/370	8.896	11.531	0.050	0.021
J03531+625	Ross 567	03:53:10.42	+62:34:08.2	NSVS	195/182	0.679	10.645	0.029	0.011
				AstroLAB IRIS	152/148	1.041	11.494	0.029	0.015
J04153-076	$o^2$ Eri C	04:15:21.73	-07:39:17.4	ASAS	190/159	4.370	9.182	0.063	0.040
J04198+425	LSR J0419+4233	04:19:52.13	+42:33:30.5	MEarth-2014-tel05	574/551	4.370	0.000	-0.015	0.008
				MEarth-2014-tel06	1807/1736	2.479	0.000	0.058	0.009
J04225+105	LSPM J0422+1031	04:22:31.99	+10:31:18.8	MEarth-2014	515/491	2.435	0.000	0.009	0.004
				ASAS	355/332	8.817	12.505	0.107	0.048
J04290+219	BD+21 652	04:29:00.14	+21:55:21.5	ASAS	435/396	6.970	8.342	0.074	0.019
				SuperWASP	2151/1707	2.553	8.596	0.118	0.041
J04376+528	BD+52 857	04:37:40.92	+52:53:37.2	SuperWASP	1958/1674	1.443	8.693	0.041	0.047
J04376-110	BD-11 916	04:37:41.88	-11:02:19.8	ASAS	545/509	9.035	10.366	0.051	0.020
J04429+189	HD 285968	04:42:55.81	+18:57:28.5	ASAS	459/429	6.970	10.018	0.067	0.018
				K2	3605/3485	0.218	0.879	0.158	...
J04429+214	2M J04425586+2128230	04:42:55.86	+21:28:23.0	ASAS	327/311	6.970	11.965	0.064	0.029
				SuperWASP	2151/1705	2.553	8.496	0.118	0.028
J04472+206	RX J0447.2+2038	04:47:12.25	+20:38:10.9	Montcabrer	192/192	0.033	11.692	0.012	0.005
				K2	3605/3572	0.218	0.975	0.022	...
J04520+064	Wolf 1539	04:52:05.73	+06:28:35.6	ASAS	301/294	8.827	11.208	0.217	0.040
J04538-177	GJ 180	04:53:49.95	-17:46:23.5	ASAS	563/530	9.038	10.897	0.045	0.019
J04588+498	BD+49 1280	04:58:50.58	+49:50:57.3	SuperWASP	3535/2696	3.536	10.039	0.071	0.015
J05019+011	1RXS J050156.7+010845	05:01:56.66	+01:08:42.9	Montcabrer	485/483	0.074	10.467	0.011	0.004
J05019-069	LP 656-038	05:01:57.47	-06:56:45.9	ASAS	619/583	9.027	12.194	0.076	0.038
J05033-173	LP 776-049	05:03:20.10	-17:22:24.5	ASAS	848/809	9.038	11.724	0.051	0.033
J05062+046	RX J0506.2+0439	05:06:12.93	+04:39:27.2	NSVS	182/172	0.556	11.864	0.029	0.018
				ASAS	478/464	8.781	12.706	0.139	0.040
J05084-210	2M J05082729-2101444	05:08:27.30	-21:01:44.4	Catalina	154/139	7.588	13.027	0.079	0.058
J05127+196	GJ 192	05:12:42.23	+19:39:56.6	ASAS	353/340	6.970	10.804	0.065	0.019
J05280+096	Ross 41	05:28:00.15	+09:38:38.3	ASAS	382/368	8.726	12.516	0.098	0.048
				MEarth-2010	842/813	0.512	0.000	0.007	0.003
				MEarth-2011	2311/2221	0.441	0.006	0.131	0.004
				MEarth-2014-tel01	1053/981	2.468	0.000	0.008	0.004
				MEarth-2014-tel05	1107/1014	1.520	0.000	0.009	0.004
J05314-036	HD 36395	05:31:27.35	-03:40:35.7	ASAS	439/412	7.435	7.955	0.034	0.015
J05337+019	V371 Ori	05:33:44.81	+01:56:43.4	ASAS	463/444	8.805	11.318	0.068	0.040
				NSVS	168/158	0.484	10.471	0.027	0.011
				Carda	171/169	0.033	10.88	0.012	0.004
J05348+138	Ross 46	05:34:52.12	+13:52:47.2	ASAS	490/471	6.970	11.859	0.058	0.028
J05360-076	Wolf 1457	05:36:00.08	-07:38:58.1	ASAS	756/711	9.036	12.871	0.126	0.061
				NSVS	162/153	0.468	11.737	0.033	0.020
J05365+113	V2689 Ori	05:36:30.99	+11:19:40.2	ASAS	692/657	8.729	8.889	0.053	0.020
J05366+112	2M J05363846+1117487	05:36:38.47	+11:17:48.8	ASAS	684/646	8.729	12.613	0.140	0.067
				NSVS	207/206	0.972	11.416	0.027	0.016
J05394+406	LSR J0539+4038	05:39:24.74	+40:38:43.8	MEarth-2014-tel04	965/928	1.485	-0.005	0.128	0.007
				MEarth-2014-tel08	1267/1198	2.517	0.000	0.015	0.006
J05415+534	HD 233153	05:41:30.73	+53:29:23.9	NSVS	66/66	0.345	9.145	0.018	0.010
J05421+124	V1352 Ori	05:42:08.98	+12:29:25.3	ASAS	519/499	6.970	11.510	0.050	0.026
				MEarth-2014-tel02	1248/1138	2.506	0.000	0.016	0.005
				NSVS	188/187	0.605	10.317	0.022	0.011
J05532+242	Ross 59 AB	05:53:14.04	+24:15:32.9	SuperWASP	2116/1889	3.591	10.397	0.083	0.038
				ASAS	318/302	6.970	10.824	0.036	0.043
J06000+027	G 099-049	06:00:03.51	+02:42:23.6	MEarth-2010	991/975	0.260	0.000	0.010	0.004
				ASAS	452/418	8.773	11.303	0.048	0.021
J06011+595	G 192-013	06:01:11.07	+59:35:50.8	SuperWASP	580/503	1.517	11.156	0.079	0.026
				MEarth-2010	908/865	0.537	0.000	0.007	0.003
				MEarth-2014	906/852	2.544	0.001	0.013	0.005
				NSVS	217/217	0.989	10.447	0.027	0.011
J06024+498	G 192-015	06:02:29.18	+49:51:56.2	MEarth-2010	1614/1550	1.539	0.000	0.010	0.005
				MEarth-2014	350/329	2.528	0.000	0.008	0.003
				SuperWASP	2913/2577	1.946	12.280	0.127	0.026
J06103+821	GJ 226	06:10:19.78	+82:06:25.7	ASAS-SN	718/698	4.323	10.474	0.023	0.006
J06105-218	HD 42581 A	06:10:34.62	-21:51:52.2	ASAS	750/708	9.041	8.141	0.056	0.019
J06246+234	Ross 64	06:24:41.32	+23:25:58.6	SuperWASP	2766/2393	3.668	12.809	0.118	0.039

**Table A.1.** M dwarfs searched for photometric periods (cont.).

Karmn	Name	$\alpha$ (J2000.0)	$\delta$ (J2000.0)	Survey	$N_{\text{obs}}/N_{\text{used}}$	$\Delta t$ [a]	$\bar{m}$ [mag]	$\sigma_m$ [mag]	$\overline{\delta m}$ [mag]
				ASAS	315/300	6.967	13.416	0.205	0.045
				MEarth-2010	675/639	0.583	0.000	0.008	0.004
				MEarth-2011	211/205	0.411	0.001	0.010	0.003
				NSVS	201/198	0.536	11.937	0.042	0.024
J06318+414	LP 205-044	06:31:50.74	+41:29:45.9	SuperWASP	6338/5690	3.555	14.621	0.207	0.143
				MEarth-2010	142/136	1.478	0.000	0.010	0.004
				MEarth-2011	519/475	0.364	0.001	0.010	0.003
J06371+175	HD 260655	06:37:10.92	+17:33:52.7	ASAS	565/532	6.970	9.606	0.040	0.019
J06396-210	LP 780-032	06:39:37.42	-21:01:33.3	ASAS	1046/981	9.041	12.617	0.107	0.096
				NSVS	126/121	0.410	11.522	0.030	0.019
J06421+035	G 108-021	06:42:11.18	+03:34:52.7	MEarth-2011	3763/3663	0.462	0.000	0.010	0.004
				MEarth-2014	500/465	2.481	0.001	0.015	0.004
				ASAS	486/475	8.581	11.999	0.079	0.043
J06548+332	Wolf 294	06:54:49.03	+33:16:05.9	SuperWASP	4132/3409	3.618	10.075	0.075	0.019
J06574+740	2M J06572616+7405265	06:57:26.16	+74:05:26.5	NSVS	307/285	0.983	11.948	0.033	0.023
				Carda	567/567	0.020	12.41	0.017	0.007
J06594+193	GJ 1093	06:59:28.69	+19:20:57.7	ASAS	447/423	6.970	11.432	0.073	0.023
				NSVS	130/127	4.474	11.148	0.022	0.015
J07001-190	2M J07000682-1901235	07:00:06.83	-19:01:23.6	ASAS	572/549	9.041	13.236	0.144	0.044
J07033+346	LP 255-011	07:03:23.17	+34:41:51.0	SuperWASP	4273/3855	1.422	13.312	0.108	0.025
				MEarth-2014	437/426	2.550	0.000	0.008	0.003
				NSVS	186/186	0.490	11.872	0.029	0.017
				Catalina	271/245	8.442	11.822	0.098	0.050
J07044+682	GJ 258	07:04:25.94	+68:17:19.6	NSVS	169/169	0.391	11.061	0.027	0.013
J07274+052	Luyten's Star	07:27:24.50	+05:13:32.9	ASAS	394/365	8.036	9.889	0.089	0.023
J07287-032	GJ 1097	07:28:45.41	-03:17:52.4	ASAS	519/497	8.956	11.497	0.045	0.030
J07319+362N	BL Lyn	07:31:57.35	+36:13:47.8	SuperWASP	8710/8313	3.643	10.381	0.065	0.022
J07353+548	GJ 3452	07:35:21.88	+54:50:59.0	SuperWASP	3527/2868	2.033	11.363	0.206	0.025
				NSVS	303/299	0.989	10.512	0.021	0.011
J07361-031	BD-02 2198	07:36:07.08	-03:06:38.5	ASAS	471/448	8.956	9.848	0.056	0.026
J07386-212	LP 763-001	07:38:40.89	-21:13:27.6	ASAS	765/709	9.038	11.675	0.057	0.037
J07393+021	BD+02 1729	07:39:23.04	+02:11:01.2	ASAS	487/469	8.956	9.591	0.036	0.017
J07403-174	LP 783-002	07:40:19.22	-17:24:44.9	ASAS	553/539	9.033	12.333	0.171	0.040
J07446+035	YZ CMi	07:44:40.18	+03:33:09.0	MEarth-2010	986/941	1.416	0.001	0.032	0.004
				ASAS	551/529	8.732	11.238	0.091	0.025
J07472+503	2M J07471385+5020386	07:47:13.85	+50:20:38.5	SuperWASP	3072/2714	2.033	12.961	0.122	0.098
				NSVS	282/266	0.973	11.865	0.031	0.017
J07558+833	GJ 1101	07:55:53.97	+83:23:05.0	MEarth-2014	775/728	2.660	0.001	0.011	0.005
				MEarth-2010	315/300	0.665	0.000	0.009	0.003
				NSVS	168/162	0.334	11.800	0.038	0.018
J07582+413	GJ 1105	07:58:12.70	+41:18:13.5	SuperWASP	7377/6608	3.599	11.866	0.100	0.032
				MEarth-2010	1193/1152	0.501	0.000	0.010	0.003
				MEarth-2014	810/748	2.602	0.001	0.012	0.005
J08119+087	Ross 619	08:11:57.58	+08:46:22.1	MEarth-2010	889/848	1.288	0.000	0.021	0.004
				MEarth-2011	923/877	0.528	0.001	0.013	0.003
				MEarth-2014	114/110	2.563	0.000	0.008	0.003
				ASAS	119/107	3.929	12.876	0.106	0.060
J08126-215	GJ 300 AB	08:12:40.88	-21:33:05.7	ASAS	779/729	9.016	12.079	0.104	0.043
J08161+013	GJ 2066	08:16:07.98	+01:18:09.2	ASAS	575/540	8.978	10.101	0.080	0.017
J08293+039	2M J08292191+0355092	08:29:21.92	+03:55:09.3	ASAS	392/372	8.580	11.400	0.074	0.023
				NSVS	165/163	0.973	10.615	0.018	0.011
J08298+267	DX Cnc	08:29:49.50	+26:46:34.8	MEarth-2014-tel01	4225/4102	2.574	0.001	0.012	0.004
				MEarth-2014-tel03	3929/3792	1.602	0.000	0.013	0.004
				MEarth-2010	1253/1227	1.608	0.000	0.014	0.005
				SuperWASP	10302/9327	3.599	12.739	0.058	0.035
J08315+730	LP 035-219	08:31:30.11	+73:03:45.9	MEarth-2014-tel04	15475/14901	2.660	0.000	0.009	0.004
				MEarth-2014-tel06	121/120	0.959	0.002	0.009	0.004
				NSVS	297/279	0.990	11.809	0.029	0.018
J08358+680	G 234-037	08:35:49.16	+68:04:09.7	NSVS	293/277	0.990	10.755	0.023	0.012
J08402+314	LSPM J0840+3127	08:40:15.97	+31:27:06.8	SuperWASP	6126/5316	3.569	12.022	0.076	0.024
				MEarth-2014	9913/9392	2.618	0.000	0.009	0.005
				NSVS	105/105	0.457	11.204	0.027	0.012
				Catalina	430/383	8.471	11.006	0.125	0.050
J08413+594	LP 090-018	08:41:20.13	+59:29:50.6	SuperWASP	527/486	1.055	14.488	0.194	0.147
				MEarth-2014	2019/1958	2.649	0.000	0.012	0.003
				MEarth-2011	153/148	0.304	0.000	0.011	0.003
				MEarth-2010	1310/1295	1.684	0.000	0.010	0.004
J08526+283	$\rho^1$ Cnc B	08:52:40.85	+28:18:58.9	MEarth-2014-tel02	864/826	2.621	0.000	0.012	0.004
				MEarth-2014-tel04	404/390	0.126	0.001	0.015	0.004
				MEarth-2010	1053/1001	0.643	0.000	0.008	0.002
				ASAS	84/84	1.394	12.532	0.185	0.042
J08536-034	LP 666-009	08:53:36.20	-03:29:32.1	Montcabrer	43/41	0.195	14.496	0.022	0.017

**Table A.1.** M dwarfs searched for photometric periods (cont.).

Karmn	Name	$\alpha$ (J2000.0)	$\delta$ (J2000.0)	Survey	$N_{\text{obs}}/N_{\text{used}}$	$\Delta t$ [a]	$\bar{m}$ [mag]	$\sigma_m$ [mag]	$\overline{\delta m}$ [mag]
J09003+218	LP 368-128	09:00:23.59	+21:50:05.4	SuperWASP MEarth-2010 NSVS Catalina	12255/11262 1201/1154 155/152 522/471	3.643 0.356 0.984 8.551	15.586 0.000 13.606 13.427	0.487 0.011 0.078 0.058	0.467 0.004 0.071 0.050
J09005+465	GJ 1119	09:00:32.54	+46:35:11.8	MEarth-2014 MEarth-2010 NSVS Catalina	1213/1136 142/137 222/213 210/190	1.600 0.630 0.983 7.888	0.003 0.001 11.907 11.911	0.025 0.008 0.028 0.090	0.005 0.004 0.016 0.050
J09028+680	LP 060-179	09:02:52.85	+68:03:46.4	MEarth-2014 NSVS	329/317 204/203	2.660 0.392	0.000 10.908	0.009 0.017	0.004 0.012
J09033+056	NLTT 20861	09:03:20.96	+05:40:14.5	MEarth-2010 Catalina	565/533 318/299	2.060 7.937	0.003 14.449	0.051 0.024	0.007 0.055
J09133+688	G 234-057	09:13:23.83	+68:52:30.5	NSVS	267/245	0.984	10.450	0.018	0.011
J09140+196	LP 427-016	09:14:03.21	+19:40:06.0	ASAS NSVS	335/310 199/194	6.410 0.984	12.199 11.220	0.082 0.024	0.037 0.012
J09144+526	HD 79211	09:14:24.86	+52:41:11.8	...	...	...	...	...	...
J09161+018	RX J0916.1+0153	09:16:10.19	+01:53:08.8	Catalina ASAS NSVS	303/288 448/423 156/151	7.951 8.953 0.973	11.774 12.925 11.760	0.110 0.200 0.034	0.050 0.097 0.014
J09163-186	LP 787-052	09:16:20.66	-18:37:32.9	ASAS	824/735	9.038	10.570	0.072	0.043
J09307+003	GJ 1125	09:30:44.58	+00:19:21.4	ASAS MEarth-2010 MEarth-2014	371/346 728/701 1096/1032	8.534 0.602 2.574	11.104 0.000 0.000	0.211 0.010 0.011	0.040 0.003 0.006
J09360-216	GJ 357	09:36:01.61	-21:39:37.1	ASAS NSVS	591/555 79/79	9.027 0.380	10.907 10.067	0.036 0.022	0.017 0.011
J09411+132	Ross 85	09:41:10.33	+13:12:34.4	ASAS	311/293	6.967	10.361	0.026	0.017
J09423+559	GJ 363	09:42:23.28	+55:59:01.6	MEarth-2010 MEarth-2014 SuperWASP NSVS	1777/1742 516/495 2563/2099 143/142	2.071 2.673 0.553 0.989	0.001 0.001 12.396 11.439	0.009 0.010 0.005 0.045	0.003 0.003 0.048 0.014
J09425+700	GJ 360	09:42:34.94	+70:02:02.4	AstroLAB IRIS	164/161	0.827	9.530	0.025	0.012
J09428+700	GJ 362	09:42:51.82	+70:02:22.2	AstroLAB IRIS	210/204	0.827	10.089	0.023	0.011
J09439+269	Ross 93	09:43:55.63	+26:58:08.6	Montcabrer	1042/975	0.214	9.814	0.008	0.004
J09447-182	GJ 1129	09:44:47.31	-18:12:48.9	ASAS NSVS	593/557 137/133	9.038 0.984	12.249 11.100	0.087 0.026	0.040 0.013
J09449-123	G 161-071	09:44:54.22	-12:20:54.4	ASAS NSVS Catalina	369/356 142/120 174/165	8.430 0.984 7.192	13.427 11.990 11.906	0.193 0.045 0.090	0.173 0.020 0.050
J09468+760	BD+76 3952	09:46:48.45	+76:02:38.8	Montsec	525/508	0.910	10.06	0.006	0.001
J09511-123	BD-11 2741	09:51:09.64	-12:19:47.8	ASAS	801/764	9.041	10.018	0.033	0.016
J09561+627	BD+63 869	09:56:08.69	+62:47:18.6	ASAS-SN	694/684	5.288	9.422	0.132	0.004
J10023+480	BD+48 1829	10:02:21.84	+48:05:20.9	SuperWASP NSVS	446/446 39/37	2.101 0.855	10.141 9.462	0.120 0.020	0.005 0.010
J10122-037	AN Sex	10:12:17.69	-03:44:44.1	ASAS	511/493	9.025	9.244	0.038	0.016
J10125+570	LP 092-048	10:12:34.81	+57:03:49.6	SuperWASP NSVS	169/163 162/156	0.011 0.989	11.670 10.663	0.019 0.039	0.017 0.011
J10167-119	GJ 386	10:16:46.00	-11:57:41.3	ASAS	568/537	9.038	11.014	0.035	0.018
J10182-204	NLTT 23956 AB	10:18:13.88	-20:28:41.4	ASAS	291/270	8.484	14.087	0.334	0.195
J10251-102	BD-09 3070	10:25:10.88	-10:13:43.4	ASAS	664/602	9.033	10.153	0.020	0.021
J10289+008	BD+01 2447	10:28:55.55	+00:50:27.5	ASAS	413/382	8.636	9.630	0.053	0.016
J10350-094	LP 670-017	10:35:01.11	-09:24:38.5	ASAS Catalina	499/475 185/175	9.008 7.318	12.064 10.934	0.067 0.163	0.048 0.050
J10354+694	LP 037-179 AB	10:35:27.26	+69:26:59.5	NSVS	163/151	0.984	10.917	0.026	0.012
J10360+051	RY Sex	10:36:01.21	+05:07:12.8	ASAS Catalina	328/311 405/366	7.751 8.570	12.677 11.322	0.103 0.156	0.045 0.050
J10396-069	GJ 399	10:39:40.61	-06:55:25.6	ASAS NSVS	666/628 125/122	9.008 0.378	11.300 10.463	0.049 0.021	0.022 0.011
J10416+376	GJ 1134	10:41:38.10	+37:36:39.8	SuperWASP MEarth-2010 MEarth-2014	4712/4062 1382/1347 224/211	4.044 0.684 2.701	12.514 10.400 0.000	0.189 0.083 0.009	0.029 0.004 0.004
J10482-113	LP 731-058	10:48:12.58	-11:20:08.2	NSVS Catalina	110/109 127/116	0.984 5.169	13.066 12.731	0.038 0.092	0.034 0.050
J10504+331	G 119-037	10:50:26.00	+33:06:05.2	SuperWASP	5090/4563	4.044	12.723	0.058	0.028
J10508+068	EE Leo	10:50:52.01	+06:48:29.3	K2 ASAS NSVS	3538/3538 357/344 145/144	0.214 7.926 0.976	1.001 11.719 10.446	0.004 0.048 0.026	...
J10564+070	CN Leo	10:56:28.86	+07:00:52.8	K2 MEarth-2010 MEarth-2014-tel01 MEarth-2014-tel04	3408/3362 773/692 2470/2318 2431/2281	0.212 0.610 2.618 0.640	1.000 0.004 0.001 0.000	0.006 0.019 0.019 0.016	...
J10584-107	LP 731-076	10:58:28.00	-10:46:30.5	Catalina	324/310	7.597	12.505	0.398	0.051
J11000+228	Ross 104	11:00:04.32	+22:49:59.3	ASAS	292/273	6.523	10.025	0.015	0.019

**Table A.1.** M dwarfs searched for photometric periods (cont.).

Karmn	Name	$\alpha$ (J2000.0)	$\delta$ (J2000.0)	Survey	$N_{\text{obs}}/N_{\text{used}}$	$\Delta t$ [a]	$\bar{m}$ [mag]	$\sigma_m$ [mag]	$\overline{\delta m}$ [mag]
J11026+219	DS Leo	11:02:38.33	+21:58:01.7	SuperWASP	8397/7293	4.044	9.983	0.056	0.013
J11033+359	Lalande 21185	11:03:20.24	+35:58:11.8	SuperWASP	12026/11565	4.044	9.731	0.074	0.011
J11054+435	BD+44 2051A	11:05:29.03	+43:31:35.7	ASAS-SN MEarth-2010 MEarth-2014-tel04 MEarth-2014-tel07	768/688 2726/2683 542/491 387/367	4.786 1.714 2.690 0.468	8.080 0.001 -0.030 -0.036	0.246 0.059 0.0025 0.168	0.0036 0.0003 0.0022 0.0022
J11055+435	WX UMa	11:05:31.33	+43:31:17.1	MEarth-2010 MEarth-2014	2726/2559 542/505	1.714 2.692	0.001 -0.001	0.058 0.010	0.0053 0.0003
J11110+304	HD 97101 B	11:11:02.46	+30:26:41.6	...	...	...	...	...	...
J11126+189	StKM 1-928	11:12:38.99	+18:56:05.4	ASAS Catalina	568/530 253/235	6.532 7.677	10.761 11.823	0.056 0.738	0.021 0.050
J11201-104	LP 733-099	11:20:06.10	-10:29:46.8	ASAS Catalina	380/363 56/55	8.674 6.997	11.212 10.269	0.051 0.069	0.043 0.050
J11289+101	Wolf 398	11:28:56.24	+10:10:39.5	MEarth-2010 MEarth-2014	3179/3017 945/896	1.613 2.635	0.000 -0.001	0.007 0.010	0.004 0.005
J11302+076	K2-18	11:30:14.44	+07:35:16.3	K2 ASAS Catalina	3313/3313 338/331 362/283	0.219 8.038 8.104	1.000 13.555 12.394	0.005 0.204 0.142	...
J11306-080	LP 672-042	11:30:41.80	-08:05:42.6	ASAS	489/458	8.704	12.043	0.070	0.031
J11417+427	Ross 1003	11:41:44.72	+42:45:07.3	HATNet SuperWASP NSVS	9096/8944 5780/4903 156/152	0.446 4.044 0.983	9.312 11.438 10.739	0.008 0.154 0.046	0.008 0.022 0.011
J11421+267	Ross 905	11:42:10.96	+26:42:25.1	SuperWASP ASAS NSVS	5425/5392 213/204 80/77	4.036 6.529 0.959	10.372 10.644 9.732	0.100 0.060 0.035	0.019 0.016 0.010
J11467-140	GJ 443	11:46:42.82	-14:00:50.5	ASAS NSVS	519/484 82/76	8.693 0.923	11.696 10.818	0.048 0.023	0.024 0.011
J11474+667	1RXS J114728.8+664405	11:47:28.57	+66:44:02.6	NSVS Catalina	196/185 67/67	0.975 7.211	13.089 13.000	0.060 0.084	0.043 0.050
J11476+002	LP 613-049 A	11:47:40.74	+00:15:20.2	K2 MEarth-2010 MEarth-2014 ASAS	3344/3323 675/667 848/791 348/337	0.219 0.599 2.602 8.679	1.005 -0.001 -0.002 13.346	0.018 0.019 0.023 0.149	...
J11476+786	GJ 445	11:47:41.44	+78:41:28.3	Montsec	627/567	0.912	10.22	0.001	0.003
J11477+008	FI Vir	11:47:44.40	+00:48:16.4	ASAS MEarth-2014-tel07 MEarth-2014-tel08 K2	386/369 786/718 824/776 3203/3203	8.681 1.118 0.618 0.219	11.127 -0.001 -0.001 1.001	0.042 0.020 0.036 0.004	0.018 0.008 0.008 ...
J11509+483	GJ 1151	11:50:57.88	+48:22:39.6	MEarth-2010	1760/1694	0.624	0.000	0.007	0.003
J11511+352	BD+36 2219	11:51:07.37	+35:16:18.9	SuperWASP	4937/4083	4.044	9.676	0.158	0.019
J12054+695	Ross 689	12:05:29.75	+69:32:22.7	MEarth-2010	1726/1685	0.668	0.003	0.105	0.003
J12100-150	LP 734-032	12:10:05.60	-15:04:15.7	ASAS	498/473	9.022	12.100	0.058	0.028
J12111-199	LTT 4562	12:11:11.80	-19:57:37.7	ASAS	529/502	9.025	11.719	0.054	0.026
J12123+544S	HD 238090	12:12:20.85	+54:29:08.7	MEarth-2010 MEarth-2014-tel05	1508/1499 232/194	0.649 2.665	-0.005 0.000	0.032 0.014	0.002 0.003
J12156+526	StKM 2-809	12:15:39.37	+52:39:08.9	SuperWASP NSVS Catalina	214/207 160/148 165/153	2.101 0.975 7.522	12.485 11.512 11.424	0.083 0.034 0.165	0.040 0.015 0.050
J12189+111	GL Vir	12:18:59.40	+11:07:33.9	MEarth-2010	1374/1355	1.594	0.001	0.014	0.004
J12230+640	Ross 690	12:23:00.25	+64:01:50.6	NSVS	251/245	0.983	10.688	0.025	0.011
J12248-182	Ross 695	12:24:52.43	-18:14:30.3	ASAS	117/117	5.433	10.022	0.397	0.036
J12312+086	BD+09 2636	12:31:15.79	+08:48:38.1	ASAS	463/428	8.096	9.679	0.069	0.016
J12350+098	GJ 476	12:35:00.70	+09:49:42.5	ASAS NSVS	379/366 177/176	8.033 0.984	11.427 10.637	0.042 0.023	0.021 0.011
J12373-208	LP 795-038	12:37:21.57	-20:52:34.9	ASAS NSVS Catalina	579/557 96/91 238/230	8.690 0.984 7.976	13.354 12.147 11.906	0.191 0.038 0.031	0.095 0.021 0.050
J12388+116	Wolf 433	12:38:52.42	+11:41:46.2	ASAS NSVS	339/320 187/182	8.005 0.984	11.521 10.500	0.043 0.023	0.023 0.016
J12428+418	G 123-055	12:42:49.96	+41:53:46.9	SuperWASP	7095/6444	4.044	11.904	0.085	0.027
J12479+097	Wolf 437	12:47:56.64	+09:45:05.0	ASAS NSVS	352/336 177/165	8.033 0.984	11.410 10.282	0.066 0.032	0.022 0.010
J13005+056	FN Vir	13:00:33.51	+05:41:08.1	MEarth-2010 MEarth-2014-tel02 MEarth-2014-tel08	1318/1269 1010/968 1142/1099	1.591 2.594 1.203	0.000 0.002 -0.001	0.007 0.009 0.009	0.003 0.004 0.004
J13102+477	G 177-025	13:10:12.69	+47:45:19.0	MEarth-2011 MEarth-2014-tel04 MEarth-2014-tel05	878/788 2183/2125 1956/1898	0.670 2.624 0.621	0.001 0.000 0.000	0.042 0.012 0.011	0.004 0.003 0.004
J13196+333	Ross 1007	13:19:40.15	+33:20:47.8	SuperWASP NSVS Catalina	14259/12982 46/45 212/187	3.077 0.855 7.123	10.673 9.863 11.612	0.048 0.026 0.050	0.016 0.011 0.050

**Table A.1.** M dwarfs searched for photometric periods (cont.).

Karmn	Name	$\alpha$ (J2000.0)	$\delta$ (J2000.0)	Survey	$N_{\text{obs}}/N_{\text{used}}$	$\Delta t$ [a]	$\bar{m}$ [mag]	$\sigma_m$ [mag]	$\overline{\delta m}$ [mag]
J13209+342	BD+35 2439	13:20:57.97	+34:16:44.7	SuperWASP NSVS	11384/9494 54/54	3.118 0.855	10.696 9.912	0.0067 0.034	0.018 0.011
J13229+244	Ross 1020	13:22:56.74	+24:28:03.4	SuperWASP MEarth-2010 MEarth-2014	7738/7005 757/733 309/303	3.077 1.479 2.591	12.716 0.000 0.000	0.079 0.009 0.009	0.033 0.004 0.004
J13283-023W	Ross 486A	13:28:21.06	-02:21:36.5	ASAS	351/333	8.667	11.236	0.042	0.018
J13293+114	GJ 513	13:29:21.31	+11:26:26.5	ASAS MEarth-2014 NSVS Catalina	338/318 248/214 133/127 301/283	7.970 2.506 0.983 7.189	12.150 0.004 11.180 11.055	0.073 0.016 0.026 0.109	0.033 0.002 0.013 0.050
J13299+102	BD+11 2576	13:29:59.79	+10:22:37.6	ASAS	568/537	9.038	11.014	0.035	0.018
J13427+332	Ross 1015	13:42:43.29	+33:17:25.5	SuperWASP	7630/7592	3.118	11.846	0.109	0.021
J13450+176	BD+18 2776	13:45:05.03	+17:47:10.5	ASAS-SN	795/771	5.093	14.076	0.686	0.033
J13457+148	HD 119850	13:45:43.54	+14:53:31.8	ASAS	314/281	6.547	8.456	0.036	0.015
J13458-179	LP 798-034	13:45:50.75	-17:58:04.8	ASAS K2	479/467 3530/3530	8.720 0.215	11.865 0.997	0.047	0.024
J13536+776	RX J1353.6+7737	13:53:38.77	+77:37:08.3	MEarth-2010	4253/4159	1.501	0.001	0.013	0.004
J13582+125	Ross 837	13:58:13.93	+12:34:43.8	ASAS Catalina	400/381 335/314	7.978 8.186	11.011 11.047	0.023 0.216	0.037 0.050
J13591-198	LP 799-007	13:59:10.46	-19:50:03.5	ASAS Catalina Montcabrer	522/512 125/120 197/190	8.719 4.789 0.134	12.701 11.291 10.674	0.104 0.131 0.023	0.040 0.050 0.003
J14010-026	HD 122303	14:01:03.25	-02:39:18.1	ASAS	367/354	8.640	9.708	0.017	0.013
J14082+805	BD+81 465	14:08:12.98	+80:35:50.0	NSVS	60/58	0.973	9.716	0.021	0.010
J14152+450	Ross 992	14:15:17.07	+45:00:53.6	SuperWASP	6217/5775	2.129	11.847	0.049	0.019
J14155+046	GJ 1182 AB	14:15:32.54	+04:39:31.2	MEarth-2014	1203/1146	2.468	0.001	0.040	0.003
J14173+454	RX J1417.3+4525	14:17:22.10	+45:25:46.1	SuperWASP Catalina	5939/5899 176/170	2.128 8.090	11.916 12.705	0.167	0.021 0.117
J14251+518	$\theta$ Boo B	14:25:11.61	+51:49:53.5	...	...	...	...	...	...
J14257+236W	BD+24 2733A	14:25:43.49	+23:37:01.1	SuperWASP	6583/6408	3.918	9.339	0.114	0.016
J14257+236E	BD+24 2733B	14:25:46.67	+23:37:13.3	SuperWASP	5013/4609	3.918	8.806	0.100	0.018
J14294+155	Ross 130	14:29:29.72	+15:31:57.9	ASAS	333/317	6.547	10.678	0.033	0.016
J14307-086	BD-07 3856	14:30:47.79	-08:38:46.6	ASAS	420/390	8.695	9.378	0.027	0.015
J14310-122	Wolf 1478	14:31:01.20	-12:17:45.2	ASAS NSVS	461/440 108/106	8.706 0.984	11.900 10.838	0.054	0.037 0.012
J14321+081	LP 560-035	14:32:08.50	+08:11:31.3	MEarth-2010 MEarth-2014 Catalina	1394/1334 557/529 377/363	1.539 0.482 8.194	0.000 0.001 13.622	0.014 0.017 0.027	0.006 0.006 0.050
J14342-125	HN Lib	14:34:16.83	-12:31:10.7	ASAS	513/477	8.728	11.339	0.037	0.019
J14524+123	G 066-037	14:52:28.54	+12:23:33.0	ASAS NSVS	406/396 188/179	7.978 0.984	11.578 10.727	0.047 0.027	0.022 0.011
J14544+355	Ross 1041	14:54:27.91	+35:32:57.0	SuperWASP MEarth-2010 MEarth-2014 NSVS Catalina	13711/12351 187/178 334/318 224/217 277/261	3.962 0.528 2.556 0.984 8.167	12.188 0.000 0.000 11.254 11.113	0.071 0.006 0.008 0.034 0.129	0.028 0.003 0.004 0.012 0.050
J15013+055	G 015-002	15:01:20.11	+05:32:55.4	ASAS	362/342	8.022	12.144	0.064	0.029
J15095+031	Ross 1047	15:09:35.59	+03:10:00.8	ASAS	550/505	8.682	11.509	0.075	0.028
J15194-077	HO Lib	15:19:26.89	-07:43:20.1	ASAS	742/685	8.711	10.574	0.046	0.014
J15218+209	OT Ser	15:21:52.92	+20:58:39.5	SuperWASP ASAS	15065/13716 300/288	3.153 6.447	10.048 10.013	0.047	0.013
J15305+094	NLTT 40406	15:30:30.33	+09:26:01.4	MEarth-2010 Catalina	762/703 370/349	4.060 8.197	0.000 13.096	0.011 0.051	0.006 0.050
J15369-141	Ross 802	15:36:58.68	-14:08:00.6	ASAS	476/456	8.176	12.771	0.113	0.055
J15412+759	UU UMi AB	15:41:16.43	+75:59:34.8	MEarth-2010 MEarth-2014	1432/1405 1047/975	2.047 2.696	0.000 0.000	0.011 0.029	0.003 0.006
J15474-108	LP 743-031 AB	15:47:24.64	-10:53:47.1	ASAS	472/444	8.717	11.310	0.070	0.021
J15499+796	LP 022-420	15:49:55.18	+79:39:51.7	MEarth-2010 MEarth-2014 NSVS	229/215 156/143 239/226	1.992 2.690 0.984	0.000 -0.001 13.144	0.000 0.009 0.049	0.004 0.003 0.038
J15598-082	BD-07 4156	15:59:53.37	-08:15:11.4	ASAS	465/425	8.716	10.478	0.043	0.022
J16028+205	GJ 609	16:02:50.98	+20:35:21.8	ASAS MEarth-2010 MEarth-2014	299/285 209/209 376/356	6.465 1.995 2.495	12.639 0.000 0.000	0.099 0.007 0.009	0.047 0.003 0.004
J16092+093	G 137-084	16:09:16.25	+09:21:07.7	ASAS	348/340	8.074	11.083	0.027	0.021
J16102-193	K2-33	16:10:14.74	-19:19:09.5	K2 NSVS	3341/3341 175/166	0.212 0.984	0.000 10.478	0.0087	...
J16167+672S	HD 147379	16:16:42.80	+67:14:19.7	ASAS-SN AstroLAB IRIS	759/722 37/36	5.836 0.3046	8.874 8.436	0.084 0.013	0.005 0.012
J16167+672N	EW Dra	16:16:45.37	+67:15:22.4	AstroLAB IRIS	71/68	0.556	10.615	0.013	0.006
J16254+543	GJ 625	16:25:24.59	+54:18:14.9	SuperWASP	19221/16794	2.312	10.205	0.084	0.049

**Table A.1.** M dwarfs searched for photometric periods (cont.).

Karmn	Name	$\alpha$ (J2000.0)	$\delta$ (J2000.0)	Survey	$N_{\text{obs}}/N_{\text{used}}$	$\Delta t$ [a]	$\bar{m}$ [mag]	$\sigma_m$ [mag]	$\overline{\delta m}$ [mag]
J16303-126	V2306 Oph	16:30:18.09	-12:39:43.4	ASAS	538/497	8.659	10.124	0.041	0.017
J16313+408	G 180-060	16:31:18.79	+40:51:51.6	HATNet SuperWASP MEarth-2010 NSVS Catalina	8406/8202 25811/23475 1249/1231 256/237 337/292	0.482 4.255 1.036 0.983 8.386	10.695 14.458 0.000 13.104 13.008	0.023 0.129 0.012 0.078 0.092	0.022 0.104 0.004 0.049 0.050
J16327+126	GJ 1203	16:32:45.25	+12:36:46.0	ASAS	385/372	6.592	12.187	0.072	0.034
J16462+164	LP 446-006	16:46:13.72	+16:28:40.7	ASAS	442/418	6.589	11.671	0.065	0.027
J16554-083N	GJ 643	16:55:25.27	-08:19:20.8	ASAS	426/391	8.665	11.769	0.085	0.059
J16555-083	vB 8	16:55:35.29	-08:23:40.1	Catalina NSVS	189/171 73/68	7.178 0.929	13.440 13.829	0.067 0.093	0.050 0.110
J16570-043	LP 686-027	16:57:05.71	-04:20:56.0	NSVS ASAS	120/120 443/410	0.973 8.626	11.177 12.286	0.026 0.059	0.015 0.034
J16581+257	BD+25 3173	16:58:08.85	+25:44:39.2	ASAS	233/219	6.566	9.665	0.052	0.012
J17033+514	G 203-042	17:03:23.85	+51:24:21.9	SuperWASP ASAS-SN	27968/26084 535/524	2.339 2.670	13.507 13.943	0.070 0.062	0.051 0.028
J17052-050	Wolf 636	17:05:13.84	-05:05:38.6	ASAS	542/519	8.665	10.103	0.027	0.015
J17071+215	Ross 863	17:07:07.52	+21:33:14.4	SuperWASP ASAS NSVS	13190/10764 235/221 142/134	2.942 6.564 4.466	11.702 11.641 10.674	0.126 0.047 0.036	0.024 0.020 0.012
J17115+384	Wolf 654	17:11:34.72	+38:26:34.1	SuperWASP	23748/22484	2.339	11.712	0.033	0.022
J17166+080	GJ 2128	17:16:40.97	+08:03:30.2	ASAS	482/460	8.110	11.477	0.047	0.022
J17198+417	GJ 671	17:19:52.67	+41:42:51.1	SuperWASP	37833/33620	4.244	11.471	0.044	0.017
J17303+055	BD+05 3409	17:30:22.73	+05:32:54.7	ASAS	358/336	7.901	9.300	0.036	0.014
J17338+169	1RXS J173353.5+165515	17:33:53.15	+16:55:12.9	MEarth-2010 NSVS	685/685 215/205	2.027 0.964	0.000 12.640	0.024 0.066	0.003 0.043
J17355+616	BD+61 1678C	17:35:34.46	+61:40:54.0	Montsec	642/613	0.912	9.410	0.016	0.002
J17378+185	BD+18 3421	17:37:53.30	+18:35:29.5	ASAS	592/559	6.566	9.577	0.030	0.013
J17542+073	GJ 1222	17:54:17.10	+07:22:44.7	ASAS MEarth-2010 MEarth-2014	414/387 638/613 689/668	8.000 2.047 2.701	13.256 0.000 0.000	0.142 0.007 0.008	0.085 0.002 0.004
J17578+046	Barnard's Star	17:57:48.49	+04:41:40.5	MEarth-2010 MEarth-2014 MEarth-2014	900/852 1045/992 535/528	0.621 2.705 2.715	0.001 -0.002 9.560	0.021 0.040 0.032	0.010 0.014 0.005
J17578+465	G 204-039	17:57:50.96	+46:35:18.2	SuperWASP	14884/13911	4.244	11.576	0.077	0.017
J18022+642	LP 071-082	18:02:16.60	+64:15:44.6	HATNet MEarth-2010 MEarth-2011	8832/8639 286/274 1813/1763	0.758 1.981 0.638	8.920 0.000 0.000	0.005 0.011 0.014	0.003 0.004 0.004
J18027+375	GJ 1223	18:02:46.25	+37:31:04.9	MEarth-2010 MEarth-2014-tel03 MEarth-2014-tel08	20385/17417 694/681 1051/1027	4.274 1.926 2.693	14.651 0.000 -0.001	0.110 0.009 0.008	0.163 0.004 0.003
J18051-030	HD 165222	18:05:07.56	-03:01:52.4	ASAS	427/384	8.622	9.383	0.036	0.016
J18075-159	GJ 1224	18:07:32.93	-15:57:46.5	K2	2783/2758	0.187	1.000	0.004	...
J18131+260	LP 390-016	18:13:06.57	+26:01:51.9	ASAS MEarth	510/491 1021/998	8.693 2.682	13.875 -0.006	0.235 0.017	0.175 0.004
J18165+048	G 140-051	18:16:31.54	+04:52:45.6	SuperWASP HATNet	5476/5040 8881/8764	3.279 0.315	12.981 9.954	0.066 0.042	0.041 0.006
J18174+483	TYC 3529-1437-1	18:17:25.14	+48:22:02.4	SuperWASP	18943/18229	4.274	11.204	0.056	0.026
J18180+387E	G 204-058	18:18:04.28	+38:46:34.2	SuperWASP	15282/14479	4.244	11.813	0.054	0.028
J18189+661	LP 071-165	18:18:57.26	+66:11:33.2	MEarth-2010 MEarth-2014-tel03 MEarth-2014-tel05	863/832 1873/1769 1694/1620	1.663 2.690 0.776	0.000 0.000 0.000	0.009 0.010 0.015	0.005 0.004 0.004
J18198-019	HD 168442	18:19:50.85	-01:56:19.1	ASAS	510/504	8.674	9.652	0.019	0.016
J18221+063	Ross 136	18:22:06.71	+06:20:37.7	MEarth-2010 MEarth-2014 ASAS	600/578 464/445 419/394	0.723 2.701 8.003	0.000 0.000 12.611	0.006 0.010 0.100	0.002 0.004 0.055
J18224+620	GJ 1227	18:22:27.19	+62:03:02.5	MEarth-2010 MEarth-2014-tel03 MEarth-2014-tel08	1205/1181 385/373 169/160	0.688 2.682 0.288	0.001 0.000 -0.002	0.009 0.023 0.014	0.003 0.005 0.004
J18319+406	G 205-028	18:31:58.40	+40:41:10.4	SuperWASP	18751/18037	4.274	11.542	0.038	0.017
J18346+401	LP 229-017	18:34:36.64	+40:07:26.7	SuperWASP	18671/17831	4.274	11.318	0.042	0.017
J18353+457	BD+45 2743	18:35:18.33	+45:44:37.9	SuperWASP MEarth-2010 MEarth-2014	13084/7411 3598/3415 405/384	4.274 1.733 2.696	9.763 0.000 0.001	0.051 0.012 0.009	0.326 0.002 0.002
J18356+329	LSR J1835+3259	18:35:37.90	+32:59:54.6	MEarth-2010	1554/1498	1.615	0.001	0.019	0.009

**Table A.1.** M dwarfs searched for photometric periods (cont.).

Karmn	Name	$\alpha$ (J2000.0)	$\delta$ (J2000.0)	Survey	$N_{\text{obs}}/N_{\text{used}}$	$\Delta t$ [a]	$\bar{m}$ [mag]	$\sigma_m$ [mag]	$\overline{\delta m}$ [mag]
J18363+136	Ross 149	18:36:19.23	+13:36:26.2	NSVS	145/138	0.967	13.185	0.090	0.081
				ASAS	284/273	6.619	12.295	0.076	0.045
				MEarth-2010	620/594	1.964	0.000	0.006	0.002
				MEarth-2011	1688/1610	0.712	0.000	0.009	0.004
				MEarth-2014	512/499	2.685	0.000	0.011	0.004
J18409-133	BD-13 5069	18:40:57.33	-13:22:45.6	ASAS-SN	548/539	3.027	10.643	0.042	0.008
				NSVS	111/110	0.885	10.403	0.023	0.012
				ASAS	484/460	8.625	12.211	0.066	0.038
				MEarth-2010	616/600	2.025	0.000	0.008	0.005
				MEarth-2011	1040/1002	0.672	0.000	0.018	0.003
J18498-238	GJ 729	18:49:49.36	-23:50:10.4	ASAS	640/633	8.646	10.545	0.038	0.018
J18580+059	BD+05 3993	18:58:00.14	+05:54:29.7	ASAS	474/451	8.085	9.226	0.045	0.019
J19070+208A	Ross 730	19:07:05.56	+20:53:16.8	MEarth-2010	639/614	0.692	0.000	0.007	0.003
				ASAS	220/209	6.534	10.781	0.023	0.015
				MEarth-2010	639/620	0.692	0.000	0.007	0.003
				MEarth-2011	917/884	0.692	0.000	0.010	0.004
				MEarth-2010	654/618	0.721	0.000	0.007	0.003
J19072+208	HD 349726	19:07:13.20	+20:52:37.3	ASAS	220/209	6.534	10.813	0.029	0.021
J19084+322	G 207-019	19:08:29.96	+32:16:52.0	MEarth-2010	1293/1210	0.513	-0.002	0.014	0.003
J19098+176	GJ 1232	19:09:50.98	+17:40:07.4	MEarth-2010	1293/1210	0.513	-0.002	0.014	0.003
J19169+051N	V1428 Aql	19:16:55.26	+05:10:08.6	ASAS	404/389	8.068	9.144	0.047	0.014
J19169+051S	V1298 Aql (vB 10)	19:16:57.62	+05:09:02.2	MEarth-2010	1446/1320	1.099	0.021	0.064	0.002
J19216+208	GJ 1235	19:21:38.68	+20:52:02.8	ASAS	198/191	6.504	13.578	0.212	0.148
J19251+283	Ross 164	19:25:08.46	+28:21:13.2	MEarth-2010	1754/1672	1.661	0.000	0.012	0.005
				MEarth-2011	2139/2097	0.675	0.000	0.010	0.003
J19255+096	LSPM J1925+0938	19:25:30.89	+09:38:23.5	NSVS	133/131	0.901	11.511	0.055	0.029
J19346+045	BD+04 4157	19:34:39.82	+04:34:57.2	MEarth-2010	1101/1070	0.781	0.002	0.027	0.009
				MEarth-2014-tel06	955/920	2.682	0.000	0.028	0.013
				MEarth-2014-tel08	931/892	0.776	0.000	0.019	0.010
J19422-207	2M J19421282-2045477	19:42:12.82	-20:45:47.8	ASAS	749/696	8.211	9.362	0.038	0.017
J19511+464	G 208-042	19:51:09.31	+46:28:59.9	Catalina	169/159	8.542	14.343	0.323	0.178
				SuperWASP	225/218	7.901	12.370	0.247	0.056
				HATNet	6164/5861	2.156	11.242	0.112	0.004
J20093-012	2M J20091824-0113377	20:09:18.24	-01:13:37.7	MEarth-2010	477/468	0.612	0.001	0.009	0.002
				MEarth-2014	298/290	2.693	0.001	0.009	0.004
				ASAS	70/67	7.981	15.123	0.498	0.040
J20198+229	LP 395-008 AB	20:19:49.25	+22:56:36.7	NSVS	126/126	0.923	12.861	0.051	0.057
J20260+585	Wolf 1069	20:26:05.29	+58:34:22.5	SuperWASP	986/887	1.281	11.852	0.033	0.028
				ASAS	225/221	6.504	12.005	0.075	0.025
				MEarth-2016-tel01	2635/2579	2.772	0.000	0.008	0.003
J20305+654	GJ 793	20:30:32.08	+65:26:58.6	MEarth-2016-tel05	2730/2692	4.060	0.000	0.010	0.003
				SuperWASP	10529/10133	2.156	12.288	0.163	0.034
				ASAS-SN	476/473	2.945	10.529	0.017	0.005
				SuperWASP	5908/5247	2.145	12.295	0.219	0.030
				ASAS	263/245	6.512	13.640	0.206	0.154
J20450+444	BD+44 3567	20:45:04.03	+44:29:56.2	MEarth-2010	377/366	1.719	0.000	0.015	0.004
				MEarth-2011	1119/1104	0.650	0.001	0.014	0.003
				MEarth-2014-tel03	1541/1458	1.686	0.000	0.011	0.003
				MEarth-2014-tel07	2773/2637	2.716	0.000	0.010	0.003
				SuperWASP	3168/2920	0.410	10.907	0.019	0.014
J20525-169	LP 816-060	20:52:33.04	-16:58:29.0	ASAS	519/504	8.540	11.443	0.036	0.019
J20533+621	BD+61 2068	20:53:19.78	+62:09:15.8	AstroLAB IRIS	101/99	0.630	8.567	0.031	0.007
				ASAS-SN	801/765	3.684	8.801	0.050	0.004
				ASAS	409/388	8.476	12.529	0.096	0.046
J20556-140N	GJ 810 AB	20:55:37.72	-14:02:07.8	Catalina	215/206	5.454	12.929	0.078	0.050
				ASAS	395/370	8.627	11.492	0.056	0.028
				ASAS	397/370	8.532	11.251	0.057	0.020
J21019-063	Wolf 906	21:01:58.66	-06:19:07.1	ASAS	217/205	6.438	12.111	0.046	0.034
J21152+257	LP 397-041	21:15:12.59	+25:47:45.4	SuperWASP	2324/2140	4.225	11.820	0.056	0.040
				ASAS	388/374	8.956	11.971	0.057	0.027
				ASAS	4464/4221	4.225	10.622	0.086	0.031
J21164+025	LSPM J2116+0234	21:16:27.29	+02:34:51.5	SuperWASP	6022/5565	1.645	11.792	0.056	0.026
				ASAS	6641/5791	4.211	11.785	0.055	0.023
				MEarth-2010	727/681	2.046	0.000	0.008	0.002
J21221+229	GSC 02187-00512	21:22:06.27	+22:55:53.1	MEarth-2014	466/442	2.683	0.000	0.015	0.005
				ASAS-SN	452/435	2.852	12.198	0.012	0.011
				ASAS	230/226	0.579	0.000	0.006	0.002
J21463+382	LSPM J2146+3813	21:46:22.06	+38:13:04.8	MEarth-2010	255/250	0.246	0.000	0.011	0.003
				MEarth-2011	727/681	2.046	0.000	0.008	0.002
				ASAS	452/435	2.852	12.198	0.012	0.011
J21466+668	G 264-012	21:46:40.22	+66:48:10.6	MEarth-2010	230/226	0.579	0.000	0.006	0.002
J21466+668	G 264-012	21:46:40.22	+66:48:10.6	MEarth-2011	255/250	0.246	0.000	0.011	0.003

**Table A.1.** M dwarfs searched for photometric periods (cont.).

Karmn	Name	$\alpha$ (J2000.0)	$\delta$ (J2000.0)	Survey	$N_{\text{obs}}/N_{\text{used}}$	$\Delta t$ [a]	$\bar{m}$ [mag]	$\sigma_m$ [mag]	$\overline{\delta m}$ [mag]
J21466-001	Wolf 940	21:46:40.40	-00:10:23.4	MEarth-2014	305/288	2.685	0.000	0.007	0.004
J22012+283	V374 Peg	22:01:13.11	+28:18:24.9	ASAS SuperWASP MEarth-2014	338/321 18405/16388 1004/938	9.011 4.222 2.701	12.681 11.690 0.000	0.088 0.074 0.036	0.038 0.039 0.006
J22020-194	LP 819-017	22:02:00.70	-19:28:59.3	ASAS	538/523	8.866	12.052	0.056	0.032
J22021+014	BD+00 4810	22:02:10.26	+01:24:00.6	ASAS	323/313	9.011	9.147	0.020	0.015
J22057+656	G 264-018 A	22:05:45.36	+65:38:55.5	NSVS	149/133	3.590	10.965	0.021	0.015
J22096-046	BD-05 5715	22:09:40.30	-04:38:26.8	ASAS	440/424	8.866	10.366	0.068	0.022
J22114+409	1RXS J221124.3+410000	22:11:24.17	+40:59:58.7	SuperWASP	6216/5736	2.107	13.332	0.057	0.038
J22115+184	Ross 271	22:11:30.08	+18:25:34.1	ASAS	382/361	6.544	10.253	0.050	0.016
J22125+085	Wolf 1014	22:12:35.96	+08:33:11.1	ASAS	252/239	8.874	12.024	0.074	0.033
J22137-176	LP 819-052	22:13:42.78	-17:41:08.2	ASAS K2	323/302 2986/2986	8.967 0.183	13.703 1.006	0.209	0.104
J22231-176	LP 820-012	22:23:06.97	-17:36:25.0	ASAS	386/363	8.967	13.313	0.133	0.063
J22252+594	G 232-070	22:25:17.06	+59:24:49.6	ASAS-SN MEarth-2016 MEarth-2010	521/512 671/656 246/242	3.022 4.063 0.611	12.965 0.000 0.001	0.027	0.017
J22298+414	G 215-050	22:29:48.86	+41:28:48.0	SuperWASP MEarth-2011 MEarth-2014	20894/18133 426/415 281/265	4.153 0.169 2.685	12.584 0.000 0.000	0.080	0.057
J22330+093	BD+08 4887	22:33:02.25	+09:22:41.1	ASAS	254/243	8.874	10.377	0.026	0.016
J22468+443	EV Lac	22:46:49.81	+44:20:03.1	SuperWASP	5963/5728	2.107	10.298	0.118	0.023
J22503-070	BD-07 5871	22:50:19.43	-07:05:24.5	ASAS	373/355	8.970	9.852	0.040	0.017
J22518+317	GT Peg	22:51:53.49	+31:45:15.3	SuperWASP	13465/12160	4.153	11.477	0.075	0.022
J22532-142	IL Aqr	22:53:16.72	-14:15:48.9	ASAS	400/379	9.003	10.206	0.084	0.017
J22559+178	StKM 1-2065	22:55:59.85	+17:48:39.9	ASAS	568/537	9.038	11.014	0.035	0.018
J22565+165	HD 216899	22:56:34.97	+16:33:13.0	ASAS	238/229	6.425	8.662	0.057	0.016
J23064-050	2MUCD 12171 (Trappist-1)	23:06:29.28	-05:02:28.6	K2 Catalina	3558/3512 314/304	0.216 0.766	1.000 15.565	0.004 0.042	...
J23113+085	NLTT 56083	23:11:23.78	+08:31:01.4	ASAS MEarth-2010 MEarth-2014	339/319 370/358 468/444	8.915 0.686 0.000	12.605 0.000 0.007	0.105 0.052 0.003	...
J23216+172	LP 462-027	23:21:37.52	+17:17:28.5	ASAS	270/250	6.948	11.749	0.054	0.025
J23245+578	BD+57 2735	23:24:30.49	+57:51:15.3	SuperWASP	2350/1898	2.099	10.350	0.120	0.028
J23340+001	GJ 899	23:34:03.28	+00:10:45.2	ASAS K2	305/287 287/284	8.967 0.018	11.190 1.000	0.038 0.001	0.019
J23351-023	GJ 1286	23:35:10.50	-02:23:21.4	NSVS Catalina	157/148 276/275	0.503 7.203	12.058 12.690	0.036 0.100	0.021 0.050
J23381-162	G 273-093	23:38:08.19	-16:14:10.0	ASAS	432/409	8.915	11.330	0.080	0.021
J23419+441	HH And	23:41:54.99	+44:10:40.8	SuperWASP	14988/13827	2.096	12.039	0.085	0.028
J23431+365	GJ 1289	23:43:06.29	+36:32:13.2	NSVS MEarth-2010 MEarth-2014-tel01	235/232 520/509 325/332	0.676 0.722 2.704	11.352 0.001 0.001	0.035 0.008 0.012	0.014 0.004 0.005
J23492+024	BR Psc	23:49:12.56	+02:24:03.8	ASAS	325/307	8.983	8.981	0.041	0.017
J23505-095	LP 763-012	23:50:31.59	-09:33:32.1	Catalina	87/87	6.071	11.313	0.319	0.05
J23548+385	RX J2354.8+3831	23:54:51.47	+38:31:36.3	SuperWASP	307/297	0.901	13.025	0.105	0.070
J23556-061	GJ 912	23:55:39.81	-06:08:32.8	ASAS	190/190	8.092	12.095	0.084	0.050
J23585+076	Wolf 1051	23:58:32.64	+07:39:30.4	ASAS	241/229	8.937	11.777	0.045	0.022

**Table A.2.** Rotation periods obtained for stars in our sample.

Karmn	$P_{\text{rot}}$ [d]	$A$ [mag]	FAP (%)	Survey	$P_{\text{rot,lit}}$ [d]	$A_{\text{lit}}$ [mag]	FAP <sub>lit</sub> (%)	Ref. <sup>a</sup>
J00051+457 <sup>b</sup>	$15.37 \pm 0.09$	0.003	$< 10^{-4}$	SuperWASP	$21.2 \pm 0.5$	...	<0.1	SM17
J00162+198E	$105 \pm 44$	0.006	$< 10^{-4}$	MEarth	104	0.0049	...	Irw11
J00162+198W	$4.83 \pm 0.06$	0.007	$< 10^{-4}$	MEarth	4.79	...	...	Nor07
J00389+306	$50.2 \pm 1.3$	0.009	$< 10^{-4}$	SuperWASP	...	...	...	...
J01019+541	$0.2779 \pm 0.0006$	0.007	$< 10^{-4}$	MEarth	0.278	...	...	New16
J01025+716	$51.5 \pm 2.6$	0.025	$< 10^{-4}$	ASAS-SN	...	...	...	...
J01026+623	$19.9 \pm 0.4$	0.006	$< 10^{-4}$	MEarth	$18.4 \pm 0.7$	...	<1	SM17
J01033+623	$1.02 \pm 0.01$	0.051	$< 10^{-4}$	MEarth	1.06	0.046	...	Irw11
J01125-169	$69.2 \pm 2.4$	0.030	0.3	ASAS	69.2	0.015	<0.1	SM16
J01339-176	$27.1 \pm 0.4$	0.064	0.05	ASAS	...	...	...	...
J01221+221	$0.564 \pm 0.001$	0.012	$< 10^{-4}$	SuperWASP	...	...	...	...
J02070+496	$7.20 \pm 0.13$	0.039	$< 10^{-4}$	SuperWASP	...	...	...	...
J02088+494	$0.74759 \pm 0.00019$	0.021	$< 10^{-4}$	SuperWASP	...	...	...	...
J02222+478	$29.5 \pm 0.4$	0.007	$< 10^{-4}$	SuperWASP	...	...	...	...
J02358+202	$31.9 \pm 0.6$	0.007	$< 10^{-4}$	SuperWASP	...	...	...	...
J02442+255	$38.7 \pm 3.7$	0.006	$< 10^{-4}$	SuperWASP	...	...	...	...
J02519+224	$0.85757 \pm 0.00003$	0.010	$< 10^{-4}$	SuperWASP	...	...	...	...
J03181+382	$77.2 \pm 3.0$	0.004	$< 10^{-4}$	SuperWASP	...	...	...	...
J03213+799	$32.4 \pm 1.0$	0.030	$< 10^{-4}$	AstroLAB IRIS	...	...	...	...
J03217-066	$21.1 \pm 0.1$	0.017	1.20	ASAS	...	...	...	...
J03473-019	$3.87 \pm 0.01$	0.048	$< 10^{-4}$	ASAS	3.88	...	...	Kir12
J04225+105	$5.48 \pm 0.01$	0.006	$< 10^{-4}$	MEarth	...	...	...	...
J04290+219	$25.4 \pm 0.3$	0.011	1.9	ASAS	...	...	...	...
J04429+189	$40.7 \pm 0.4$	0.013	0.5	ASAS	38.92	...	...	KS07
J04429+214	$47.8 \pm 1.1$	0.045	0.049	ASAS	...	...	...	...
J04472+206 <sup>c</sup>	$0.3426 \pm 0.0003$	0.015	$< 10^{-4}$	K2	...	...	...	...
J05019+011	$2.12 \pm 0.02$	0.023	$< 10^{-4}$	Montcabrer	...	...	...	...
J05062+046	$0.8650 \pm 0.0006$	0.012	0.38	NSVS	0.89	...	...	Kir12
J05280+096	$17.2 \pm 0.1$	0.054	0.92	ASAS	...	...	...	...
J05314-036	$33.8 \pm 0.6$	0.011	0.0025	ASAS	33.61	...	...	KS07
J05365+113	$12.3 \pm 0.1$	0.022	$< 10^{-4}$	ASAS	12.04	...	...	Kir12
J06000+027	$1.81 \pm 0.01$	0.014	$< 10^{-4}$	MEarth	1.81	...	...	Irw11
J06024+498	$105 \pm 6$	0.011	$< 10^{-4}$	MEarth	99.6	0.0176	...	Irw11
J06103+821	$44.6 \pm 1.0$	0.010	$< 10^{-4}$	ASAS-SN	...	...	...	...
J06105-218	$27.3 \pm 0.2$	0.009	9.6	ASAS	27.3	0.029	11.4	SM16
J06318+414 <sup>d</sup>	$0.29952 \pm 0.00007$	0.024	$< 10^{-4}$	SuperWASP	0.300	...	...	New16
J06421+035	$83.4 \pm 7.0$	0.013	$< 10^{-4}$	MEarth	...	...	...	...
J06548+332	$18.1 \pm 0.3$	0.006	$< 10^{-4}$	SuperWASP	...	...	...	...
J07033+346	$8.04 \pm 0.03$	0.016	$< 10^{-4}$	SuperWASP	...	...	...	...
J07319+362N	$16.4 \pm 0.3$	0.029	$< 10^{-4}$	SuperWASP	...	...	...	...
J07353+548	$21.8 \pm 1.0$	0.008	$< 10^{-4}$	SuperWASP	...	...	...	...
J07361-031	$12.2 \pm 0.1$	0.017	0.038	ASAS	12.16	...	...	Kir12
J07446+035	$2.78 \pm 0.01$	0.025	$< 10^{-4}$	MEarth	2.77	...	...	Kir12
J07472+503	$1.32 \pm 0.01$	0.029	$< 10^{-4}$	SuperWASP	...	...	...	...
J07558+833	$1.11 \pm 0.01$	0.010	$< 10^{-4}$	MEarth	1.11	...	...	Irw11
J08119+087	$5.42 \pm 0.15$	0.004	$< 10^{-4}$	MEarth	...	...	...	...
J08161+013	$40.7 \pm 0.4$	0.009	1.0	ASAS	...	...	...	...
J08298+267	$0.45900 \pm 0.00001$	0.005	$< 10^{-4}$	MEarth	0.459	...	...	New16
J08315+730	$105 \pm 11$	0.005	$< 10^{-4}$	MEarth	...	...	...	...
J08402+314	$118 \pm 14$	0.005	$< 10^{-4}$	MEarth	110.7	...	...	New16
J09140+196	$89.9 \pm 2.0$	0.043	1.8	ASAS	...	...	...	...
J09423+559	$74.3 \pm 2.8$	0.011	$< 10^{-4}$	MEarth	72.8	...	...	Irw11
J09425+700	$21.0 \pm 0.4$	0.040	$< 10^{-4}$	AstroLAB IRIS	...	...	...	...
J09428+700	$23.9 \pm 0.6$	0.023	$< 10^{-4}$	AstroLAB IRIS	...	...	...	...
J09439+269	$13.7 \pm 0.9$	0.009	$< 10^{-4}$	Montcabrer	...	...	...	...
J10122-037	$21.6 \pm 0.2$	0.017	$< 10^{-4}$	ASAS	21.56	...	...	Kir12

**Table A.2.** Rotation periods obtained for stars in our sample (cont.).

Karmn	$P_{\text{rot}}$ [d]	$A$ [mag]	FAP [%]	Survey	$P_{\text{rot,lit}}$ [d]	$A_{\text{lit}}$ [mag]	FAP <sub>lit</sub> [%]	Ref. <sup>a</sup>
J10354+694	118±10	0.022	< 10 <sup>-4</sup>	NSVS	...	...	...	...
J10416+376	54.3±4.4	0.004	< 10 <sup>-4</sup>	MEarth	...	...	...	...
J10508+068 <sup>e</sup>	64±19	0.010	< 10 <sup>-4</sup>	K2	...	...	...	...
J10564+070	2.704±0.003	0.003	< 10 <sup>-4</sup>	K2	...	...	...	...
J11026+219	14.6±0.2	0.046	< 10 <sup>-4</sup>	SuperWASP	14	...	...	Fek00
J11302+076	36.4±0.3	0.007	< 10 <sup>-4</sup>	K2	38.6	...	0.1	Clo17
J11417+427	71.5±5.1	0.003	< 10 <sup>-4</sup>	HATNet	73.5	...	...	Har11
J11421+267	44.6±2.0	0.009	< 10 <sup>-4</sup>	SuperWASP	44.1±0.2	...	...	Lot18
J11476+002	11.60±0.04	0.041	< 10 <sup>-4</sup>	K2	11.6	...	...	Kir12
J11477+008	163±3	0.014	10.0	ASAS	165.1	0.0078	0.2	SM16
J11509+483	125±23	0.006	< 10 <sup>-4</sup>	MEarth	132	...	...	Irw11
J11511+352	22.8±1.0	0.010	< 10 <sup>-4</sup>	SuperWASP	...	...	...	...
J12054+695	100±10	0.008	< 10 <sup>-4</sup>	MEarth	96.2	...	...	Irw11
J12189+111	0.49102±0.00003	0.013	< 10 <sup>-4</sup>	MEarth	0.49	...	...	Irw11
J12230+640	32.9±1.1	0.027	< 10 <sup>-4</sup>	NSVS	...	...	...	...
J12350+098	36.6±1.3	0.027	0.00039	NSVS	...	...	...	...
J12428+418	16.2±0.1	0.014	< 10 <sup>-4</sup>	SuperWASP	...	...	...	...
J13005+056	0.60022±0.00004	0.005	< 10 <sup>-4</sup>	MEarth	0.6	...	...	Irw11
J13102+477	28.8±0.8	0.017	< 10 <sup>-4</sup>	MEarth	28.8	0.0091	...	New16
J13536+776	1.23±0.01	0.017	< 10 <sup>-4</sup>	MEarth	1.2313	...	...	Wes15
J14152+450	52.8±1.4	0.009	< 10 <sup>-4</sup>	SuperWASP	...	...	...	...
J14257+236W	111±12	0.059	< 10 <sup>-4</sup>	SuperWASP	...	...	...	...
J14257+236E	17.6±0.5	0.009	< 10 <sup>-4</sup>	SuperWASP	...	...	...	...
J15218+209	3.37±0.01	0.023	< 10 <sup>-4</sup>	SuperWASP	3.3829	...	...	Nor07
J15305+094	0.3048±0.0006	0.002	0.0003	MEarth	0.305	0.0031	...	New16
J15412+759	83.4±10.4	0.004	< 10 <sup>-4</sup>	MEarth	...	...	...	...
J16102-193	6.263±0.015	0.018	< 10 <sup>-4</sup>	K2	6.3±0.2	...	...	Dav16
J16254+543	76.79±0.13	0.006	< 10 <sup>-4</sup>	SuperWASP	77.8±5.5	...	<1.2	SM17
J16303-126	119±1	0.010	0.7	ASAS	119.3	0.0059	<0.1	SM16
J16313+408	0.512±0.001...	0.008	< 10 <sup>-4</sup>	HATNet	0.51	...	...	Har11
J16554-083N	6.52±0.01	0.028	0.006	ASAS	...	...	...	...
J16570-043	0.547±0.001	0.028	1.4	NSVS	1.21	...	...	Kir12
J16581+257	23.8±0.1	0.012	0.0019	ASAS	...	...	...	...
J17052-050	50.2±1.3	0.012	0.00033	ASAS	...	...	...	...
J17115+384	62.6±2.0	0.008	< 10 <sup>-4</sup>	SuperWASP	...	...	...	...
J17198+417	71.5±2.6	0.005	< 10 <sup>-4</sup>	SuperWASP	...	...	...	...
J17338+169	0.26593±0.0003	0.031	< 10 <sup>-4</sup>	MEarth	0.27	...	...	Nor07
J17355+616	19.3±0.3	0.015	< 10 <sup>-4</sup>	Montsec	16.3±4.2	...	<0.1	SM17
J17578+465	30.3±0.9	0.006	< 10 <sup>-4</sup>	SuperWASP	31.64	...	...	Har11
J18022+642	0.28027±0.00002	0.005	< 10 <sup>-4</sup>	MEarth	0.28	...	...	New16
J18075-159	3.866±0.008	0.005	< 10 <sup>-4</sup>	K2	...	...	...	...
J18131+260	2.28±0.01	0.027	< 10 <sup>-4</sup>	MEarth	2.28	...	...	Har11
J18174+483	15.8±0.1	0.022	< 10 <sup>-4</sup>	SuperWASP	...	...	...	...
J18319+406	50.2±1.3	0.014	< 10 <sup>-4</sup>	SuperWASP	...	...	...	...
J18346+401	40.2±0.8	0.008	< 10 <sup>-4</sup>	SuperWASP	...	...	...	...
J18353+457	34.0±2.9	0.042	< 10 <sup>-4</sup>	SuperWASP	34.5±4.7	...	<0.1	SM17
J18356+329	0.118±0.001	0.008	< 10 <sup>-4</sup>	MEarth	0.118±0.01	...	...	Hal08
J18363+136	50.2±1.6	0.010	< 10 <sup>-4</sup>	MEarth	1.017	...	...	New16
J18482+076	2.76±0.01	0.007	< 10 <sup>-4</sup>	MEarth	2.756	...	...	New16
J18498-238	2.87±0.01	0.017	< 10 <sup>-4</sup>	ASAS	2.869	0.005	...	KS07
J18580+059	35.2±0.3	0.014	< 10 <sup>-4</sup>	ASAS	36.3±0.1	...	<0.1	SM17
J19072+208	3.80±0.01	0.013	0.91	ASAS	...	...	...	...
J19084+322	74.1±2.8	0.005	< 10 <sup>-4</sup>	MEarth	...	...	...	...
J19098+176	80.1±3.2	0.005	< 10 <sup>-4</sup>	MEarth	...	...	...	...
J19169+051N	46.0±0.2	0.008	2.0	ASAS	46	0.0045	<0.1	SM16
J19169+051S	23.6±0.3	0.008	< 10 <sup>-4</sup>	MEarth	...	...	...	...
J19216+208	133±9	0.016	< 10 <sup>-4</sup>	MEarth	154.7	...	...	New16

**Table A.2.** Rotation periods obtained for stars in our sample (cont.).

Karmn	$P_{\text{rot}}$ [d]	$A$ [mag]	FAP [%]	Survey	$P_{\text{rot,lit}}$ [d]	$A_{\text{lit}}$ [mag]	FAP <sub>lit</sub> [%]	Ref. <sup>a</sup>
J19346+045	$12.9 \pm 0.8$	0.006	0.33	ASAS	...	...	...	...
J19511+464	$0.59278 \pm 0.00012$	0.007	$< 10^{-4}$	SuperWASP	0.59	...	...	Har11
J20198+229	$1.13 \pm 0.01$	0.028	$< 10^{-4}$	SuperWASP	...	...	...	...
J20260+585	$57.7 \pm 0.4$	0.004	$< 10^{-4}$	MEarth	142.09	...	...	New16
J20305+654	$32.8 \pm 0.5$	0.023	$< 10^{-4}$	ASAS-SN	...	...	...	...
J20336+617	$12.6 \pm 0.7$	0.018	$< 10^{-4}$	SuperWASP	...	...	...	...
J20405+154	$106 \pm 6$	0.009	$< 10^{-4}$	MEarth	104.6	...	...	New16
J20450+444	$19.9 \pm 0.6$	0.011	$< 10^{-4}$	SuperWASP	...	...	...	...
J20525-169	$67.6 \pm 0.6$	0.026	0.00085	ASAS	67.6	0.01	$< 0.1$	SM16
J20567-104	$9.63 \pm 0.01$	0.018	0.28	ASAS	...	...	...	...
J21012+332	$29.4 \pm 0.9$	0.016	$< 10^{-4}$	MEarth	29.12	...	...	Wes15
J21152+257	$34.8 \pm 0.2$	0.033	1.2	ASAS	...	...	...	...
J21221+229	$41.0 \pm 1.7$	0.009	$< 10^{-4}$	SuperWASP	...	...	...	...
J21348+515	$54.3 \pm 1.5$	0.011	$< 10^{-4}$	SuperWASP	...	...	...	...
J22012+283	$0.44571 \pm 0.00002$	0.007	$< 10^{-4}$	SuperWASP	0.45	...	...	GR98
J22021+014	$29.5 \pm 0.1$	0.009	4.5	ASAS	31	...	...	Tes04
J22114+409	$30.0 \pm 1.3$	0.010	$< 10^{-4}$	SuperWASP	...	...	...	...
J22115+184	$36.3 \pm 0.2$	0.018	$< 10^{-4}$	ASAS	...	...	...	...
J22252+594	$64.6 \pm 2.1$	0.014	$< 10^{-4}$	ASAS-SN	...	...	...	...
J22298+414	$99.8 \pm 1.2$	0.007	$< 10^{-4}$	SuperWASP	...	...	...	...
J22468+443	$4.38 \pm 0.03$	0.091	$< 10^{-4}$	SuperWASP	4.376	...	...	Tes04
J22518+317	$1.63 \pm 0.01$	0.016	$< 10^{-4}$	SuperWASP	1.64	...	...	Nor07
J22532-142	$81.0 \pm 0.8$	0.014	0.00018	ASAS	96.7	...	...	Riv05
J22565+165	$39.5 \pm 0.2$	0.013	2.5	ASAS	$37.5 \pm 0.1$	...	...	SM15
J23064-050	$3.304 \pm 0.011$	0.004	$< 10^{-4}$	K2	$3.295 \pm 0.003$	...	...	Vid17
J23216+172	$74.7 \pm 0.7$	0.026	0.55	ASAS	...	...	...	...
J23419+441	$106 \pm 6$	0.027	$< 10^{-4}$	SuperWASP	99.58	...	...	New16
J23431+365	$83.6 \pm 7.0$	0.046	$< 10^{-4}$	NSVS	...	...	...	...
J23548+385	$4.70 \pm 0.04$	0.038	$< 10^{-4}$	SuperWASP	4.76	...	...	KS13

<sup>a</sup> References. GR98: Greimel & Robb (1998); Fek00: Fekel & Henry (2000); Tes04: Testa et al. (2004); Riv05: Rivera et al. (2005); KS07: Kiraga & Stępień (2007); Nor07: Norton et al. (2007); Hal08: Hallinan et al. (2008); Har11: Hartman et al. (2011); Irw11: Irwin et al. (2011); Kir12: Kiraga (2012); KS13: Kiraga & Stępień (2013); SM15: Suárez Mascareño et al. (2015); Wes15: West et al. (2015); Dav16: David et al. (2016); New16: Newton et al. (2016); SM16: Suárez Mascareño et al. (2016); SM17: Mascareño et al. (2018); Clo17: Cloutier et al. (2017); Vid17: Vida et al. (2017); Lot18?:

<sup>b</sup> J00051+457 = GJ 2: the periodogram of the ASAS light curve displays several secondary peaks around 15.37 d, including at 21.2 d as found by Suárez Mascareño et al. (2015).

<sup>c</sup> J04472+206 = RX J0447.2+2038: we also measured  $P_{\text{rot}} = 0.342 \pm 0.002$  d in the Montcabrer dataset (see Fig B.7).

<sup>d</sup> J06318+414 = LP 205-044: the periodogram of the SuperWASP light curve displays a second peak at 0.482 d of approximately the same power as at 0.299 d.

<sup>e</sup> J10508+068 = EE Leo: we increased the frequency search to less than half of the inverse of the time baseline of about 80 d, so the tabulated period is uncertain.

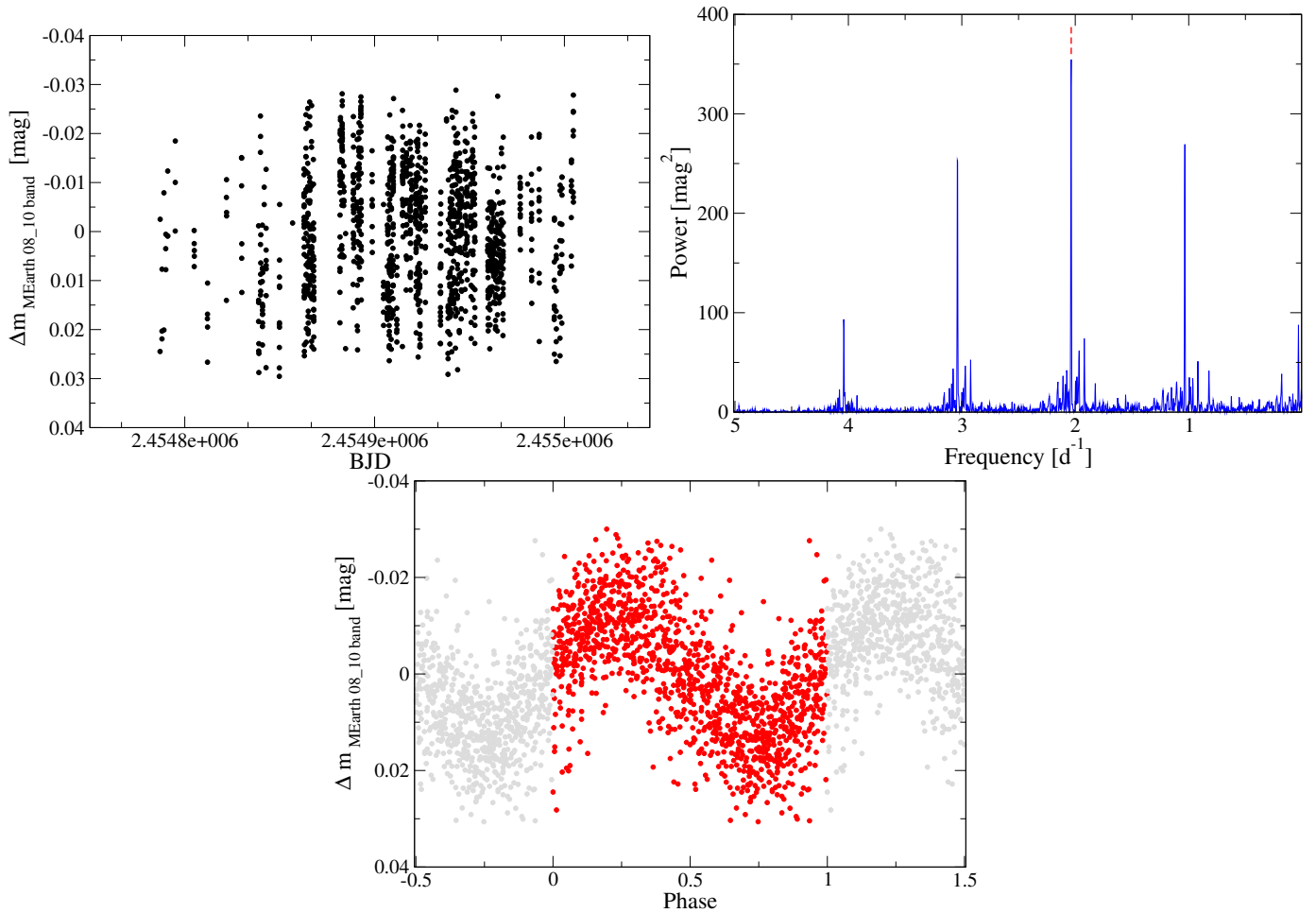


**Fig. B.1.** MEarth RG715-band photometric data (*top left*), Lomb–Scargle periodogram (*middle*), and phase-folded rotation curve for  $P=0.491$  d (*bottom*) for the M5.0 V star J12189+111 = GL Vir.

## Appendix B: Example light curves and periodograms

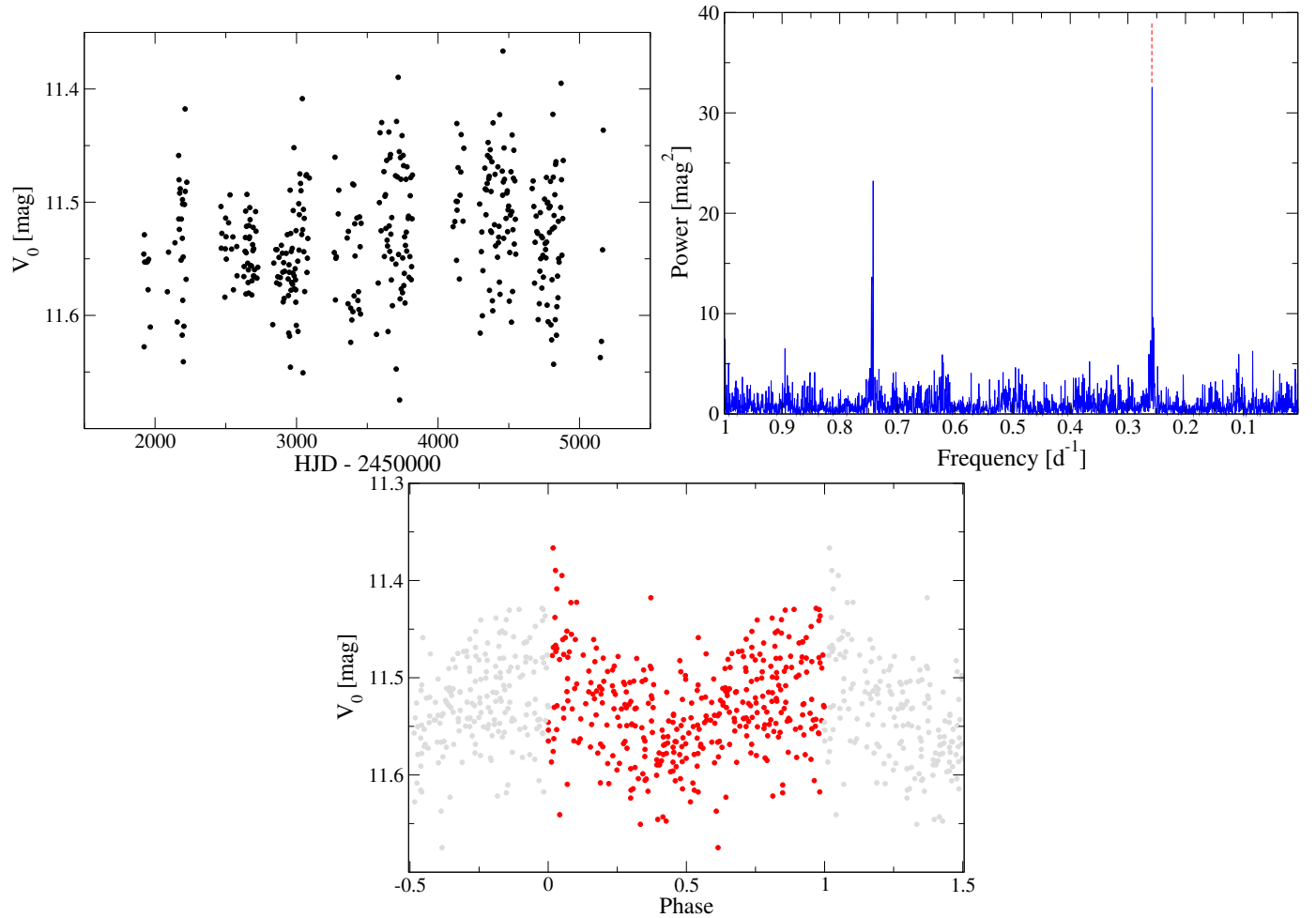


**Fig. B.2.** ASAS-3  $V$ -band photometric data (*top*), Lomb-Scargle periodogram (*middle*), and phase-folded rotation curve for  $P=3.87$  d (*bottom*) for the M3.0 V star J03473-019 = G 080-021.

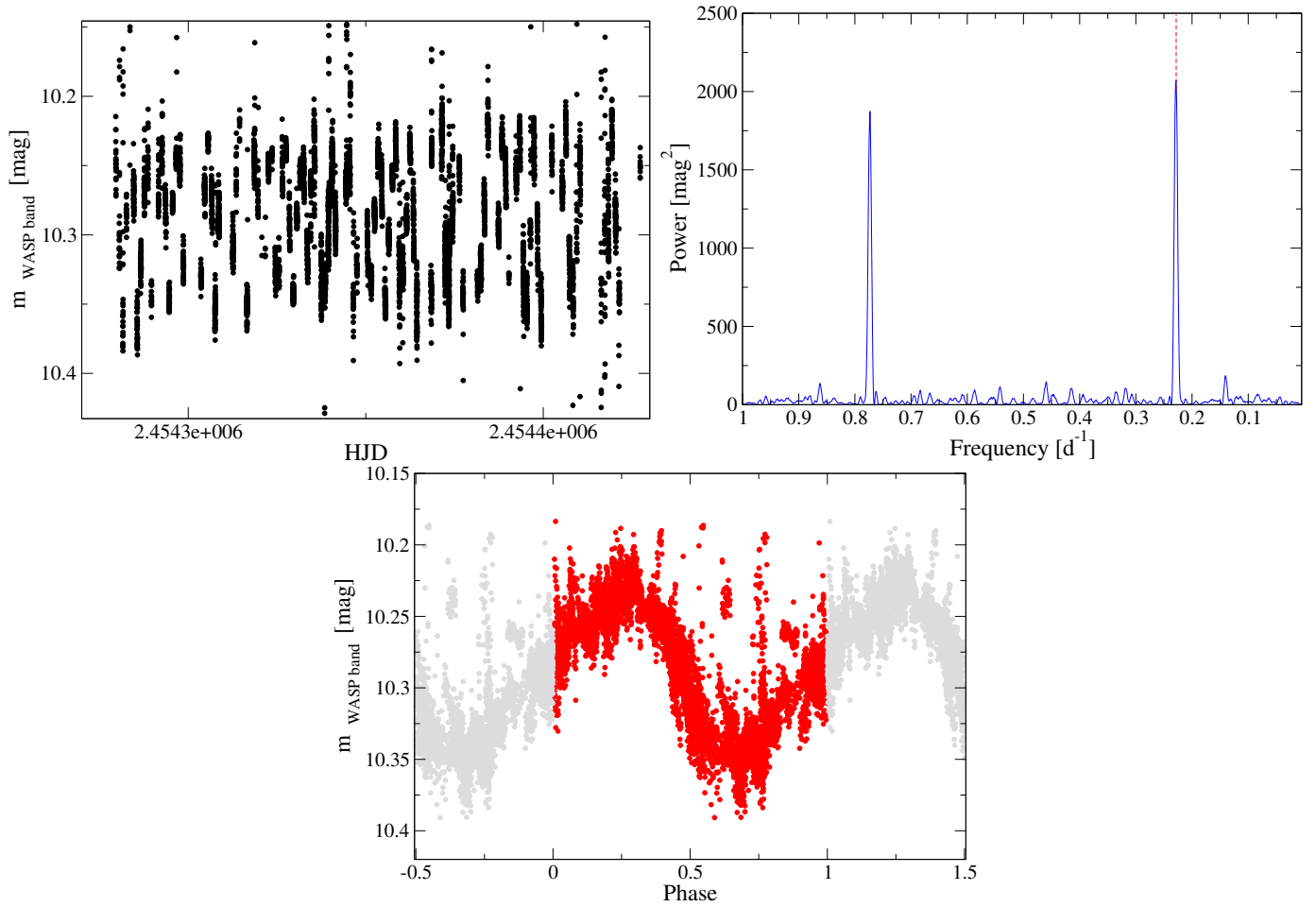


**Fig. B.3.** SuperWASP broad-band photometric data (*top*), Lomb–Scargle periodogram (*middle*), and phase-folded rotation curve for  $P=4.379$  d (*bottom*) for the M3.5 V star J22468+443 = EV Lac.

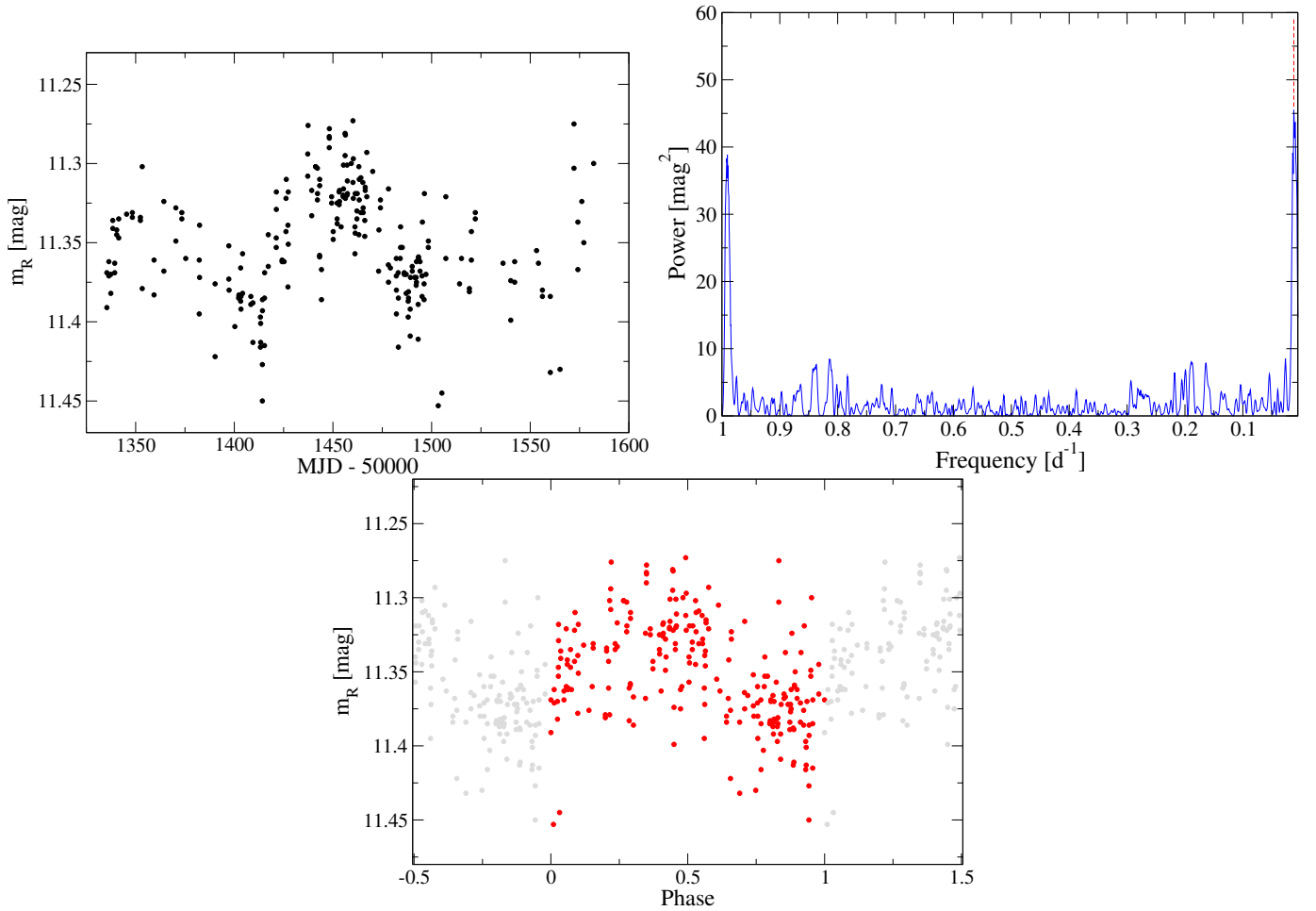


**Fig. B.4.** NSVS clear-band photometric data (*top*), Lomb-Scargle periodogram (*middle*), and phase-folded rotation curve for  $P=87$  d (*bottom*) for the M4.0 V star J23431+365 = GJ 1289.

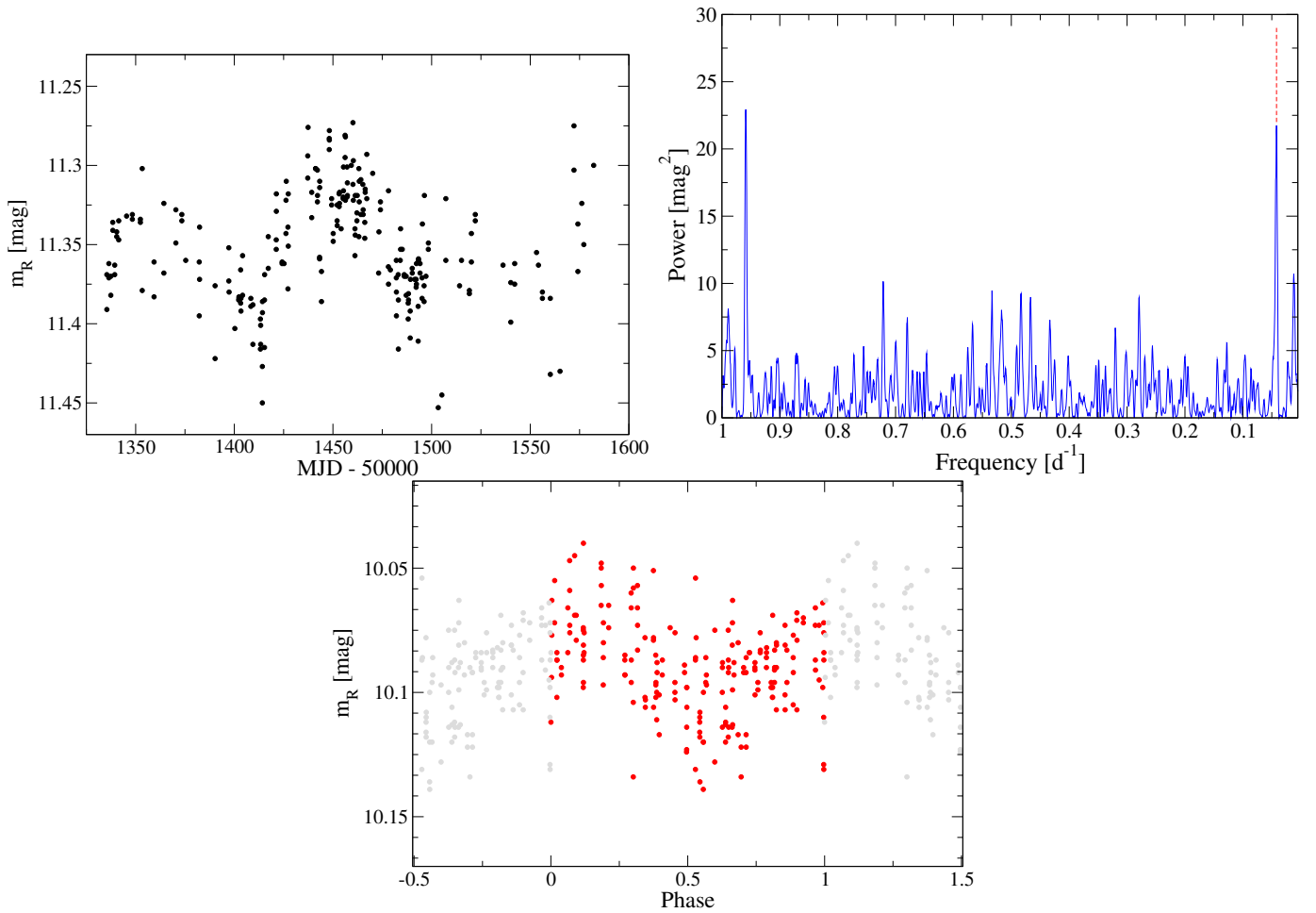


**Fig. B.5.** AstroLAB IRIS \$R\$-band photometric data (*top*), Lomb-Scargle periodogram (*middle*), and phase-folded rotation curve for \$P=23.9\text{ d}\$ (*bottom*) for the M3.0 V star J09428+700 = GJ 362.

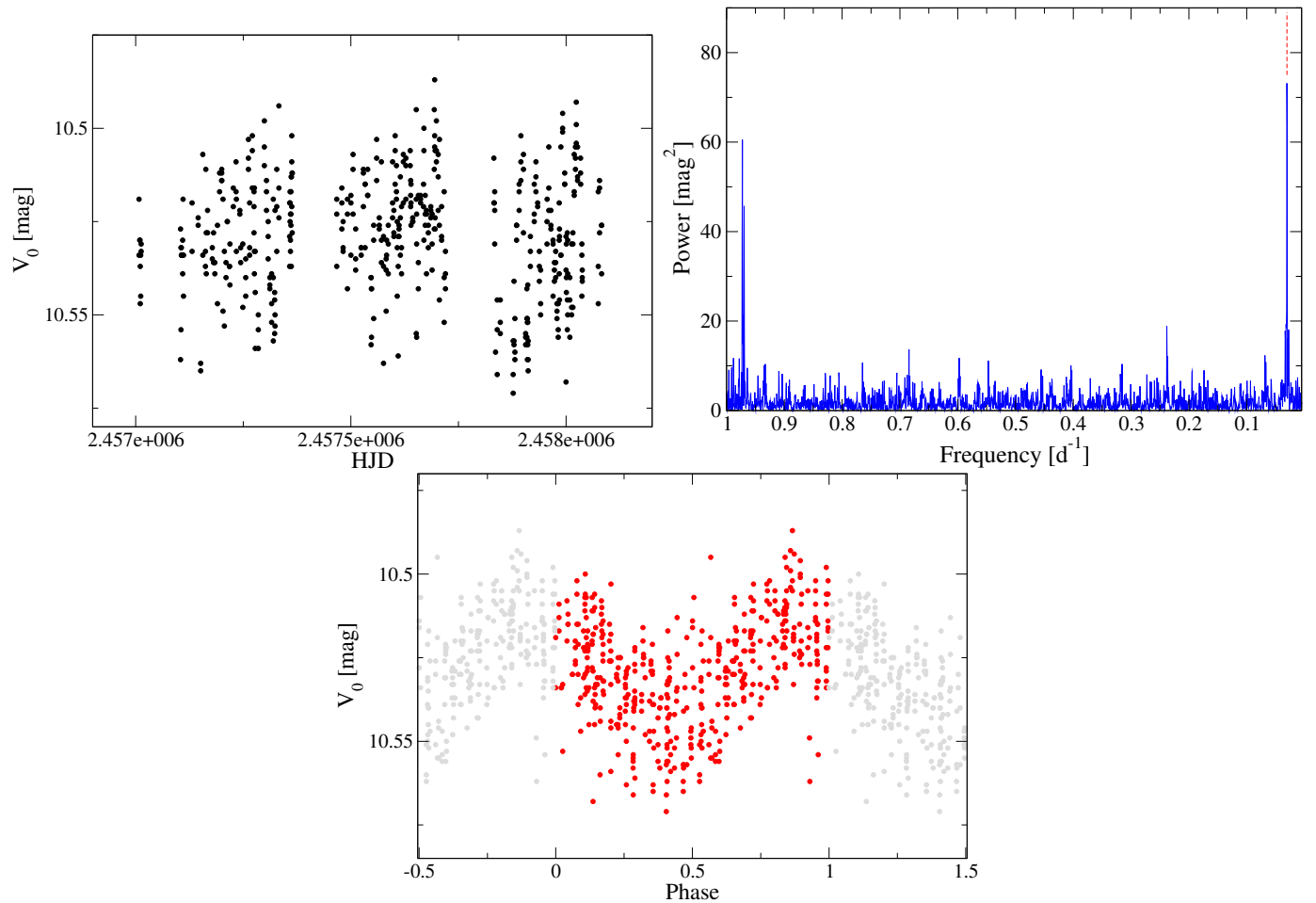


**Fig. B.6.** ASAS-SN  $V$ -band photometric data (*top*), Lomb–Scargle periodogram (*middle*), and phase-folded rotation curve for  $P=32.8$  d (*bottom*) for the M2.5 V star J20305+654 = GJ 793.

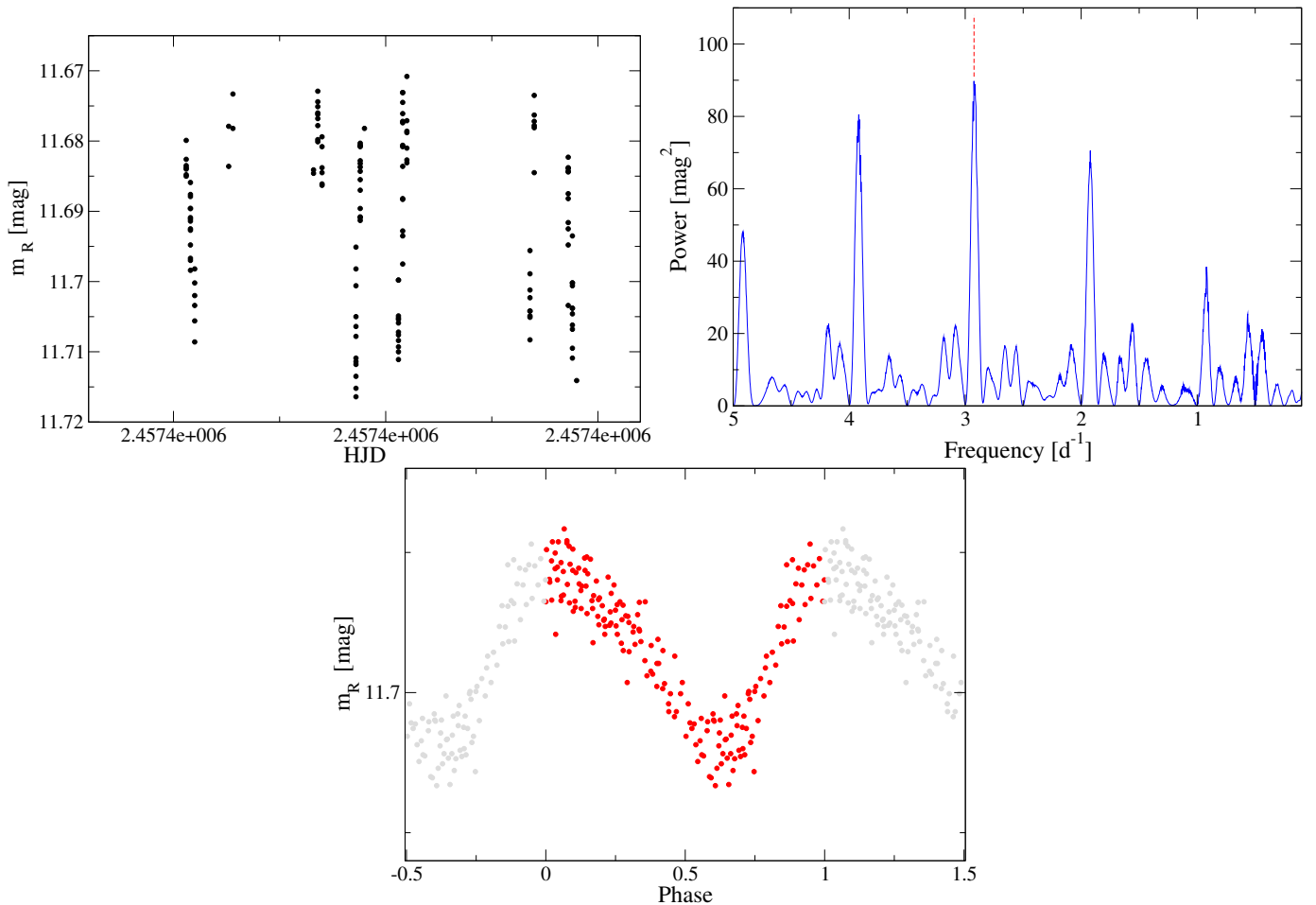


**Fig. B.7.** Montcabrer  $R$ -band photometric data (*top*), Lomb–Scargle periodogram (*middle*), and phase-folded rotation curve for  $P=0.342\text{ d}$  (*bottom*) for the M5.0 V star J04772+206 = RX J0447.2+2038 (compare with Fig. B.8).

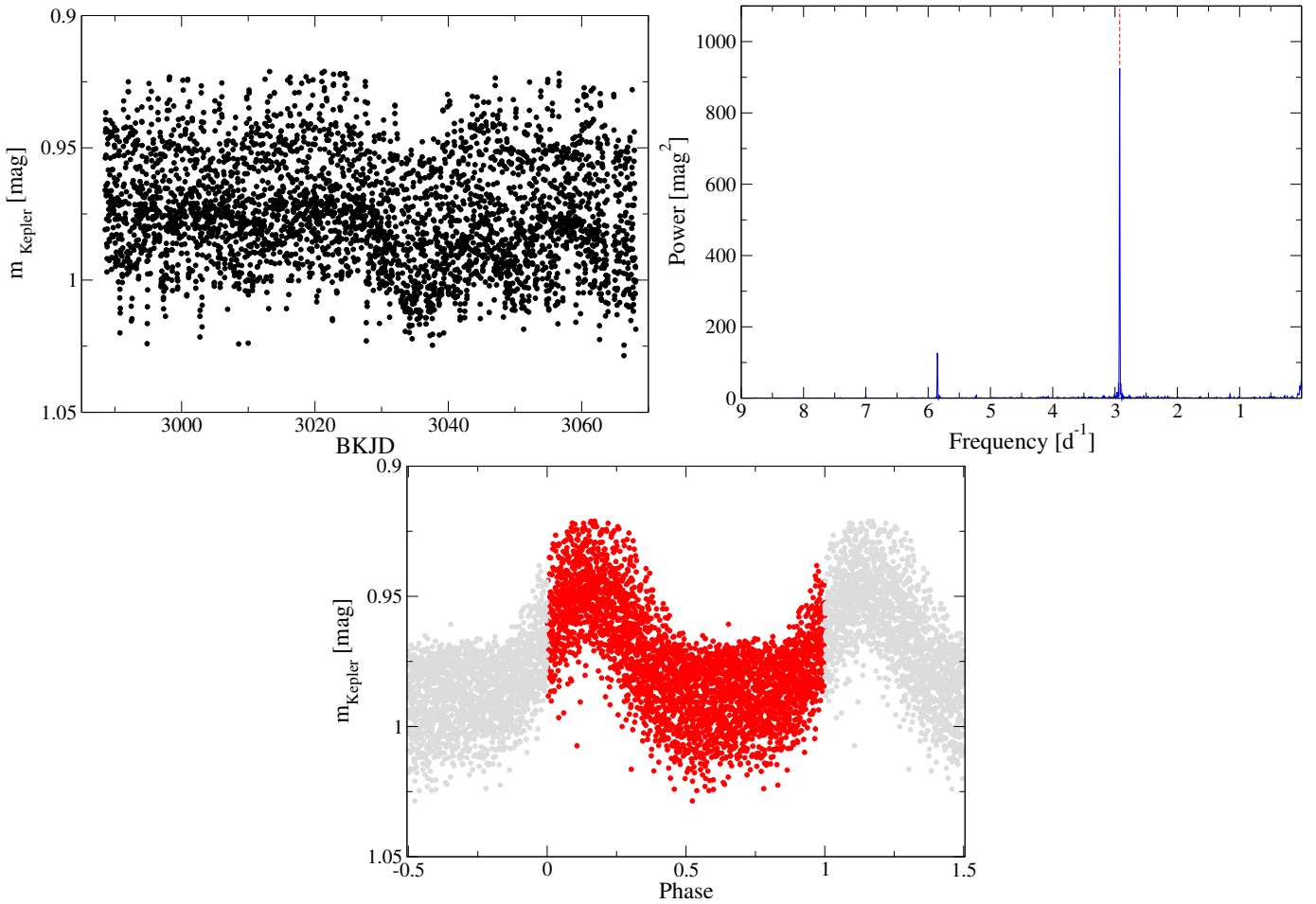


**Fig. B.8.** K2 photometric data (*top*), Lomb–Scargle periodogram (*middle*), and phase-folded rotation curve for  $P=0.342\text{ d}$  (*bottom*) for the M5.0 V star J04772+206 = RX J0447.2+2038 (compare with Fig. B.7).

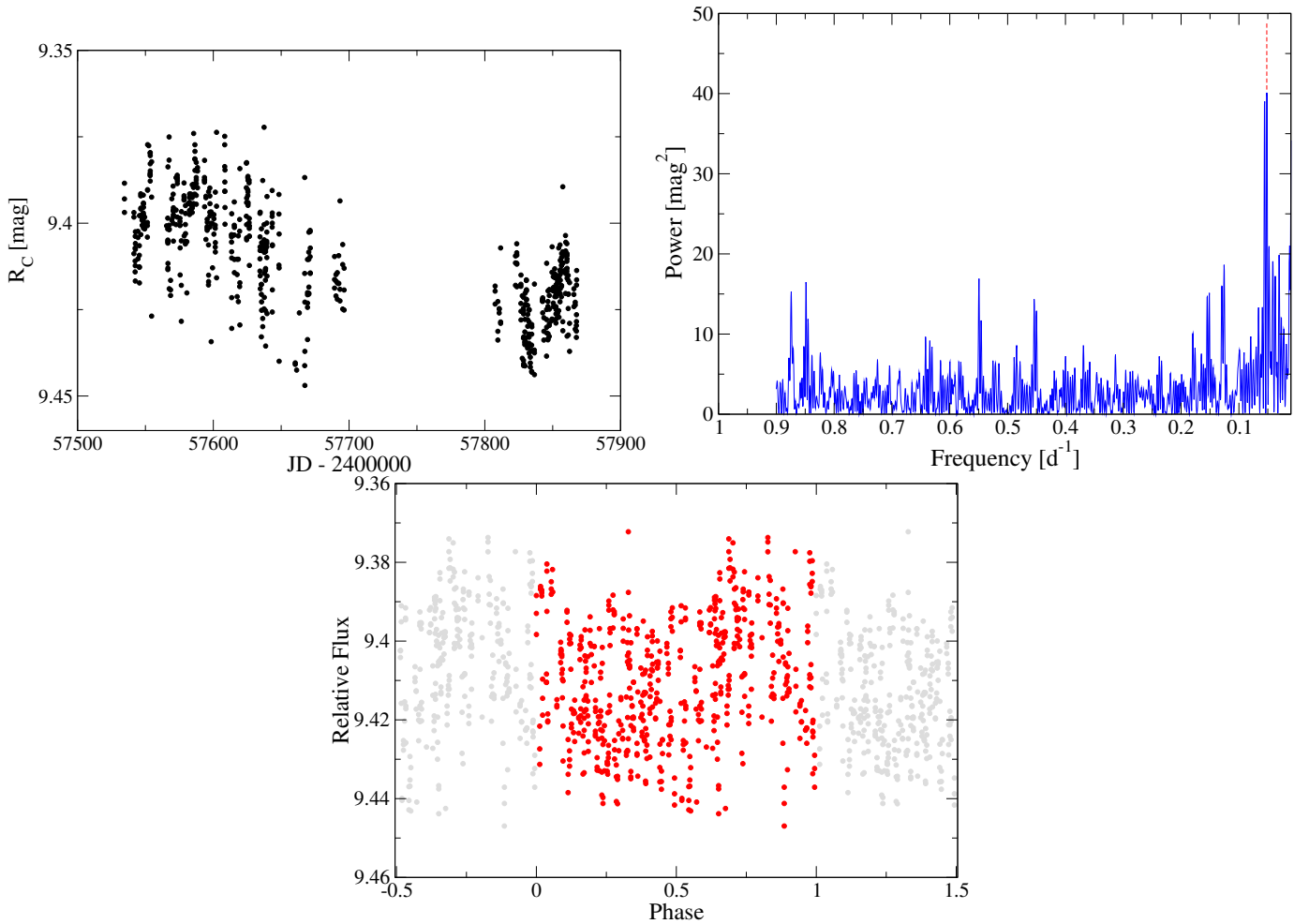


**Fig. B.9.** Montsec  $R_C$ -band photometric data (*top*), Lomb-Scargle periodogram (*middle*), and phase-folded rotation curve for  $P=19.3$  d (*bottom*) for the M0.5 V star J17355+616 = BD+61 1678C.

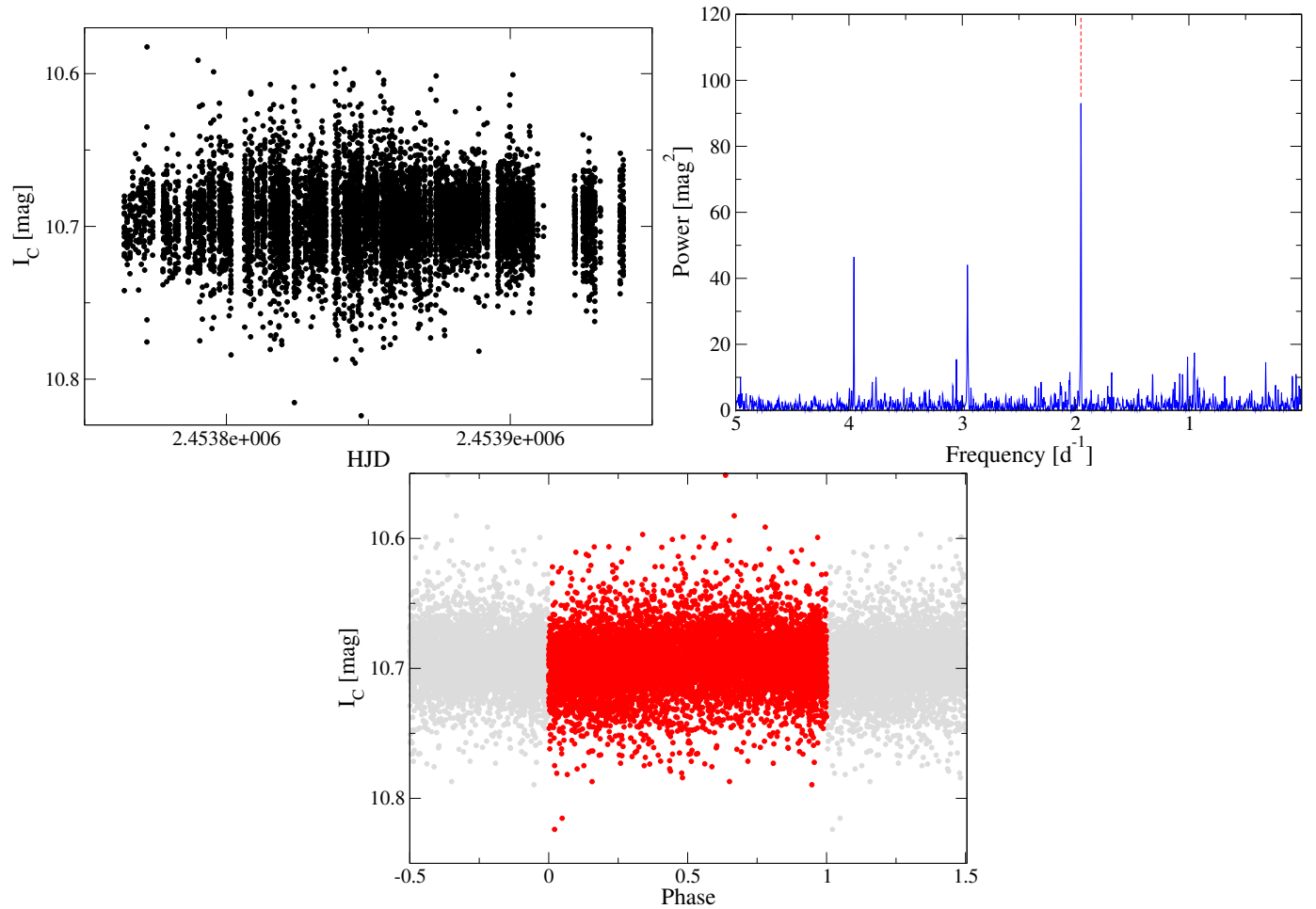


**Fig. B.10.** HATNet \$I\_C\$-band photometric data (*top*), Lomb-Scargle periodogram (*middle*), and phase-folded rotation curve for \$P=0.512\$ d (*bottom*) for the M5.0 V star J16313+408 = G 180–060.